2012-01-01

Comparison Study Between Fem And Sem For Wave Propagation Models Applied To Solids

Shaddy Roberto Castillo Ponton
University of Texas at El Paso, srcastillo@miners.utep.edu

COMPARISON STUDY BETWEEN FEM AND SEM FOR WAVE PROPAGATION MODELS APPLIED TO SOLIDS

SHADDY ROBERTO CASTILLO PONTON

Department of Civil Engineering

APPROVED:

Jack Chessa, Ph.D., Chair

Cesar Carrasco, Ph.D.

Hong-Sioe Oey, Ph.D.

Soheil Nazarian, Ph.D.

Benjamin C. Flores, Ph.D.
Dean of the Graduate School

Dedication

I want to dedicate this little piece of work, which has taken these last few months to complete, to my friends and family; without them the long nights would have felt longer and the hard problems much harder. Special thanks to Dr. Chessa for guiding me through this process and for being an outreaching hand of support when doubts surrounded me the most. Likewise, special thanks to Dr. Oey, with whom I was fortunate enough to work with, and whose advice went always beyond the academic interest. I thank each and every one of them and those that I have unintentionally left out of this space. I dedicate this work to you all.

"I know well enough that every word I utter carries with it something of myself, of my special and unique self with its particular history and its own particular world"
-Carl Jung

"Les choses qui paraissent obscures la veille sont parfois trop claires le lendemain "-Alexandre Dumas

COMPARISON STUDY BETWEEN FEM AND SEM FOR WAVE PROPAGATION MODELS APPLIED TO SOLIDS

by

SHADDY ROBERTO CASTILLO PONTON, B.S. CE

THESIS

Presented to the Faculty of the Graduate School of

The University of Texas at El Paso

in Partial Fulfillment

of the Requirements

for the Degree of

MASTER OF SCIENCE

Department of Civil Engineering

THE UNIVERSITY OF TEXAS AT EL PASO

December 2012

Acknowledgements

Special thanks to all the authors on whom I have found the source of inspiration and whose contribution on this topic to the academic world is nothing short of amazing. Special thanks to Dr. Chessa for granting me access to his large repository of code, which has allowed saving a few hundred lines of code in the process.

Abstract

Wave propagation is a field whose application has spread across many disciplines. In the field of structural engineering, wave propagation methods have focused their attention specifically in the area of structural health monitoring and active control of vibrations and noise. Likewise, the development of new methods and their application have been successful in the area of material science with a special emphasis on the field of structural integrity evaluation of anisotropic and inhomogeneous structures (laminated composite structures). The current available analysis tools are inadequate to handle the modeling of complex structures. One-dimensional wave propagation problems in solids are still a prevalent mean to approximate solutions for more sophisticated problems in mechanics. Fundamental solutions to one-dimensional problems provide the basis for understanding the fundamental principles that govern multidimensional wave propagation behavior. As boundary conditions become non-trivial and the quest of analytical closed-form solutions to the equations becomes cumbersome, D'Alembert's approach to wave propagation problems may involve a complex procedure that may render the quest for the solution very difficult if not impossible. Although many transformation approaches may seem promising, utilization of numerical procedures such as finite element analysis or the newest spectral element method has quickly become the academic norm for analysis of propagation problems.

The aim of this study is to gain insight in the analytical, numerical and experimental aspects that FE and SE wave propagation models provide. For the first part of this paper we will study wave propagation through a cylindrical rod, although it has been treated extensively in literature because of its simple structural shape, studying these types of problems allows us to compute accurate analytical and numerical solutions. The study of these problems provides the fundamentals to understand and interpret solutions that lead toward accurate multidimensional extension of the wave propagation theory. For the second part of this study, we will extend our models to two-dimensional wave propagation in plates. SEM and FEM plate models were developed based on different levels of spatial and temporal discretization. If not assessed carefully, numerical models may be often affected by phenomena not present in the physical system that has been introduced due to round-off errors, incompatibility of time integrations schemes, and/or ill-conditioned matrices. Proper identification and correction of any factors that may lead to unstable systems is necessary. Based on the models presented in this paper, a conclusion regarding the choice of the best-suited method for the modeling and assessment of wave propagation problems has been drawn based on their respective conditioning and stability characteristics.

Table of Contents

List of Figures

List of Illustrations

Chapter 1: Introduction

Wave propagation is a field whose application has spread across many disciplines. In the field of structural engineering, wave propagation methods have specifically focused in the area of structural health monitoring and active control of vibrations and noise. Likewise, the development of new methods and their application have been successful in the area of material science with a special emphasis on the field of structural integrity evaluation of anisotropic and inhomogeneous structures (Gopalakrishnan, Chakraborty, & Roy Mahapatra, 2007).

The current available analysis tools are inadequate to handle the modeling of complex structures. Dynamic analyses are traditionally performed using the conventional Finite Element Method (FEM); Unfortunately, FEM advantages are quickly overturned when the problem posed involves complex geometries as high-order discretization of the domain in question increases the time and computational cost to obtain the solution. Improving the accuracy of the FE solution is possible through a technique referred to as hp-refinement. Hp-refinement consists of two techniques: the first technique involves decreasing the element size, h, while holding the polynomial order fixed and is classified as an h-refinement. The error typically decreases as a power of h, where the exponent is determined by the polynomial order and smoothness of the solution. In contrast, improving the accuracy by raising the polynomial order, p, given a fixed element discretization, is classified as a p-refinement and it is typically associated with spectral convergence (Pozrikidis 2010). FE hp-refining techniques fail as the polynomial order, p, and the element size, h, reach a certain limit; the state of the system then renders the numerical process unstable for reasons that will be explained in the following section. A response to the undermining condition caused by the element's size and polynomial interpolation degree has been the utilization of Spectral Element (SE). Spectral elements are formed by the deployment of the interpolation nodes throughout the domain at a specific set of points given by the zeros of a family of

orthogonal polynomials. This, besides offering certain mathematical advantages in the system calculation process, allows a simplified system that conveys more relevant information.

1.1 THE SPECTRAL ELEMENT METHOD

The terminology spectral means that error decreases faster than any power of $1/p$, where p is the order of the polynomial expansion. Hp-refinement is the combination of both strategies to increase the accuracy of the solution. For inhomogeneous and nonlinear equations, the node distribution plays an important factor in the accuracy and convergence of the solutions. Theoretical analysis of the interpolation errors has shown that given a fixed number of interpolation nodes to be distributed over an element, the highest interpolation accuracy has been achieved by distributing the nodes at the positions corresponding to the zeros of certain families of orthogonal polynomials. If performed correctly, the result is a *Spectral Element Expansion* and an associated *spectral element method (*Pozrikidis 2010).

FEA modal expansions are generally performed using Lagrange interpolation, which are generally successful at low-order polynomials. As the number of interpolation points is raised, oscillations occur near the ends of the domain in question. The *Runge effect [Fig. 1],* is detrimental to the accuracy of the interpolation and consequently to the reliability of the finite element solution. The potential failure is circumvented by deploying the points at the zeros of a set of families of orthogonal polynomials.

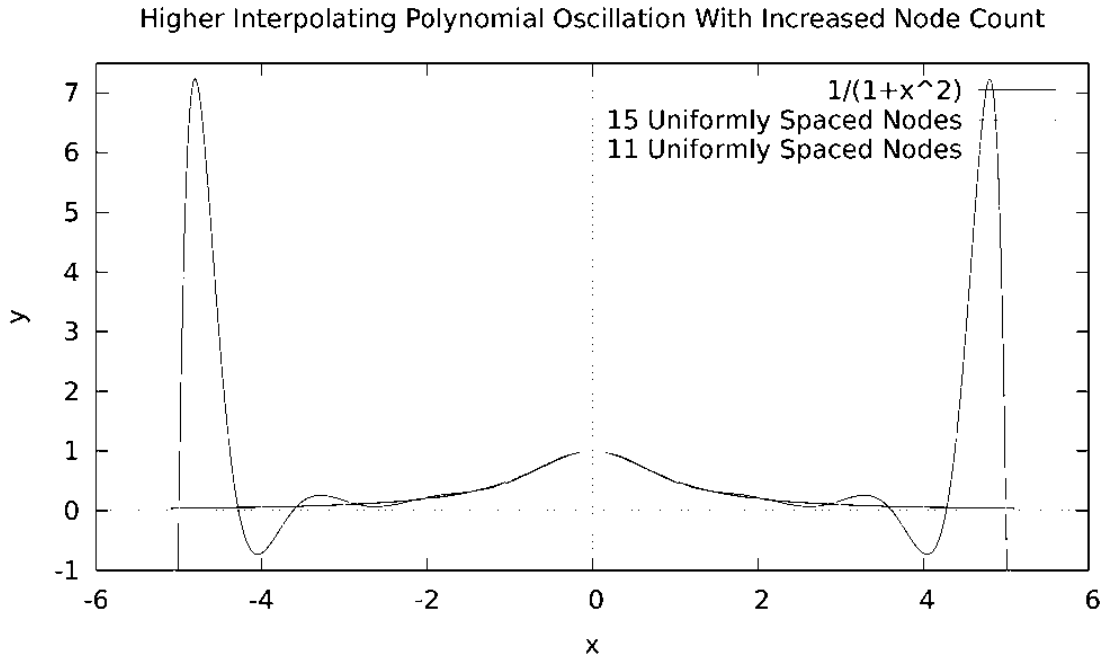

Figure 1.1: Runge effect present in High-order Lagrange Interpolation

The main reason for choosing the zeros of this set of families of orthogonal polynomial is because the interpolation is guaranteed to vary in the range of (-1,1), independent of the order of the polynomial interpolation. This property ensures the suppression of the Runge oscillations and a spectral convergence, that is, a convergence faster than any power of $1/p$. Lagrange polynomials fail in performance because physically they are reconstructed from evenly spaced data, this means that equal attention is paid to the middle as well as to the ends of the interpolation domain. Insufficient information beyond the boundaries of the domain is given which results in oscillations at the ends of the interpolation domain. Karniadakis & Sherwin (Karniadakis et al. 1999) present graphs of the condition number for the mass matrix calculated using Lobatto spectral elements and evenly spaced node elements. Their research had demonstrated that the mass matrix for the evenly spaced nodes was significantly worse conditioned for polynomial orders higher than five. A high condition number carries and increase risk in numerical instability and failure due to the growth of the computer round-off error (Pozkiridis 2010).

Chapter 2: Wave Propagation Problems

As was previously mentioned in the introductory part, dynamic analyses are traditionally performed using conventional FEM techniques. Wave propagation problems commonly introduce a high frequency input content for which many vibrational modes participate in the motion. At higher frequencies, wavelengths are very small and to effectively capture these modes using FE techniques, a restriction on the domain discretization and element size is imposed. Element size should be of the same order of the signal's wavelength. A fine mesh although ensuring an accurate distribution of the inertia, increases the computational cost of the solution enormously.

Finite Element solutions in dynamics are obtained using two different methods: the modal and the time marching scheme methods. Modal methods cannot be applied to multi-modal problems because of the need to determine natural frequencies and modal shapes for both low and high frequency modes. The extraction of eigenvalues is one of the well-known computationally expensive problems in mechanics. Thus, modal methods do not suit wave propagation problems. In contrast, various time marching schemes have been developed for the FEM. For these methods, the analysis is performed over a small time step, this being a fraction of the total time for which the response histories are required. For some marching schemes the constraints posed on the time step in conjunction with very large mesh sizes make the Finite Element solution for wave propagation problems prohibitibe (Lee 2009).

Numerical methods such as the finite element approach result in large-sized systems due to their inability to approximate the mass distribution accurately. The necessary method of choice should approximate the solution to the governing differential equations as closely as possible, which would result in a more accurate representation of the mass distribution of the element. If the solution procedure involves solving the wave governing differential equations in the time domain it will result very difficult to come up with a solution that works in both the time and spatial domain and that accurately models the

system's boundary conditions. A common method of approach to circumvent the temporal domain problem consists in ignoring the inertial part of the wave equation and to solve the static part of the equation exactly, which would allow the calculation of the mass and stiffness matrices. This method would ensure a stiffness matrix that is nearly exact and a mass distribution that is approximate.

Alternatively, the governing wave equation can be transformed to the frequency domain and solved exactly. This is a simpler option since the transformation into the frequency domain eliminates the time variable from the equation and introduces the frequency, ω, as a parameter. For 1-D systems, the transform method reduces the set of Partial Differential Equations (PDE) into a set of Ordinary Differential Equations (ODE), which are less complex to solve than the original wave equation as the time dependence is removed. Different transformation methods can be used to tackle these types of problems. Laplace, Fourier and Wavelet transforms are three commonly used transform methods. Once the transform method is selected and applied to the given set of PDEs, the governing equation in the frequency domain is solved exactly and all the relevant parameters in the Frequency Domain (FD) are obtained. The time domain solutions are obtained through the application of inverse transformations of the FD solutions. In summary, transformation methods yield a solution for two different domains (time and frequency) through the use of forward and inverse transforms which implies the need for an efficient way of obtaining these forward and inverse transforms, either analytically or numerically, to obtain the respective domain solutions. Sometimes this key feature limits the scope of the analysis of wave propagation problems using transform methods.

Chapter 3: 1-D Wave Propagation

1D Wave propagation problems in solids are still a prevalent mean to obtain approximate solutions for complex problems in mechanics. As boundary conditions become non-trivial, finding analytical closed-form solutions becomes challenging. D'Alembert's approach can be applied in many cases but often times it cannot offer a closed-form solution to the problem in the time domain (Schwarz et al. 2010). As boundary conditions become more complex, analytical solutions become more scarce and difficult to obtain. Solutions to one-dimensional problems form the basis for the understanding of models and are used as foundation for the extension process to multi-dimensional scenarios. Understanding wave propagation characteristics in simple structures is essential for their successful evaluation and application in more complex situations (van Hoof 1994).

Dynamic problems demand an effective method of acquisition and representation of all the factors that interfere in the process. A sufficiently accurate dynamic response can only be acquired by capturing all the necessary range of high frequency wave modes. The element size, h, must be sufficiently small in the order of the size of the shortest wavelength of the vibrating structure. In literature, two kinds of numerical methods have been applied to wave propagation problems[4]. The first one is conventional finite element analysis for which it has already been mentioned that the numerical capabilities are often overturned by the high computational costs. The second one is referred to as Spectral Element Methods (SEM) which itself is divided into two branches: Fast-Fourier Transform (FFT) based SEM and the orthogonal polynomial based SEM. SEM based on FFT techniques involves the analysis of the system's responses measured (in the time domain) and transforming it into a frequency domain (FD) so an analysis of the components of the pulse can be performed. FFT methods allow a single element to model sufficiently wave propagation in large uniform structures, which is well

suited for 1D and 2D problems[4]. On the other hand, orthogonal polynomial based SEM techniques are best suited to model situations involving complex geometries. It is for this reason that the Spectral Element Methods is well suited to handle wave propagation problems. The difference between FEM and SEM is the formulation of the modal interpolations and the location of the nodal points. SEM are deployed systematically in each element at the locations of the zeros of a given family of orthogonal polynomials (e.g. Legendre, Cherbysev, Lobatto, Lobatto-Legendre,etc.) Among the properties of the spectral elements we can find numerical stability, lower computational cost because efficiency is gained by efficient element discretization. Spectral element methods allow a more natural diagonalization of the mass matrix process, which at the same time assists in the overall computational cost of the operation. This method has been successfully applied in many different fields, especially those of fluid dynamics, seismology and acoustics (Lee 2009).

Conventional finite element models are formulated by using frequency independent polynomial interpolation functions, this means that FEM cannot capture all necessary high frequency wave modes of interest[7]. FEM solutions become significantly inaccurate at high frequencies when the order of the wavelength modeled is very small. As a rough guide, the mesh size should be 10-20 times smaller than the wavelength of the highest frequency mode of interest. Unfortunately, this approach results in a system that is extremely large which from a computation point of view renders the method too prohibitive for complex or large structures. This problem can be to a degree circumvented by making the shapes functions frequency dependent, these dynamic shape functions can capture the necessary frequencies that compose a given wave mode. This concept has led to the development of what is known as the Dynamic Stiffness Method (DSM.)

Recently, the focus of the spectral element method has been towards the simulation of wave propagation in complex structures for damage detection (e.g. 1D structures rod/beams). As the industry leans toward more advanced Non-Destructive Testing methods (NDT), it has become more important to

understand the wave propagation behavior the material is subjected to before and after the existence of defects such as cracks, or delamination in the case of composite materials, and how waves are diffracted or dispersed by these during the testing process. 3D SEM Wave propagation analyses of composite materials have not been widely reported in literature. Although numerical simulation has been explored for some years, in most related work, analyses have been simplified to focus on one-dimension or two-dimensional models that have concluded in approximated results for complicated layups with or without damage (Li et al. 2012.)

SEM combines accuracy and flexibility. This makes it highly desirable for modeling elastic wave propagation problems. For the purpose of this paper a comparison between FE and SE techniques has been performed. For the SEM case, high-order spectral elements based on Lobatto polynomials will be used. The Finite Element analysis will consist in linear elements whose number, or size, will increase or decrease depending on the level of accuracy desired. The comparison consists in the analysis and interpretation of a set of metrics (deviation, error, SSE, etc.) taken throughout the domain in question during the extent of each simulation. These set of metrics are considered to characterize in the best manner possible the level of performance and accuracy that each method provides for any of the simulation's scenarios given a fixed number of degrees of freedom (although SEM was allowed to vary in order as long as the number of nodes did not drastically differ from the one specified). Levels of dispersion and the cumulative error were likewise recorded using as base the analytical solution calculated via D'alembert's wave solution theory.

3.1 Spectral Element Method Basis

The domain of study is discretized into a given set of spectral elements each represented by an interpolation basis of degree p. To perform the discretization process each element must be mapped from its physical domain to a master domain characterized by coordinate ξ in the coordinate space Λ=[-

1,1] using an invertible mapping. The individual element discretization occurs by deploying the nodal points at the position of the zeros of the Lobatto polynomials throughout this master domain. The interpolation functions (basis functions) are calculated using Gauss-Lobatto-Legendre polynomials of degree N. Each interpolation function fulfills the required kronecker-delta property, δ_{ij}, which returns a value for the ith function evaluated at the ith node equal to one and which vanishes at any other nodal position. Equation 1, shown next, represents the formula for the interpolation basis where P'_N represents the derivative of the Legendre Polynomial of degree N. The mapping formulation guarantees the interpolation function to vanish at the element's end points as well as the interior nodal points defined using the Lobatto orthogonal polynomial of choice.

$$\left(1-\xi^2\right)P'_N(\xi)=0,$$

Equation 3.1: Interpolation Basis

The integrals are numerically calculated using a Gauss-Lobatto quadrature that renders the exact value of the integral depending on the degree of choice. Gauss-Lobatto quadratures integrate exactly functions of degree (2*k*-1) or lower, *k* being the quadrature's order. This quadrature characteristic in conjunction with an important orthogonal polynomials' mathematical property of allow a natural and straightforward diagonalization process to calculate the mass matrix. For this paper, computational cost has not been directly measured but the focus has rather been the accuracy provided by each method. For this reason, the diagonalization option has been set aside and the work for this paper has been entirely performed using full Mass matrices to avoid any loss in information that could be presented during the diagonalization procedure. This has simplified the finite element processing and post-processing sections of the code since FE's diagonalization is not as simple or natural as that for spectral based elements.

3.2 Wave Propagation Governing Equations

$$c_0^2 \frac{\partial^2 u}{\partial x^2} = \frac{\partial^2 u}{\partial t^2}, \quad \text{with initial conditions } u(x,0) = 0, \quad \left.\frac{\partial u}{\partial t}\right|_{t=0} = \dot{u}(x,0) = 0.$$

Equation 3.2: Wave equation

For this paper, a 1-Dimensional rod of length L and constant cross section A is considered. The mechanical properties of the rod are denominated E, for the elastic Young's modulus and ϱ for its mass density. Hence, the rod's one-dimensional speed *c*, is obtained via the formula:

$$c = \sqrt{\frac{E}{\rho}}$$

Equation 1.3: Wave Speed

To simplify the problem the following assumptions have been made: the mechanical model of the rod is completely isotropic having its longitudinal axis resting on the x-coordinate. The wave propagation for which this paper is concerned of is that occurring in the longitudinal direction thus any phenomena occurring in the y-direction is neglected. At time t=0 the rod is subjected to a sinusoidal force/pulse at the left end of the rod with a duration of 0.2 seconds. Damping is not considered for this problem, as the main concern is the natural numerical stability and level of dispersion that Finite Elements and Spectral Elements methods provide and how well they compare against each other.

Following Galerkin's method (which allows the transformation from a partial differential wave equation into an ordinary differential equation) in conjunction with the central time difference integration scheme, the wave equation can be rewritten into matrix form as:

$$\mathbf{M\ddot{U} + KU = F},$$

Equation 3.2: Wave Equation in its ODE form

Where M denotes the global mass matrix, K is the global stiffness matrix and F is the vector of time-dependent forces applied at the left end of the rod. U denotes the global vector of unknown nodal displacements. Both Neumann and Dirichlet conditions are initially zero.

Equation 3.3: Central Time Difference Formula

From analytical considerations it follows that we generally encounter two types of basic waves that propagate in a solid medium, each characterized by its own specific propagation velocity, c. These waves are referred to as dilatational (or longitudinal) wave and distortional (or transverse wave). When a wave of either type reaches the domain boundaries both reflection and refraction will occur and generally a wave of each type will reflect and refract. For problems involving wave propagation in finite solids or for small time periods there may not be analytical solutions available so a numerical approach is necessary.

Numerical modeling of wave propagation involves a spatial and temporal discretization of the governing equation, the SE and FE methods take care of the spatial discretization of the domain in question resulting in a semi-discrete system of ODEs. The numerical integration of the governing ODE involves the selection of a time integration scheme which influences directly on the accuracy of the solution. For this reason it is necessary to select a mesh capable of detecting minimal changes and a time integration method that is stable for and during the solving process.

Propagation of waves across a cylindrical rod has been treated extensively in literature and practice. Its simple structural shape enables us to easily interpret and analyze numerical and experimental results allowing us a step-by-step extension towards multi-dimensional more complex analyses. The analytical analysis of wave propagation in a rod can be based on elementary theory or be

based on the exact equations of motions. Elementary theory does not originate from the governing equations of motions but from considering the motion of an element in a structure. For this theory certain assumptions must be considered e.g parallel cross sections perpendicular to the longitudinal axis remain plane and parallel and there is a uniform distribution of stress throughout the material. Elementary theory gives more insight on the general aspects of wave propagation while exact analysis gives a more accurate representation of the wave behavior. It is important to mention that numerical modeling often introduces phenomena/noise that is not present in the physical system. For this reason it is necessary to analyze the results and compare them against the analytical solution to check the presence of numerical dispersion, instability, or incorrect set up of boundary conditions. The numerical dispersion is caused by the spatial and temporal discretization of the system. A serious problem during the modeling stage is the presence of numerical dispersion since it is not immediately obvious whether it is an accurate representation of what is physically occurring or whether it is a consequence of the selection of a given set of numerical schemes or mathematical basis formulation to tackle the problem. A wave is said to propagate non-dispersively in a medium if each harmonic component of the wave propagates at the same velocity, so proper identification of the component of the web is necessary for its accurate representation.

3.2.1 Numerical dispersion associated to temporal discretization

Schreyer showed that the temporal discretization influences the numerical procedure in two ways: by introducing (i) numerical damping and (ii) numerical dispersion[6]. Schreyer showed that the two

characteristics could be deduced for any time integration algorithm by the calculation of the eigen values of the amplication matrix **A.**

Comparison of dispersion associated with both spatial and temporal discretization indicates that a given combination may result in cumulative dispersion or in other cases it may result in a counterbalancing effect. Spatial discretization is naturally constrained to a fixed degree as it directly influences the size of the system. Spatial discretization must not render a system too large or too little, as it will have direct influence on the system's overall computational cost and accuracy of the solution. In the other hand, the chosen time scheme will have a larger selection of choices and its full influence will depend on the size and type of system that has resulted from the spatial discretization. In regards to time integration schemes, Krieg and Key stated: *a good time integrator will introduce errors of a type and will tend to offset the errors introduced by discretization in space* (van Hoof, 1994).

Time integrations schemes can be implicit or explicit. Usage of explicit integration schemes results in the consideration of stability criterions for the selection of a time step size, this results in conditionally stable explicit time integration schemes. When unconditionally stable implicit integration schemes are used the choice of the time step size is based on the degree of accuracy desired, this means that the cost per time step is high but the time step selection is not bounded by consideration of the solution's stability criterion. Mesh refinement yields a more accurate approximation to the wave velocity, and its oscillatory behavior near the wave's front. However, h-refinement introduces the presence of higher frequencies that will affect the approximation that to compensate its fault, it will require the time step of choice to be sufficiently small. When the time step is too large the high frequencies cannot be represented accurately, this is a phenomena known as *aliasing*. The selections of a

time step as well as the level of mesh refinement are highly correlated. An admissible value for both is the key to an accurate approximation to the physical representation of the system.

Schreyer analyzed and categorized the many different integration schemes that exist. He proved that the central difference method with a lumped mass matrix is nondispersive when a given set of conditions is satisfied. However, this is only true for 1D wave propagation with evenly spaced nodes. Integrations methods can be classified as unconditionally stable or conditionally stable. An integration method is stable if the solution is bounded for any set of initial conditions. An integration method is called unconditionally stable if the solution for any set of initial conditions does not grow unboundedly for any given time step Δt. The integration is conditionally stable if the condition described above holds provided that the ratio $\Delta t/T$ is below a certain value referred to as the *stability limit* [Bathe (1982)]. Hughes (Bathe, 1982) (Hughes & Belytschko, 1983)[(Hughes 1983)] found that the central difference method is only conditionally stable. Likewise, Newmark-β methods are implicit and unconditionally stable. Newmark's method is one of the most effective and popular techniques for structural dynamics problems because it introduces no numerical damping. Krieg and Key showed that errors of lumped mass with explicit integration and/or consistent mass with implicit integration are compensatory. In the other hand, systems with lumped mass matrices and implicit integration schemes or consistent mass and explicit integration schemes are cumulative in nature. This is in part due to the fact that the central difference schemes shorten the time period of study while Newmark's method elongates that period. Consistent masses underestimate the periods while lumped masses overestimate the periods. Krieg and Key's study resulted in the classification of the central difference time integration scheme as conditionally stable when the system is conformed by a diagonal matrix. Several other alternatives exist to improve accuracy but at a much greater expense (van Hoof, 1994).

The final choice for spatial and temporal discretization largely depends on the size and type of system in question. Wave propagation problems must be dealt with properly. The wave behavior must be correctly modeled and an accurate representation of the wave expansion, reflection and diffraction is highly important for the solution obtained to be of reasonable value. The solution requires the use of a small time step to minimize the error due to time integration but on the other hand, the time step must not be smaller than necessary, since this would render the solution more costly than what is actually needed. Depending on the size of the system the error may be largely contributed by the spatial discretization, a proper analysis should be performed for an efficient deployment of nodal points and the set up of boundary conditions to model the given scenario correctly.

Chapter 4: Analysis and Data Interpretation of Numerical approximation

4.1 WAVE PROPAGATION PROBLEM SET UP

For this paper, a 1D rod of length L=10 and constant cross-section A=1 is considered. The mechanical properties of the rod are the following: (i) elastic Young's modulus E=500 N/m^2 (ii) mass density ϱ=1 N/m^3. Hence, the rod's one-dimensional speed *c* is obtained via Eq 3. The Dirichlet boundary conditions indicate a right fixed end while neumann's boundary conditions indicate a sinusoidal pulse of period T=0.4 with a duration of 0.2 s occurring at the left end of the rod.

To simplify the problem the following assumptions have been made: the mechanical model of the rod is one-dimensional having its longitudinal axis resting on the x-coordinate. The wave propagation for which this paper is concerned of is that occurring in the longitudinal direction thus that occurring in the y-direction is neglected. Damping is not considered for this problem, as the main concern is the natural numerical stability and level of dispersion that Finite Elements and Spectral Elements methods provide and how well they compare against each other.

The second part of this report concerns the aspects and effects of the numerical modeling of wave propagation. Both the spatial and the temporal discretization introduced errors, which influence the accuracy of the solutions. The combined effects of the procedures performed need to be examined and properly interpreted before a conclusion regarding the selection of the best method for treatment of wave propagation problems can be stated.

Theory and empirical research has provided enough information regarding the wave behavior near fixed boundary conditions. It is known that a travelling wave as soon as it reaches a fixed boundary

nodal point at either end of the material, both reflection and refraction take place. Most generally, four separate waves are generated: a wave of each type is reflected, and a wave of each type is refracted. This means that when a stress pulse reaches a free end of the bar, it will be reflected. In order to investigate the nature of the reflected pulse, the boundary conditions must be applied such that no stress normal to the end of the rod is developed. The shape of the reflected pulse results in that of the incident pulse but with opposite sign. This means that a compression pulse will be reflected as a tension pulse or vice-versa. At the ends of the rod, the displacements and hence the velocities are a superposition of both incident and reflected pulse and the resulting value will be twice the corresponding values as the pulse travels along the rod.

For this paper, a model based on the conditions described above was tested using FEA with a given number of linear elements. During this procedure the metrics that were continuously recorded were: (i) the areas under the wave curve for the analytical and the numerical approximation, (ii) the difference between these areas (iii) the difference between the analytical solution and the numerical approximation, from here it is necessary to remark the two types of error measurement procedures utilized: the first one is comprised by the summation of the mean square errors per time step throughout the components and the second one involves the total sum of the standard difference per time step among the elements components.

4.2 FINITE ELEMENTS

This section deals with the analysis and interpretation of the results from each of the tests. For this section different parameters were taken into account and the few selected were considered the most descriptive of the method's performance. These are now utilized as metrics to measure the accuracy of

the wave behavior model given method and discretization specification set up to the problem. A description of the graphs utilized follows:

(i) *Wave Representation given a configuration.*- This graph is presented so that a general picture of the model behavior can be seen. It compares the analytical solution to the numerical approximation at a random time step. From this graph a general idea of the accuracy of the test can be concluded preliminarily without the need of analyzing numerical data. Although the numerical values cannot be compared up close, it shows identifiable sections where the approximation does not meet the requirements as it may present oscillations or distorsions of some sort.

(ii) *Areas vs time step.*- This graph depicts the area under the wave curve for both the analytical and numerical approximation solutions. Unlike the *wave representation* graph, it may be easier to spot trends such as area loss due to numerical dispersion/dissipation. Similarly, one does not need to be acquainted with numerical data as the graph simplifies the information such that one can determine graphically what is occurring in the test.

(iii) *Dispersion as measured by area difference.*- This graphs contains the plot of the difference between the area under the propagating wave for both analytical solution and the numerical approximation. Increase in the difference of areas is a clear proof of numerical dispersion/dissipation in the process, which will render the numerical solution less accurate as the test time increases.

(iv) *Root Mean Square Error graph (MSE).*- This graphs shows the plot of the total mean square error (sum of the difference between the analytical solution and the numerical approximation squared) for each time step. This graph describes how well the numerical approximation approaches the analytical solution as time progresses during the test. Plots

that seem to remain constant near are often sought, as it would depict an exact solution for each of the time steps.

(v) *Standard Error and MSE.*- Similar to the graph described above, the only difference is that the Standard Error contains the sum of the individual difference per node of each of the components of the bar given a time step. Unlike the procedure above, these quantities have a positive or negative value, so it can be easier to spot whether an over or an under approximation are taking place. It is important to notice that at low-order MSE errors, the plot should be depicted by an almost horizontal line on top of the x-axis (y=0).

4.3.1 The Analysis and the Interpretation

4.3.1.1 FEA using 50 linear elements

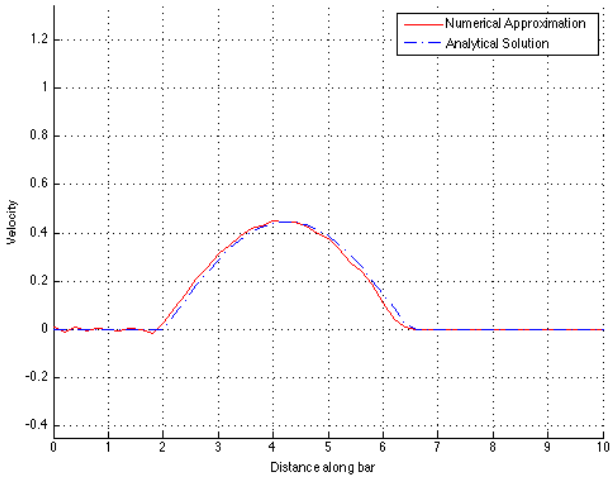

Figure 4.1: Wave Representation using 50 linear elements

Figure 2 on top, depicts a numerical approximation that can be quickly described as inaccurate. There seems to be oscillations at the left end of the wave and throughout its initial part of the crest. This is a first indication that what we will be analyzing is not encouraging for this specific set up. One thing that should not discourage us from pursuing the FEA method in wave equation is the fact that we have just started and we have done so very poorly, using only 50 linear elements so there is much more room for improvement.

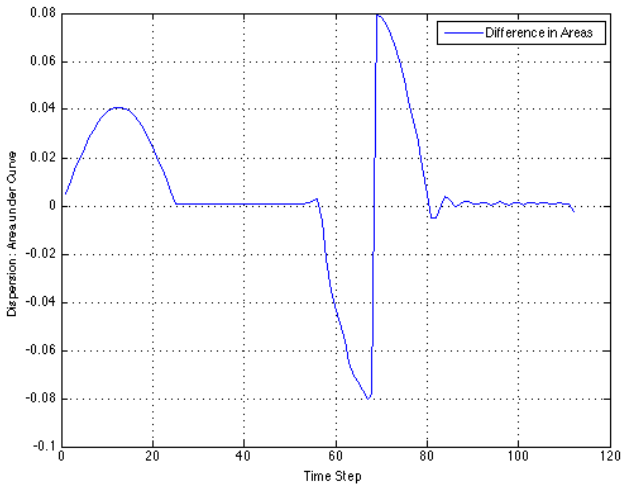

Figure 4.2: Dispersion as measured by areas

Figure 3 indicates the presence of some dispersion in the numerical approximation, the highest being of the order of 0.08. No statement can be done yet regarding the dispersion at this element discretization level since no point of comparison exists yet, we shall go back to this point later on in this section.

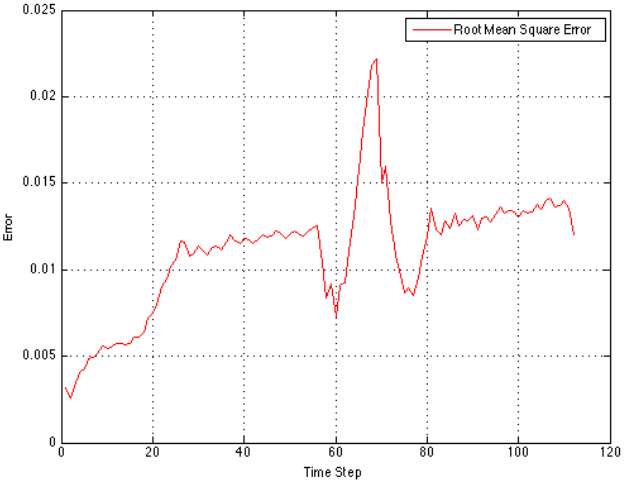

Figure 2.3: Root mean square error

Figure 4 indicates the presence of error increase in the numerical approximation, the highest being of the order of 0.02 but quickly dropping back and leveling below 0.015. No statement can be done yet regarding the MSE significance since no point of comparison exists yet, we shall go back to this point again later on in this section.

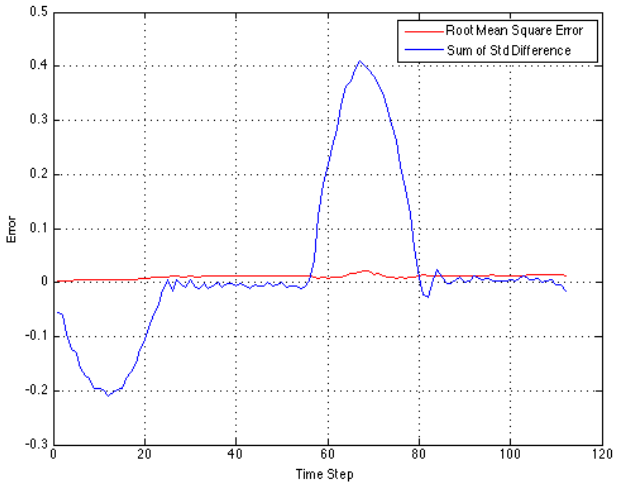

Figure 4.4: Standard error and MSE

Figure 5 depicts the MSE and the standard error, the MSE seems to be growing up slowly as the time progresses during the test, this is an indication that the accuracy of the solution is dependent on time. The Standard Sum cannot indicate us anything just yet.

4.3.1.2 FEA using 100 linear elements

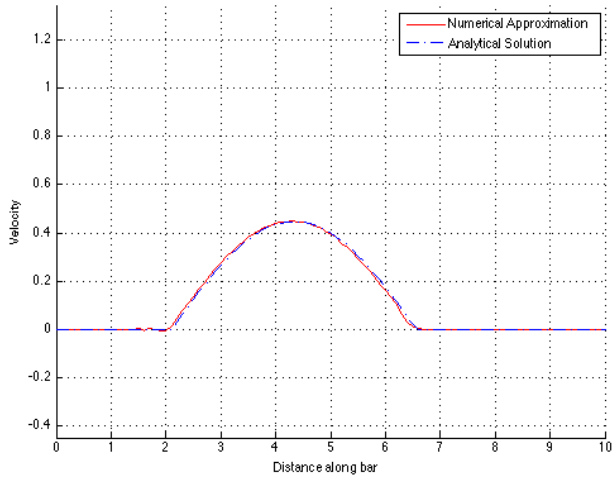

Figure 4.5: Wave Representation using 100 elements

Figure 6 on top, shows good improvements over the numerical approximation using 50 linear elements. There seems to be some oscillations left at the left end of the wave but the approximation has somewhat stabilized close to the analytical solution throughout its initial part of the crest. This is encouraging; by doubling the number of elements we have been able to make increase our accuracy notably.

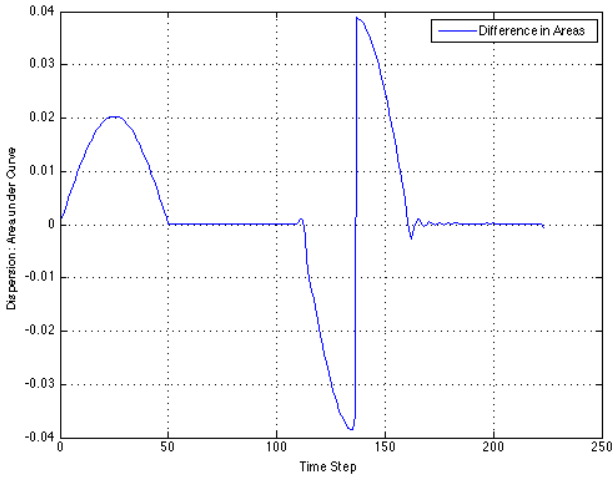

Figure 4.6: Dispersion as measured by areas

Figure 7 indicates the presence of dispersion in the numerical approximation, the highest being of the order of 0.04. In comparison with the 50 linear elements solution, by doubling the number of elements we have decreased the maximum error by half.

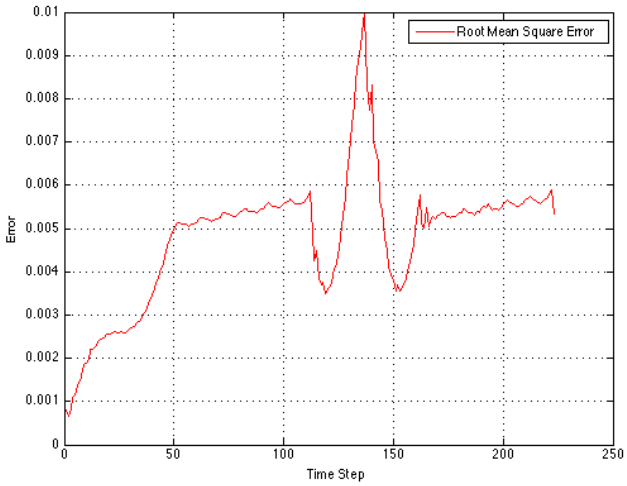

Figure 4.7: MSE using 100 linear elements

Likewise, Figure 8 shows a decrease in the error of the numerical approximation; in fact the MSE has been almost halved. By having 100 elements only we have obtained a decent solution to our wave propagation problem. It is important to mention that the MSE seems to be stabilizing at a point below .006 meaning that the solution will reach certain stability as time progresses.

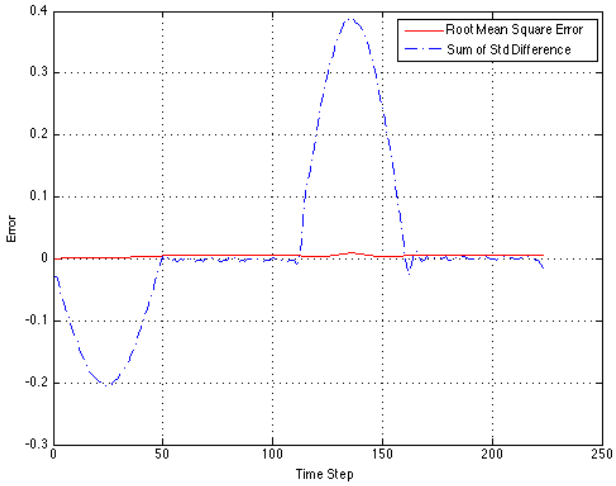

Figure 4.8: Standard Error and MSE using 100 elements

Figure 9 almost depicts an MSE error that is close to zero but contains a bump near the time step at which the wave hits the right end of the rod. This means that the solution is not quite well at representing what is physically happening, that is, at the appearance of the refraction and reflection waves.

4.3.1.3 FEA using 250 linear elements

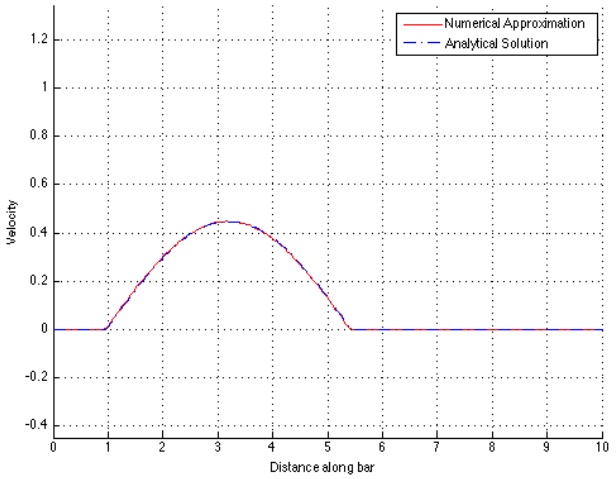

Figure 4.9: Wave Representation using 250 elements

Figure 10 on top, indicates that the approximation using 250 linear element is very accurate. The presence of the existing oscillations near the left end of the wave and the near the crest of the wave is almost null. This is encouraging; by doubling the number of elements we have been able to render almost an exact numerical approximation.

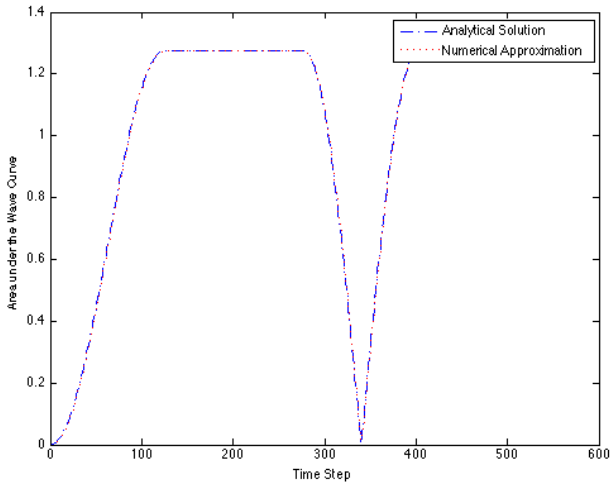

Figure 4.10: Area under curve vs time step

Figure 11 shows the stabilization of the areas under the wave curves. It is in the same order of the analytical wave area.

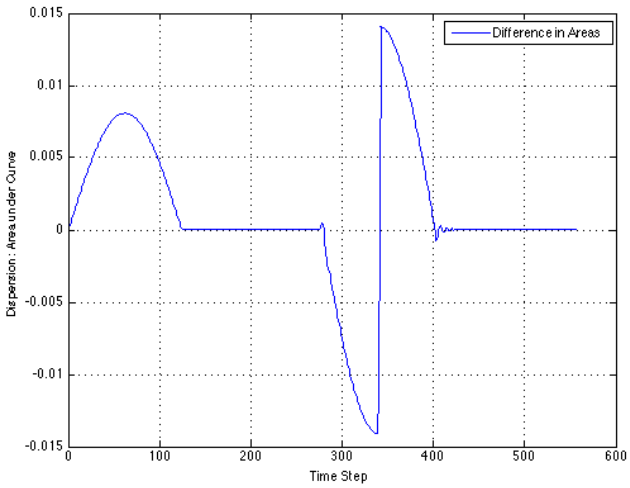

Figure 4.11: Dispersion as measured by difference in areas

Figure 12 once again shows that by doubling the number of elements (in comparison with the previous set up) we have almost made the error decrease by half. The order of the area difference is minimal and an encouraging statement regarding the solution can be done at this point.

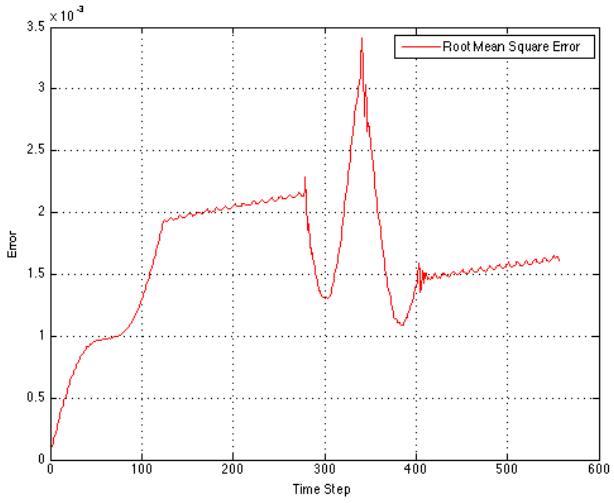

Figure 4.12: MSE using 250 elements

The order of the MSE as lowered in order dramatically, it's in the order of $3x10^{-3}$ in comparison with the original 0.01 from the previous set up.

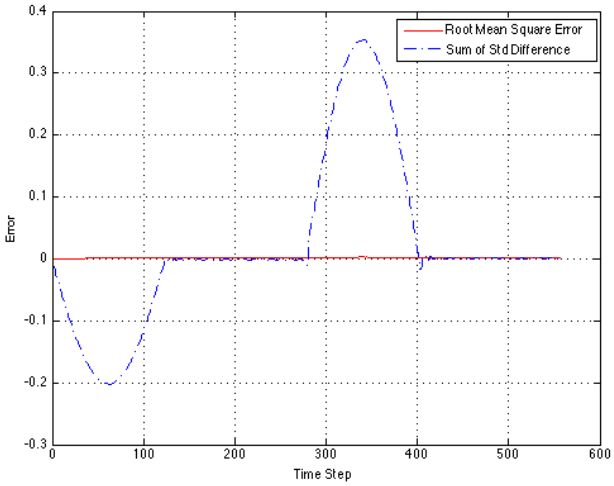

Figure 4.13: Standard error and MSE for 250 elements

Figure 14 confirms what we have been stating regarding this current set up. The MSE is close to zero throughout the test and the sum of the standard difference is zero is now more often encountered. The maximum difference seen is in the order of 0.35 which then stabilizes at zero once more for the rest of the testing period.

4.3.1.4 FEA using 500 linear elements

Since we have been able to establish an ongoing trend as the number of elements composing the representation of the bar. We will let the reader take his or her own conclusions regarding this last set up. It will suffice to mention that the level of accuracy has increased considerately and the error of the approximation has diminished almost to the point of being negligible. The effect of almost all detrimental phenomena due to the numerical basis of the approximation has diminished as the number of elements used to model the wave behavior on the road has increased.

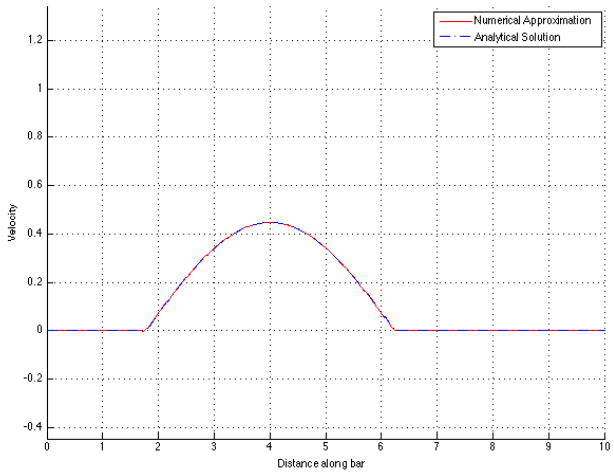

Figure 4.14: Wave representation using 500 elements

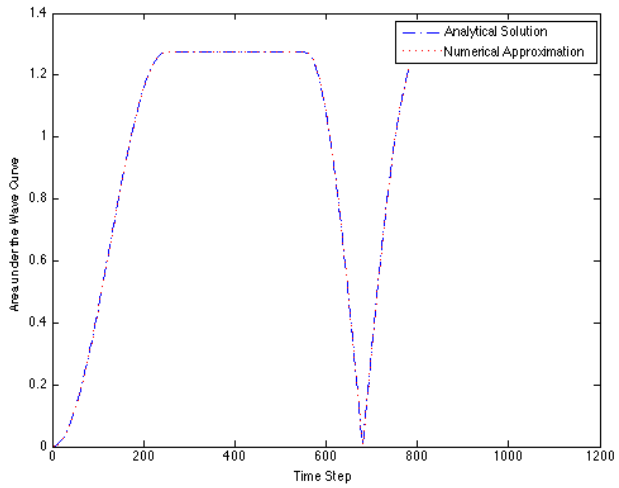

Figure 4.15: Area under curve vs time step

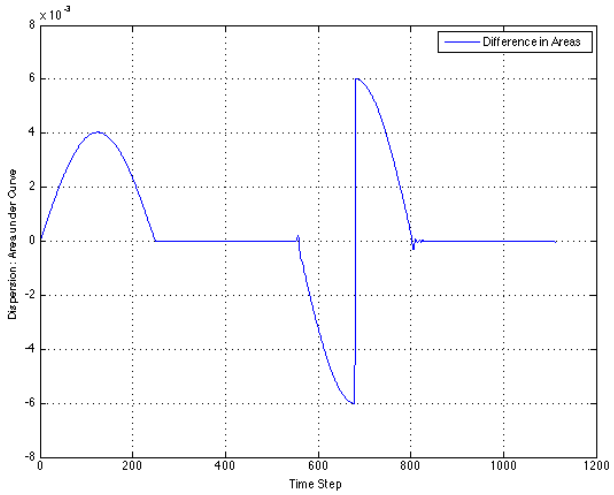

Figure 4.16: Dispersion as measured by difference in area

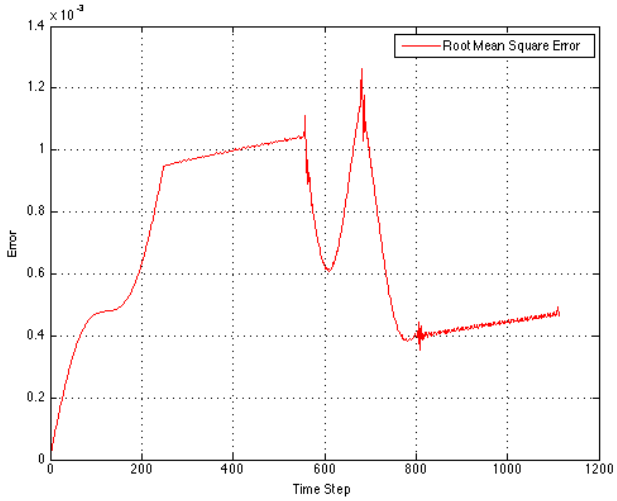

Figure 4.17: MSE using 500 elements

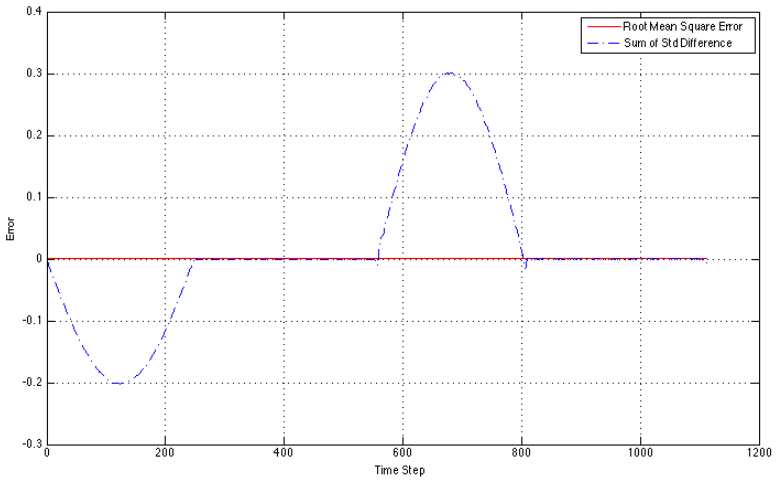

Figure 4.18: Standard error and MSE

4.4.1 The Analysis and the Interpretation

4.4.1.1 SPECTRAL ELEMENTS

Spectral elements have some nice properties that have already been well described during the introductory text for this paper. They have been able to circumvent some of the weaknesses conventional finite elements has had. For wave propagation problems, the spectral elements have been able to achieve a high lever of accuracy at a lower number of elements [nodal points] as we will later be seen during this section.

4.4.1.2 15 Elements with p=3 [61 nodes]

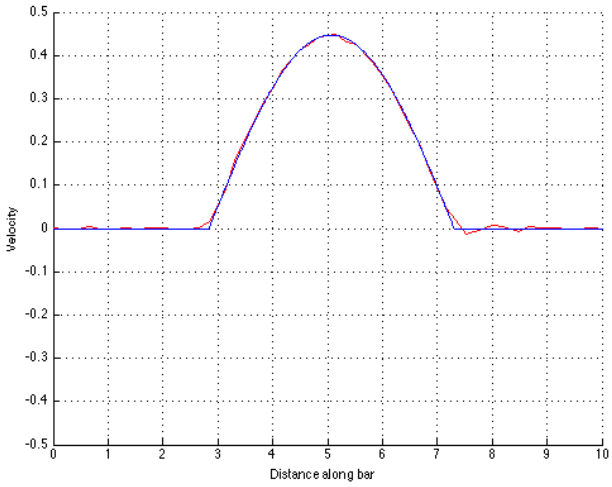

Figure 4.19: Wave representation with NE=15, P=3

Figure 20, on top, shows that for a low number of elements with an interpolation degree P=3, the numerical approximation is not accurate. There exists the presence of oscillation along the bar, especially at the right end of the wave.

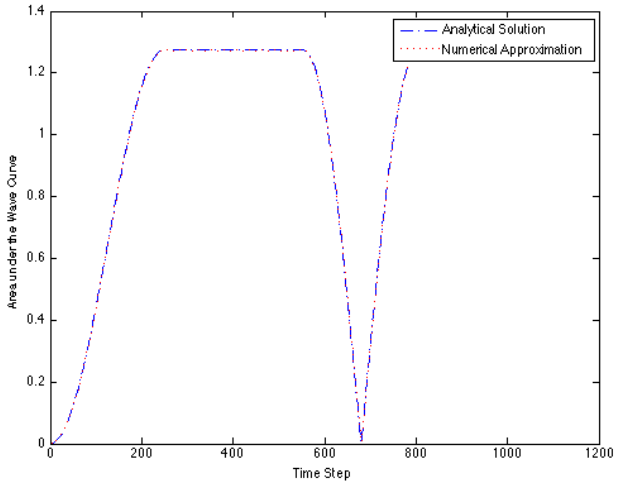

Figure 4.20: SEM: 61 nodes - Area vs Time Step

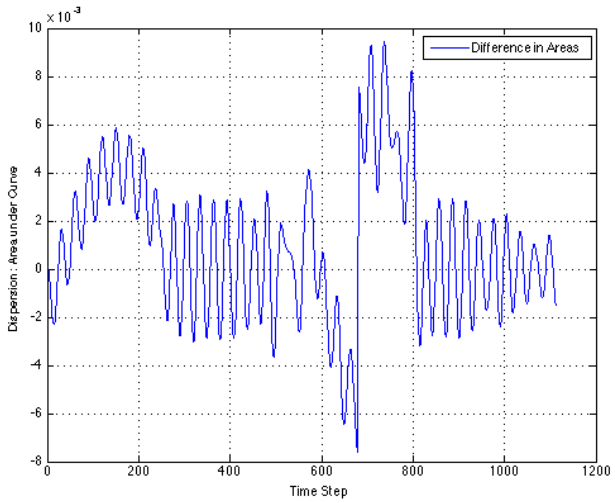

Figure 4.21: Dispersion measured as difference in area

Figure 22 describes that the spectral element solution achieves instantly a higher level of accuracy than that of conventional FEA. Figure 23, shown below, is also quite an encouraging proof that we are heading on the right track since the highest error is in the order of $3.5x10^{-3}$ in comparison with the 0.02 obtained in the initial 50 linear element set up.

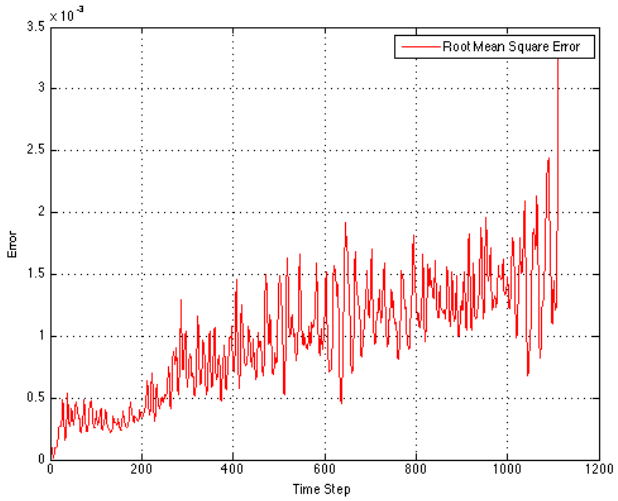

Figure 4.22: MSE

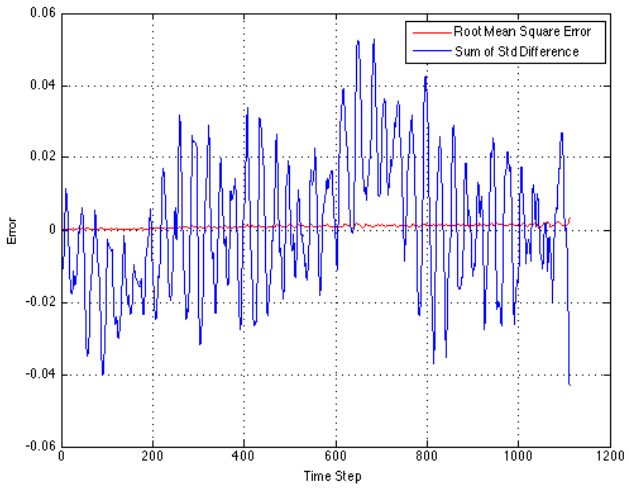

Figure 4.23: Standard error and MSE

4.4.1.3 33 elements with p=3 [100 nodes]

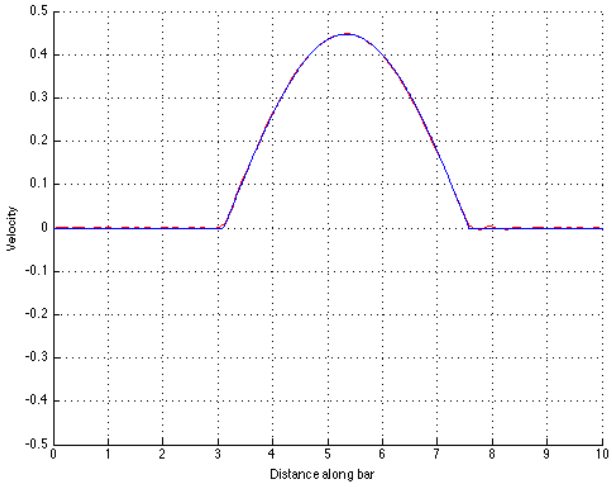

Figure 4.24: Wave representation with NE=33, P=3

Figure 25, depicts close to little or no oscillation at the right end of the propagated wave. The condition is stable and close to the analytical solution along the rest of the bar. The number of element has nearly doubled and it seems that the error depicted in Figure 27 has been reduced by almost 30%. The amount of dispersion for a low order solution using spectral elements is close to null. The numerical

approximation is more stable at keeping track of the dynamic changes occurring during wave propagation.

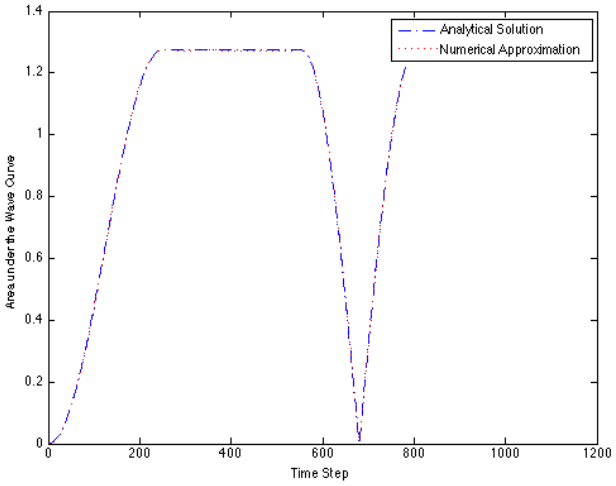

Figure 4.25: Area vs Time step

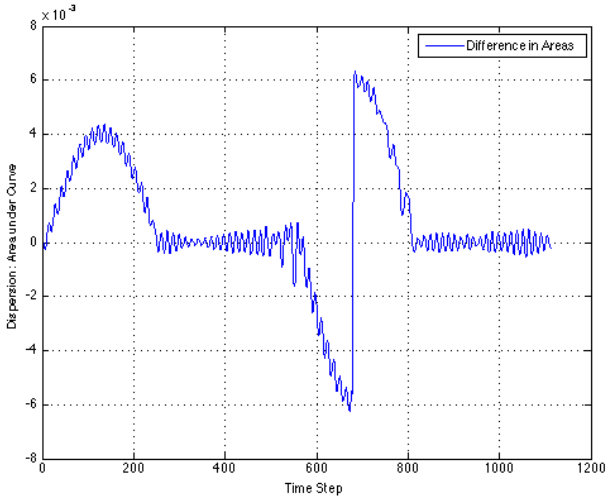

Figure 4.26: Dispersion as measured by difference in area

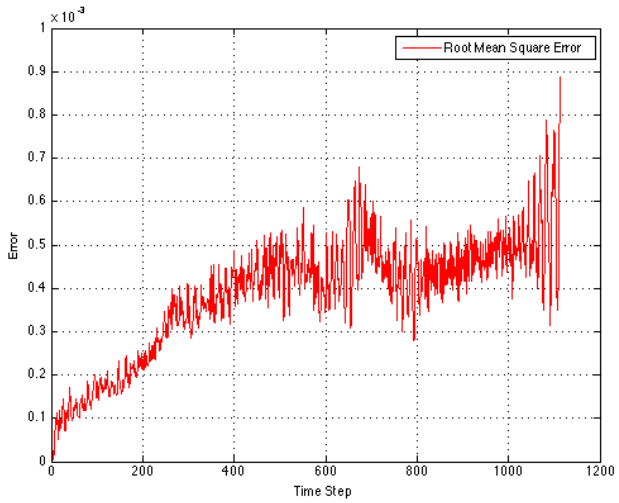

Figure 4.27: MSE

Figure 28, shown above, demonstrates what had been described throughout the past sections of this paper. The SE solution error seems to be stabilizing at a given level at a faster pace than did the FE solution. It does contain some oscillation but the mean value of these oscillations doesn't seem to overcome the level $0.5x10^{-3}$.

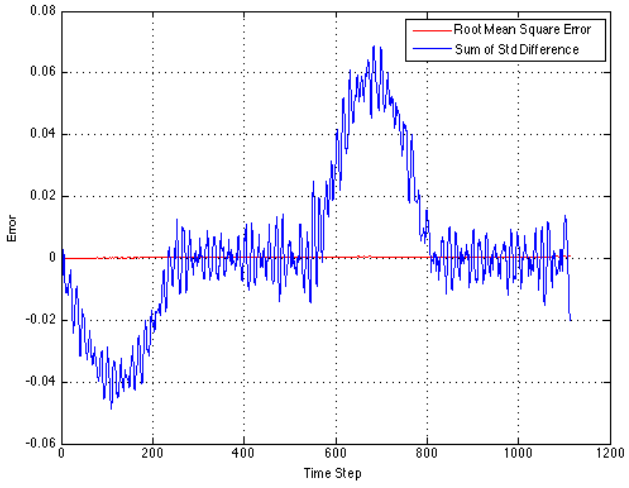

Figure 4.28: Standard Error and MSE

4.4.1.4 100 elements with p=4 [401 nodes]

This and the following cases are left for the reader to interpret as in the case with FEA, the explanation may be self-evident and to repeat it here might be rather repetitive to the reader, as it follows the continuing trend we have seen here as every time the number of elements has been increased with the interpolation degree held constant.

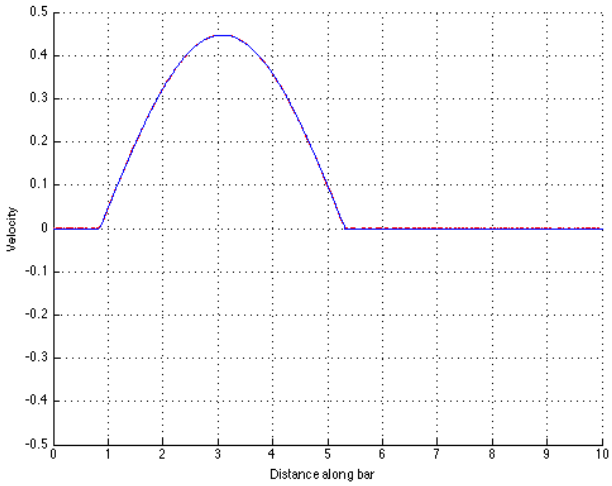

Figure 4.29: Wave Representation using NE=100 ,P=4

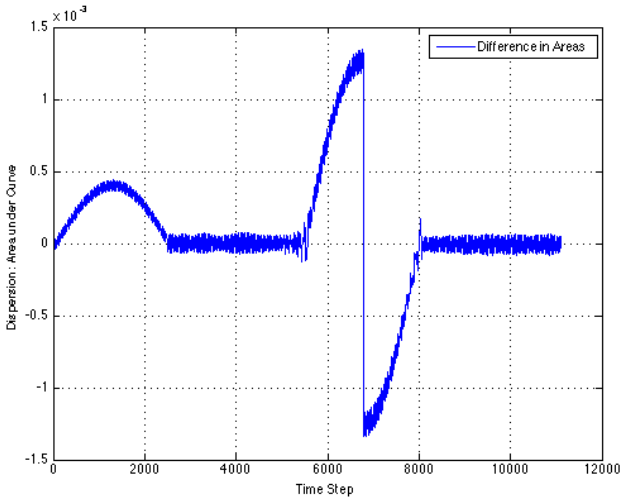

Figure 4.30: Dispersion as measured by difference in area

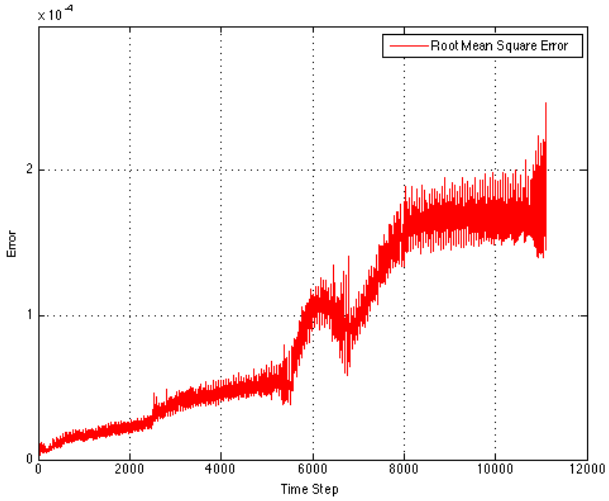

Figure 4.31: MSE

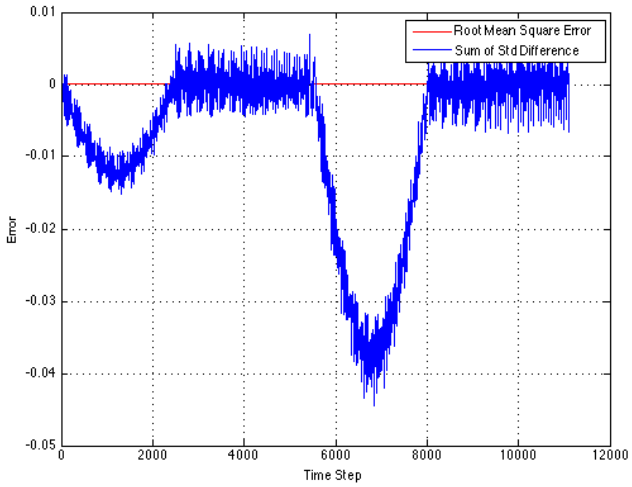

Figure 4.32: Standard Error and MSE

4.4.1.5 125 elements with p=4 [501 nodes]

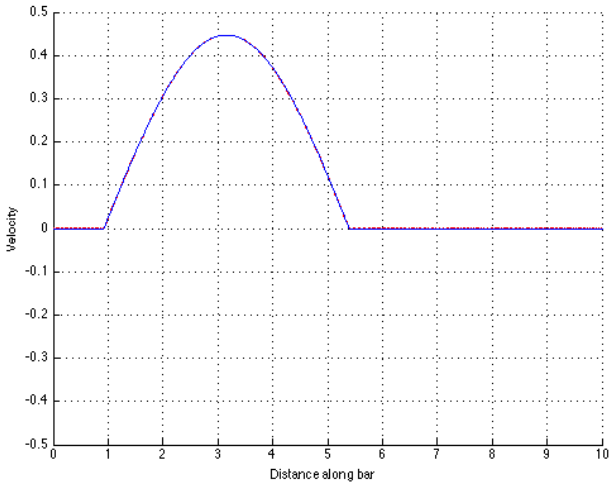

Figure 3.33: Wave Representation with NE=125, P=4

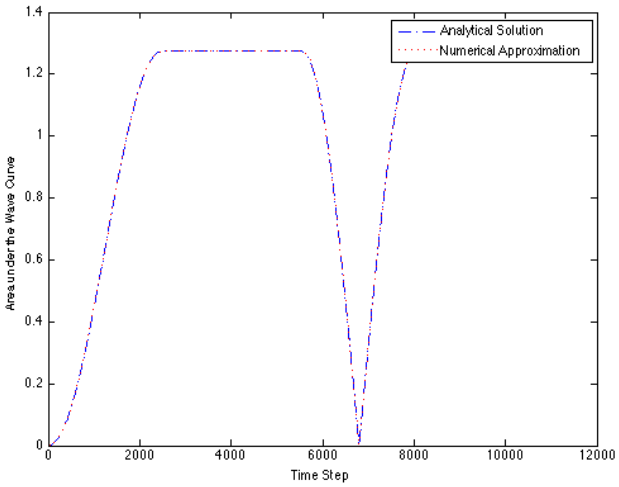

Figure 4.34: Area vs Time step

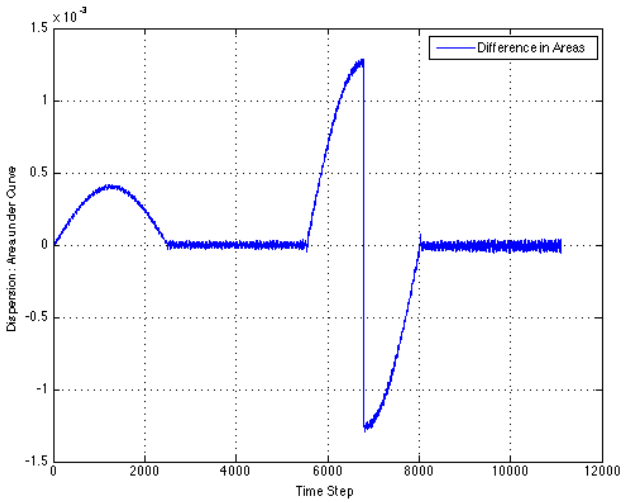

Figure 4.35: Dispersion as a measure of area difference

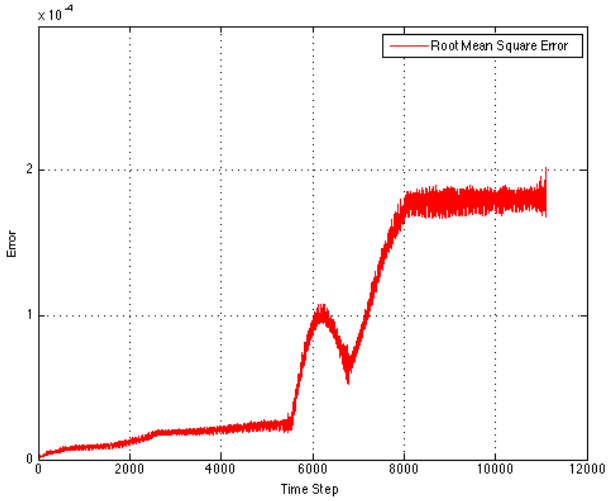

Figure 4.36: MSE

4.5 Conclusions

The Spectral Elements have put in evidence their efficiency at treating wave propagation problems in comparison to conventional FEA. The only problems that they pose are the sometimes the complex formulation of their interpolation functions at higher dimensions. This problem may even overturn whatever qualities they may have at the treatment of these types of problems.

Spectral Elements do have in comparison to conventional FE a lower dispersion degree regardless of the time scheme chosen. In the other hand, they may have a more limiting stability number so that would mean that the time step would have to be lower for the solution to be stable at higher interpolation degrees. This is something to think about since it may overturn the computational advantages that would often be the advantage of the time spent on problem formulation.

Chapter 5: 1-D Dissipation and Dispersion

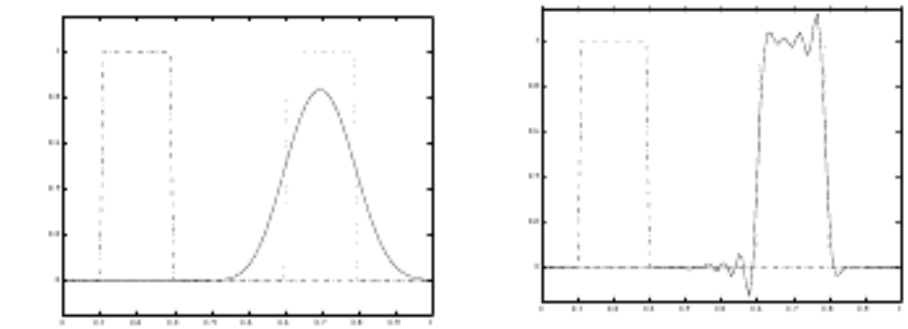

Figure 5.1: Dissipation and Dispersion phenomena

Dissipation and dispersion are two problems that arise from the use of low-order polynomials. While dissipation leads to decay of the waveform and can be depicted as a loss of energy, dispersion leads to its gradual separation into a train of oscillations. Numerous studies have shown that higher order finite elements are found to have much more efficiency towards numerical dispersion than linear and even quadratic elements.

Dispersion errors are caused by the approximation of wave velocities, which result in unwanted oscillations that pollute the results [as depicted in the illustration above (a)]. This is a phenomenon that is especially problematic in large-scale wave propagation models. When the propagating wave traverses long distances, the dispersion error accumulates and the numerical deficiencies grow resulting in a solution with erratic/chaotic behavior. A common side effect of dispersion is the increase in amplitude as the wave disperses. It is important to reduce the dispersion error especially for long-range wave propagation problems. This reduction can be performed straightforwardly by mesh refinement or by reduction of the time step size. It is important to mention

that both of these error-reduction techniques are accompanied by a significant increase in the computational cost.

Although it is usually detrimental to our solutions, introduction of dissipation/dispersion via damping or other numerical artifices is sometimes necessary to counteract natural numerical errors and would lastly result in a numerically stable or even more accurate solution. Because the spectral element method is composed of higher order elements, considerable reduction of the dispersion and dissipation error is achieved. Solutions that are obtained via numerical methods are never exact. Wave propagation constitutes a problem involving an infinite number of unknowns, approximated by a finite number of discretizing or basis functions. For obvious reasons, it is not possible to solve a problem that involves an infinite number of unknowns, as it is not practical to solve a problem constituted by a large number of unknowns. It is desirable, then, to solve a problem with the minimum requirements to achieve a nominal tolerable error. Errors that result from the finite discretization can be divided into two categories: a) Numerical dispersion and dissipation b) numerical reflection errors.

For this section we will present an analysis on the dissipative/dispersive performance based on a one-dimensional long-range wave propagation scenario. The scenario consists of a one-dimensional metal rod with the same mechanical properties as those presented in the previous section, however, a tenfold increase in the rod's length has taken place. This length's increase is in part to have a wavelength that is considerably smaller such that boundary conditions do not affect the wave propagation inside the domain in question, which is in turn a rough representation of wave propagation through an infinitely large medium.

To compare the performance, we will make use of a time series, that is, a plot of the analytical and the approximated wave propagation projection presented at specific time intervals. This will give a general insight into the dissipative/dispersive behavior of the numerical solution.

5.1 FEM

As it has been continuously repeated throughout the extent of this paper and corroborated by the previous section, linear finite elements are not very efficient at handling wave propagation problems. Unless *hp*-refinement techniques are used, our numerical approximation will suffer from the phenomena inherent to low-order approximations. This section will give the reader a clearer picture by providing graphical examples of the dissipative and dispersive errors that are generated during long-range wave propagation problems. As was described in the introductory portion of this chapter, the model consisted in the same mechanical rod that was presented in the previous section but whose length had suffered a tenfold increase in size. The tenfold increase is to simulate an infinite medium. This is because the wavelength is sufficiently small in comparison to the domain's size, which permits a sufficiently free flow for the travelling wave since it's not highly influenced by the boundary conditions, imposed at either ends.

For the FEM, we have tested the scenario using 50, 100, 200, 300, and 500 linear elements. The images that compose the time series were captured at the following times: t= .4025, 0.8050, 1.2075, 1.6100, 2.0124, 2.4149, 2.8174, 3.2199, 3.6224, 5.0249, and 5.427 seconds.

5.1.1 FEM using 50 linear elements

The FEM model consisting of 50 linear elements is shown next; it can be easily perceived that the approximation to the analytical solution is not accurate and as the time progresses the approximation seems to be dissipating, or losing area, and that by the time the test is concluded the wave's peak velocity has been reduced by almost 25%, likewise the wave travelling speed has been reduced in such way that the numerical approximation lags the analytical solution. This huge loss in area was not initially captured for the problem in the previous section, which is an indication of the bad performance of low-order elements for long-range propagation problems. We likewise encounter large oscillations following the projected wave, these indicators of dispersion attenuate with time but its magnitude is and remains considerably large overall.

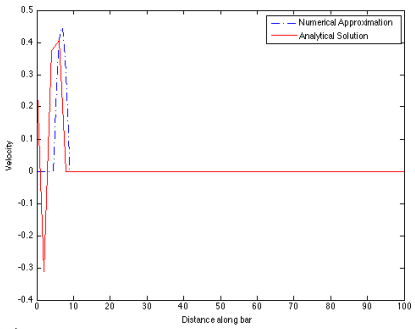
Numerical Approximation
Analytical Solution
Velocity
Distance along bar

(a)

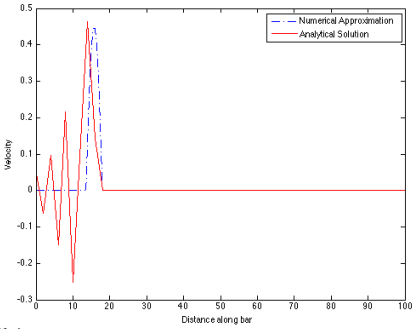
Numerical Approximation
Analytical Solution
Velocity
Distance along bar

(b)

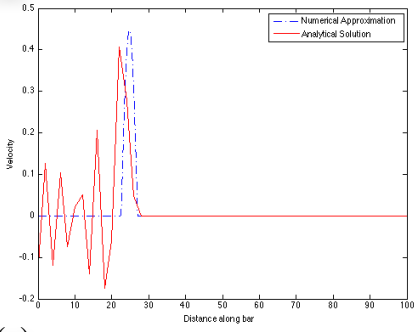
Numerical Approximation
Analytical Solution
Velocity
Distance along bar

(c)

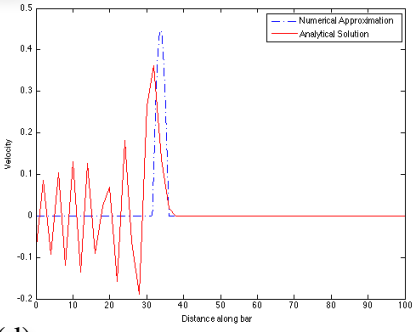
Numerical Approximation
Analytical Solution
Velocity
Distance along bar

(d)

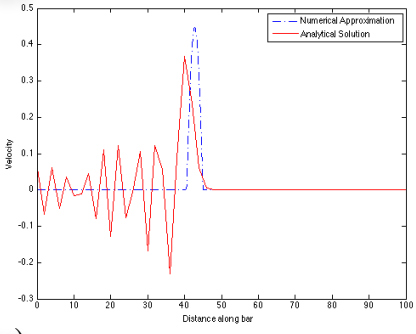
Numerical Approximation
Analytical Solution
Velocity
Distance along bar

(e)

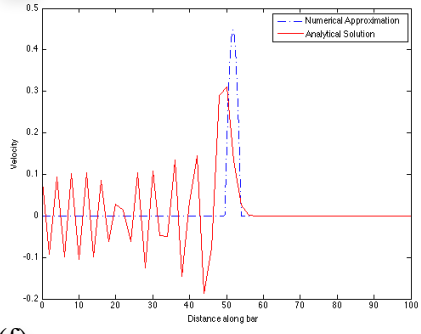
Numerical Approximation
Analytical Solution
Velocity
Distance along bar

(f)

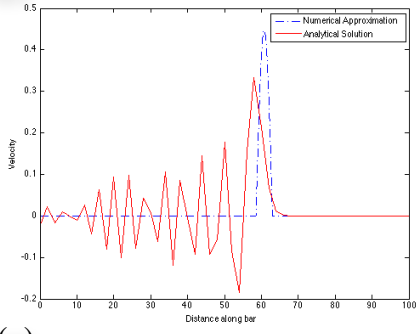
Numerical Approximation
Analytical Solution
Velocity
Distance along bar

(g)

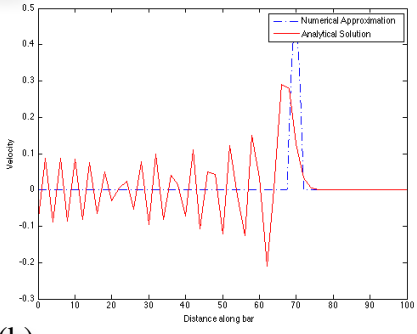
Numerical Approximation
Analytical Solution
Velocity
Distance along bar

(h)

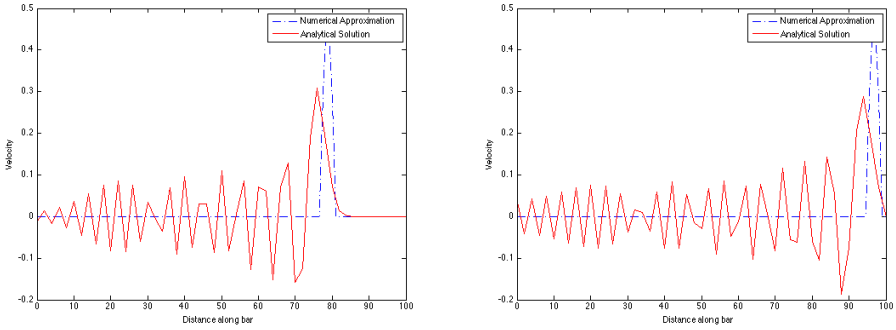

(i) (j)

Figure 5.2: 50 Linear FE Wave Projection (a)t=.4025 (b)t= 0.8050 (c)t=1.2075 (d)t= 1.6100 (e)t= 2.0124 (f) t= 2.4149 (g)t= 2.8174 (h)t= 3.2199 (i)t= 3.6224 (j)t=5.0249

5.1.2 FEM using 100 linear elements

By doubling the number of elements in the domain, we obtain a more accurate solution that is accompanied by a considerable reduction in the level of dispersion. Unfortunately, the approximation seems to initially overestimate the analytical solution by almost 20% but as dispersive behavior seems to take place, the solution stabilizes, more or less, within an acceptable range; however, the approximation seems to lag behind the analytical solution again although now at a lower level.

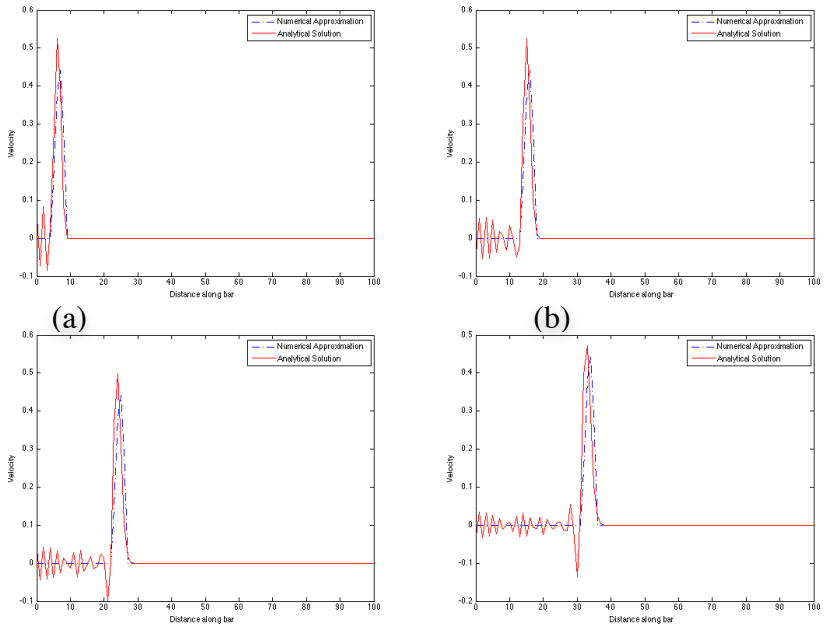

(a) (b)

(c) (d)

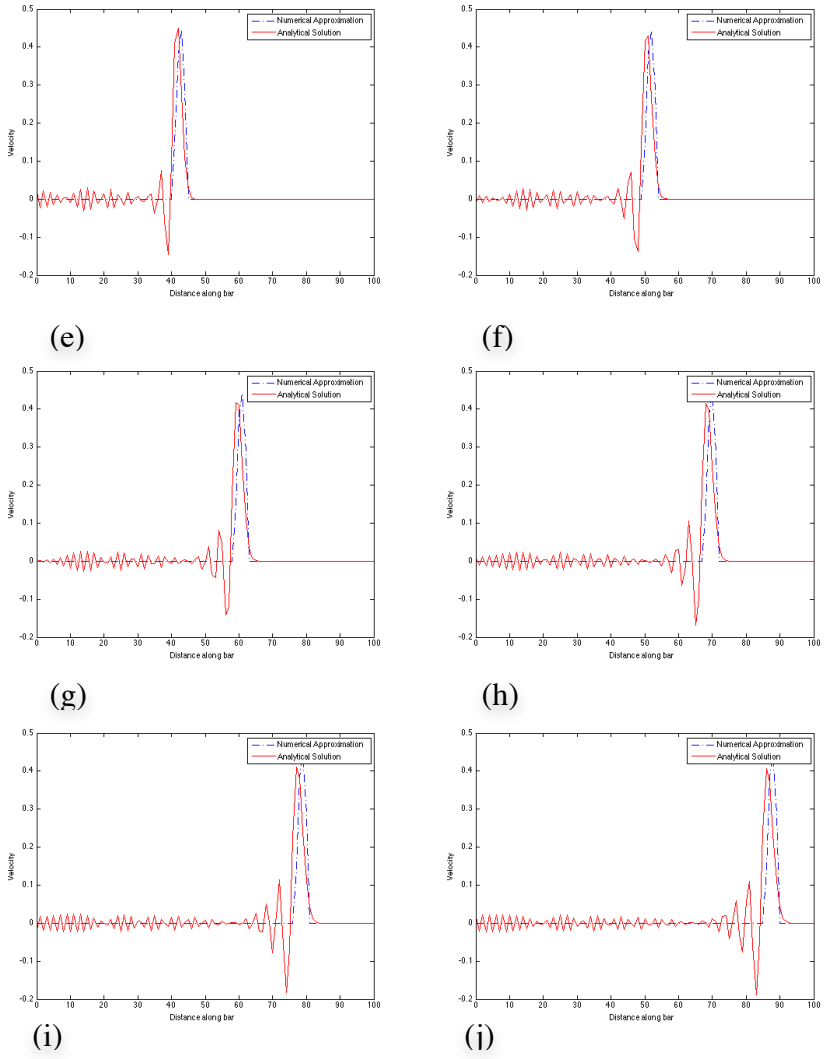

Figure 5.3: 100 Linear FE Wave Projection (a) t=.4025 (b)t= 0.8050 (c)t=1.2075 (d)t= 1.6100 (e)t= 2.0124 (f) t= 2.4149 (g)t= 2.8174 (h)t= 3.2199 (i)t= 3.6224 (j)t=5.0249

5.1.3 FEM using 200 linear elements

It is only by quadrupling the domain that we start getting really nice solutions. The approximation using 200 linear elements has a good fit to the analytical solution, with a slight overestimation, but it still presents some small level of dispersion lagging the projected wave for a short time period. Like in the previous scenarios, the solution lags behind the analytical solution in the last

stages of the propagation. The most important characteristic find in this scenario is that the solution's area under the curve is very stable throughout the test and suffers minimal change.

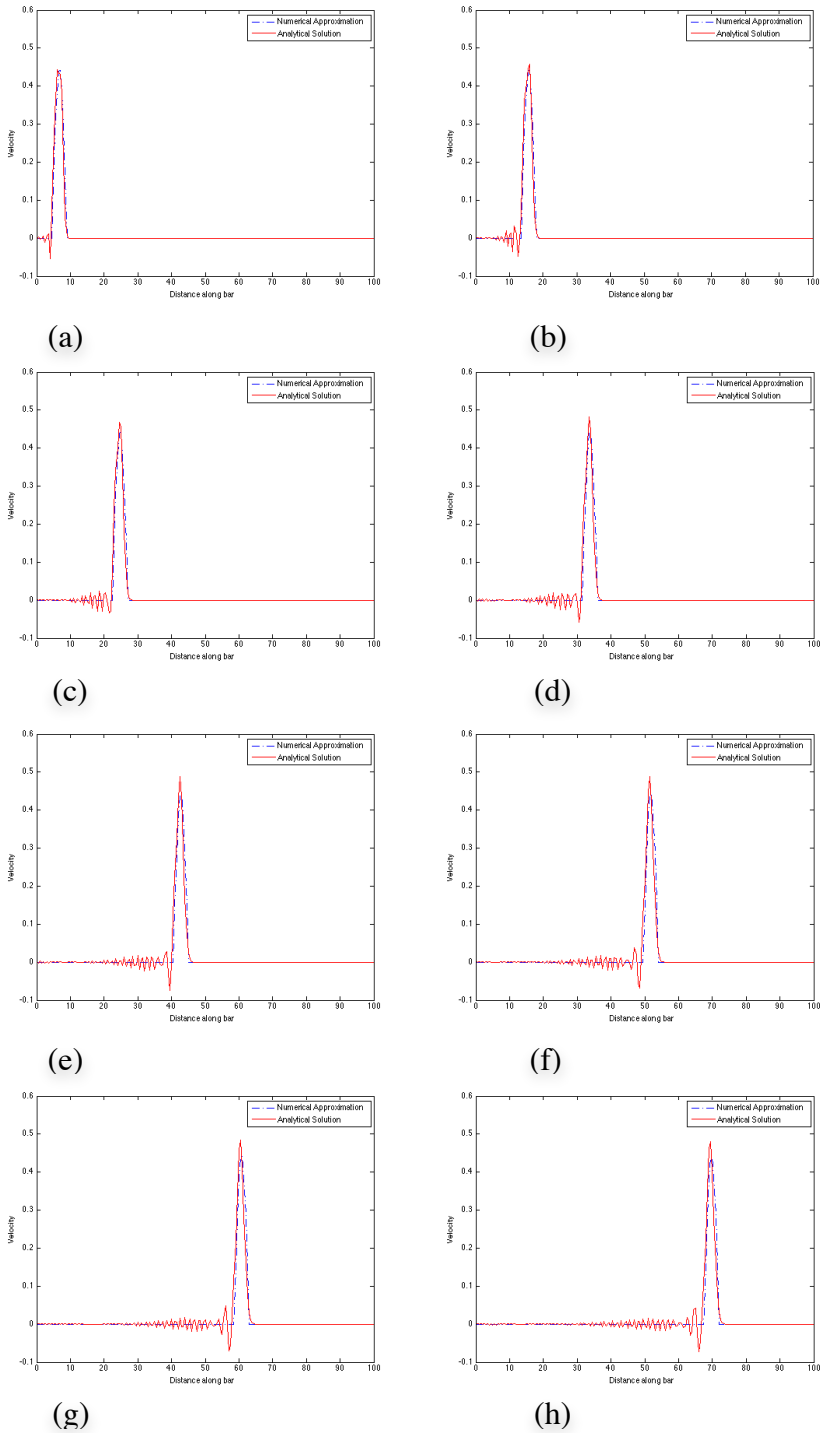

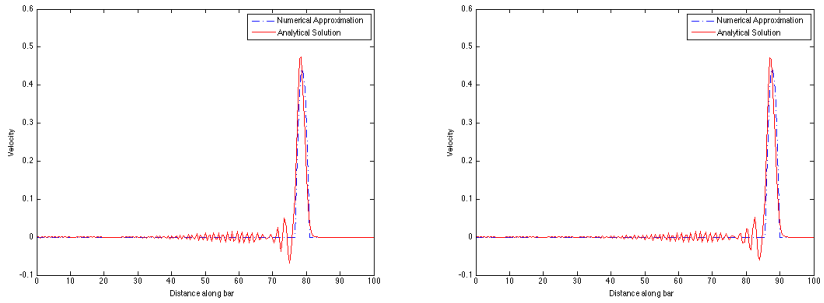

(i) (j)

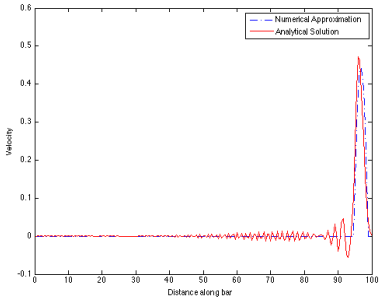

(k)

Figure 5.4: 200 Linear FE Wave Projection (a)t=.4025 (b)t= 0.8050 (c)t=1.2075 (d)t= 1.6100 (e)t=2.0124 (f) t= 2.4149 (g)t= 2.8174 (h)t= 3.2199 (i)t= 3.6224 (j)t=5.0249 (k)t=5.427

5.1.4 FEM using 300 linear elements

Not many new things can be stated regarding the performance of the FE model using 300 linear elements, except that the solution is able to accurately represent the wave propagation and little to no dissipation is present. The solution behaves incredibly well with time, although there is still the problem with the lagging dispersion, but it seems to attenuate enough to become negligible as the test progresses and most importantly we are accurately describing the wave itself.

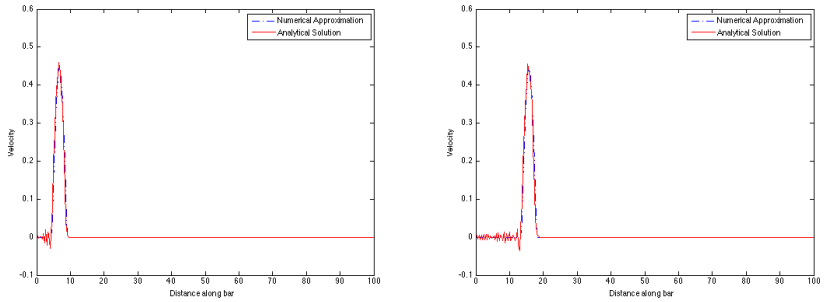

(a) (b)

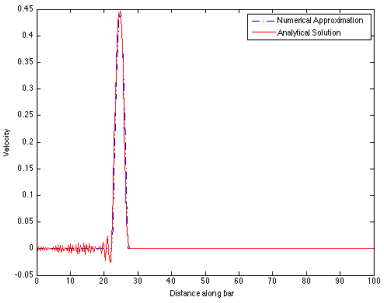
Numerical Approximation
Analytical Solution
Velocity
Distance along bar

(c)

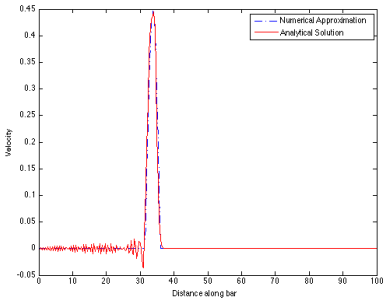
Numerical Approximation
Analytical Solution
Velocity
Distance along bar

(d)

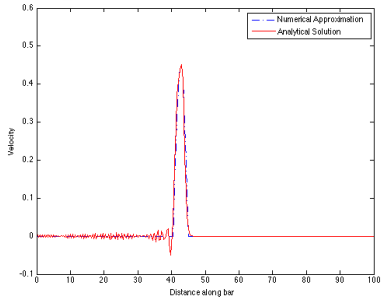
Numerical Approximation
Analytical Solution
Velocity
Distance along bar

(e)

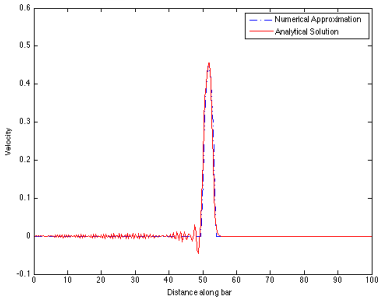
Numerical Approximation
Analytical Solution
Velocity
Distance along bar

(f)

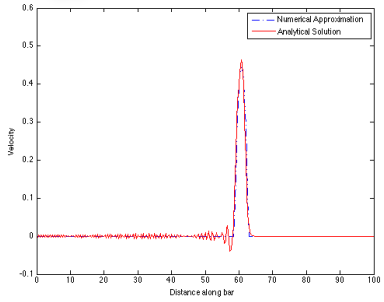
Numerical Approximation
Analytical Solution
Velocity
Distance along bar

(g)

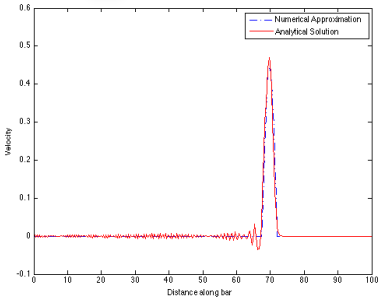
Numerical Approximation
Analytical Solution
Velocity
Distance along bar

(h)

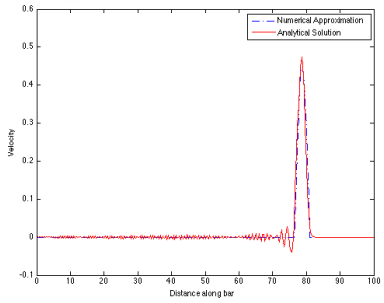
Numerical Approximation
Analytical Solution
Velocity
Distance along bar

(i)

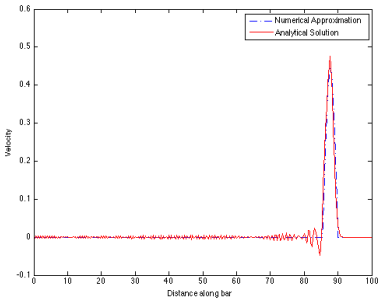
Numerical Approximation
Analytical Solution
Velocity
Distance along bar

(j)

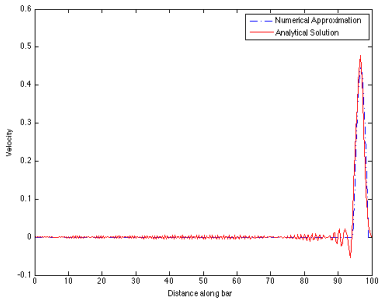

(k)

Figure 5.5: 300 Linear FE Wave Projection (a)t=.4025 (b)t= 0.8050 (c)t=1.2075 (d)t= 1.6100 (e)t= 2.0124 (f) t= 2.4149 (g)t= 2.8174 (h)t= 3.2199 (i)t= 3.6224 (j)t=5.0249 (k)t=5.427

5.1.5 FEA using 500 linear elements

Higher discretization of the domain, a tenfold increase of what we had initially started with, results in a very accurate solution, however the presence of dispersion is not effectively reduced by further domain discretization, this is something to be tackled by an increase in the element order and whose result we will analyze in the next section that deals with the spectral element method performance.

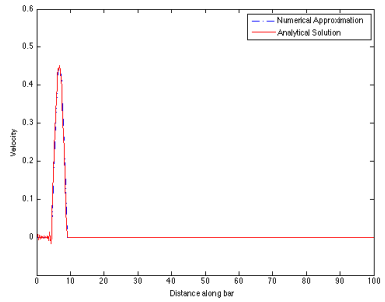

(a)

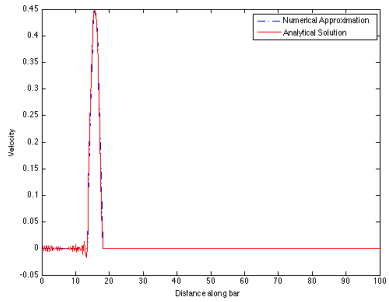

(b)

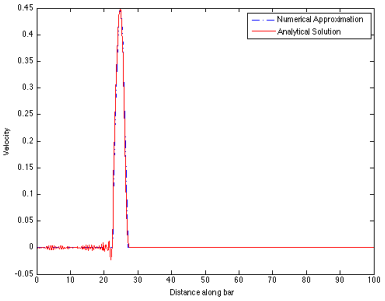

(c)

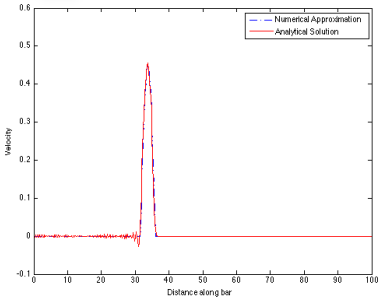

(d)

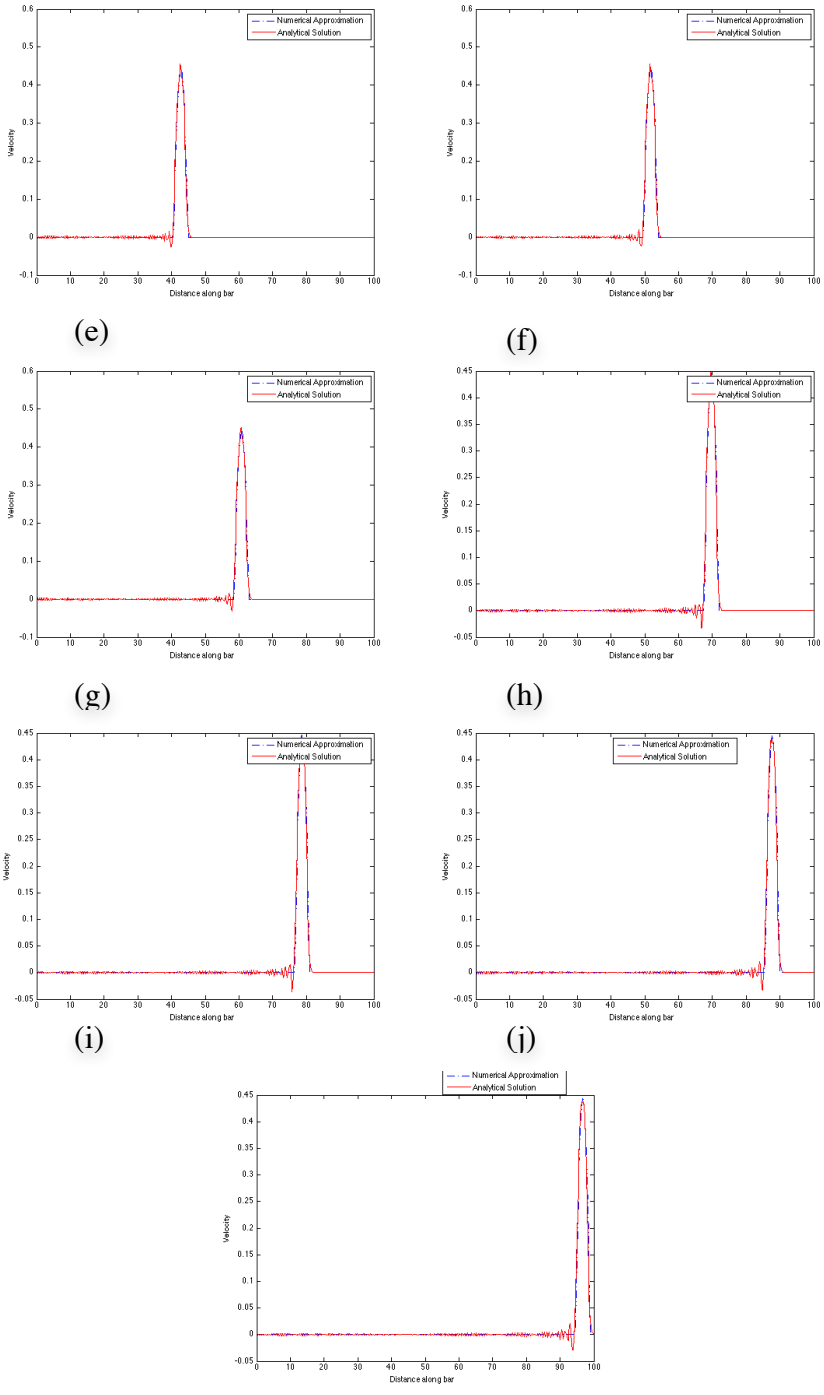

Figure 5.6: 500 Linear FE Wave Projection (a)t=.4025 (b)t= 0.8050 (c)t=1.2075 (d)t= 1.6100 (e)t=2.0124 (f) t= 2.4149 (g)t= 2.8174 (h)t= 3.2199 (i)t= 3.6224 (j)t=5.0249 (k)t=5.427

5.2 SEM

As we mentioned during the introductory part of this chapter, a response to the presence of dispersion and dissipation has been the use of spectral elements. The spectral elements are high-order elements that are able to detect the quick changes in the behavior of the solution, which in turn results in a higher accuracy level. The model tested is analogous to that previously described during the FEM section of this chapter, however due to the high-order nature of the spectral elements and that we are trying to compare their performance based on a nodal number basis, the scenarios simulated considered a high number of different order bases with different number of elements. The scenarios tested were the following:

1. 20 SE model using 3^{rd} order polynomial basis [61 Nodes].
2. 40 SE model using 3^{rd} order polynomial basis [121 Nodes].
3. 80 SE model using 3^{rd} order polynomial basis [241 Nodes].
4. 120 SE model using 3^{rd} order polynomial basis [361 Nodes].
5. 20 SE model using 4^{th} order polynomial basis [81 Nodes].
6. 40 SE model using 4^{th}order polynomial basis [161 Nodes].
7. 80 SE model using 4^{th} order polynomial basis [321 Nodes].
8. 120 SE model using 4^{th} order polynomial basis [481 Nodes].
9. 20 SE model using 6^{th} order polynomial basis [121 Nodes].
10. 40 SE model using 6^{th}order polynomial basis [241 Nodes].
11. 80 SE model using 6^{th} order polynomial basis [361 Nodes].

5.2.1 SEM using 20 elements based on 3rd order polynomials

The performance of the SE solution using 20 elements based on 3rd order polynomials can be closely compared to the FE solution using 50 linear elements [61vs50 nodes.] The behavior is closely related. The SE solution has some dissipation throughout the test; however, the reduction of its peak value is in the order of 10-15% at its worst. The dissipation, although present, seems to be occurring at a lower degree. Unfortunately, dispersion seems to be occurring before and after the propagating wave but the values seem to stabilize with time and this introduced noise seems to have a lower frequency than the noise introduced by the FE solution.

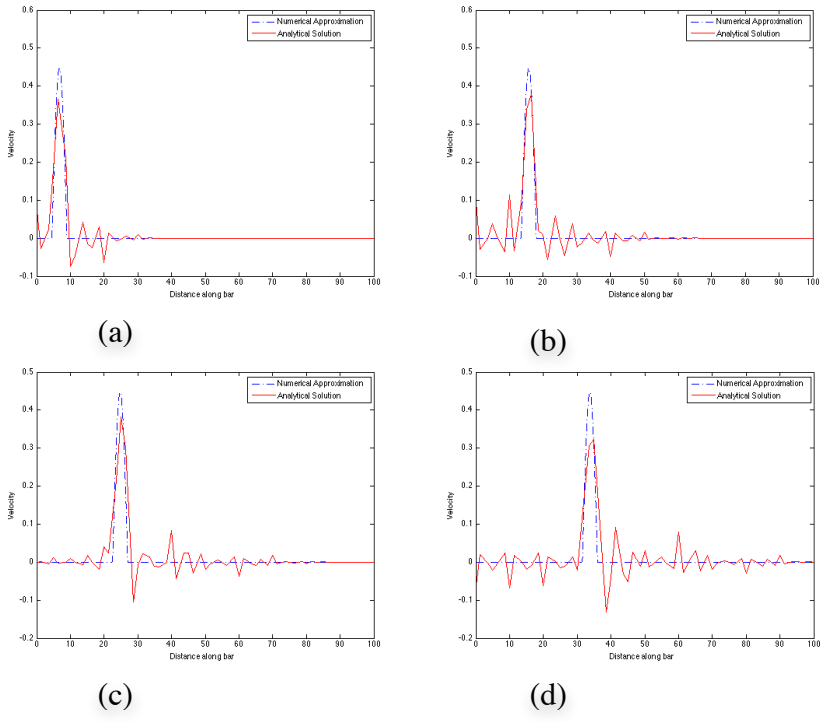

(a) (b)

(c) (d)

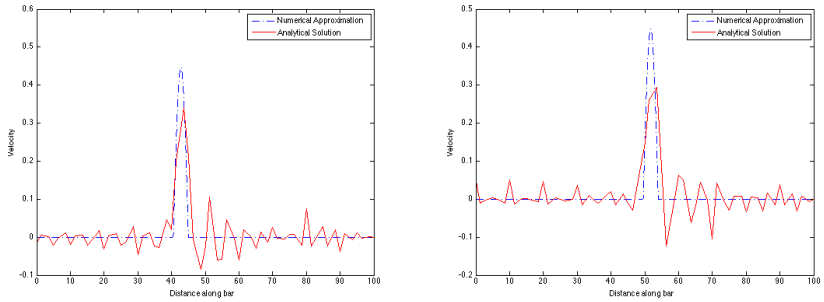

(e)

(f)

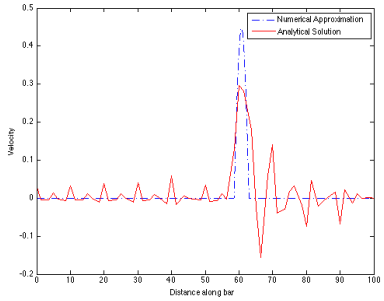

(g)

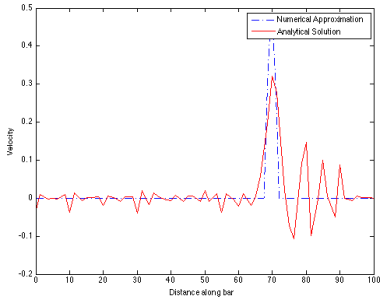

(h)

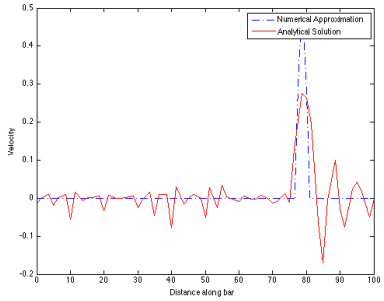

(i)

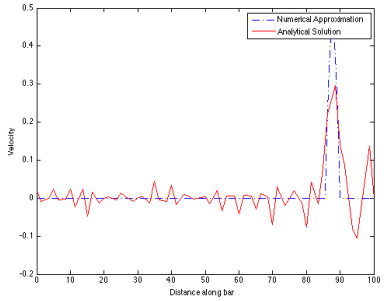

(j)

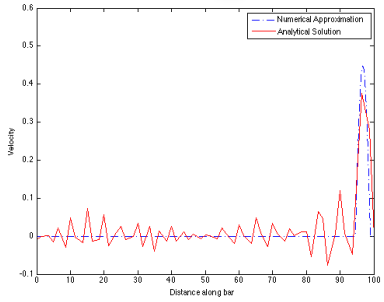

(k)

Figure 5.6: 20 elements with P=3 SE Wave Projection (a)t=.4025 (b)t= 0.8050 (c)t=1.2075 (d)t=1.6100 (e)t= 2.0124 (f) t= 2.4149 (g)t= 2.8174 (h)t= 3.2199 (i)t=3.6224 (j)t=5.0249 (k)t=5.427

5.2.2 SEM using 40 elements based on 3rd order polynomials [121 Nodes]

By doubling the number of elements in the domain, we obtain a very accurate solution. Unfortunately, dispersion is still present but at a rather low level but this is counter-balanced by the little dissipation now present in the system. The solution behaves considerably well overall, the largest difference between the analytical solution and our approximation occurs at the last image captured (t= 5.8s) and it can be mostly attributed to the fact that the solution is reaching the right end of the bar and is getting ready to reflect.

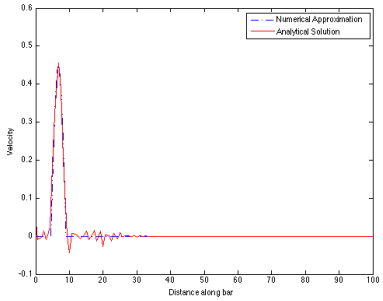

(a)

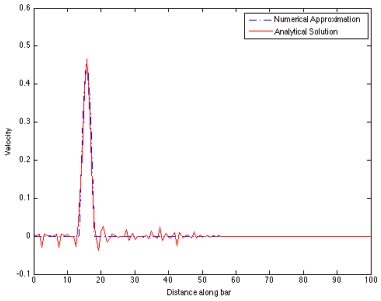

(b)

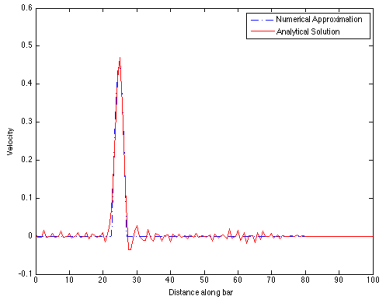

(c)

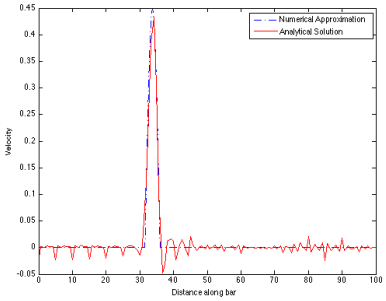

(d)

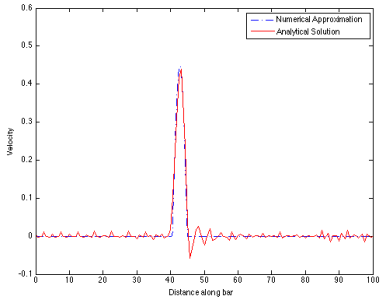

(e)

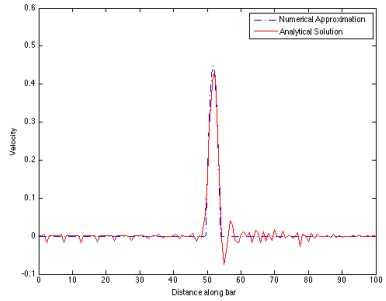

(f)

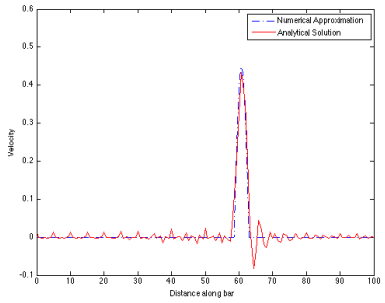

(g)

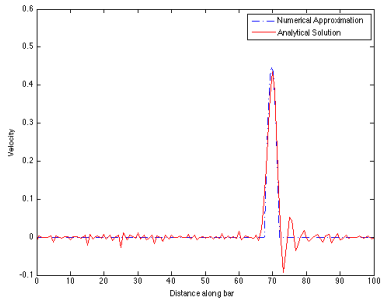

(h)

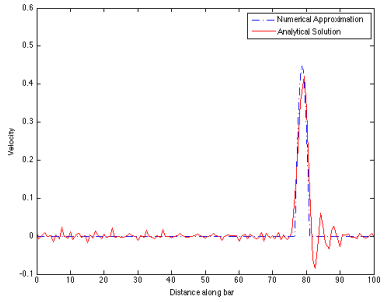

(i)

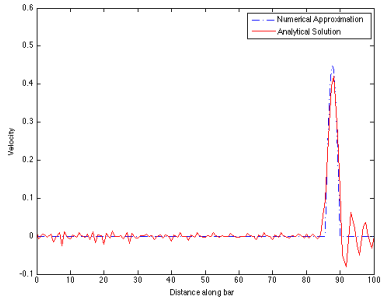

(j)

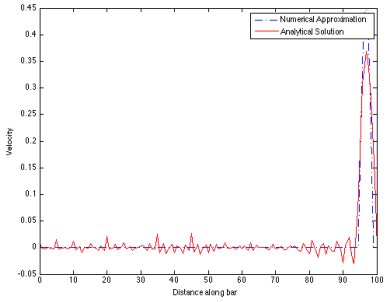

(k)

Figure 5.7: 40 elements with P=3 SE Wave Projection (a)t=.4025 (b)t= 0.8050 (c)t=1.2075 (d)t=1.6100 (e)t= 2.0124 (f) t= 2.4149 (g)t= 2.8174 (h)t= 3.2199 (i)t=3.6224 (j)t=5.0249 (k)t=5.427

5.2.3 SEM using 80 elements based on 3rd order polynomials [241 Nodes]

Quadrupling the initial number of elements almost results in eliminating all traces of dispersion (although some rest throughout the test near the right end of the projected wave), likewise, dissipation levels are almost negligible. The solution obtained accurately models the analytical solution and we have done so by mere mesh refinement.

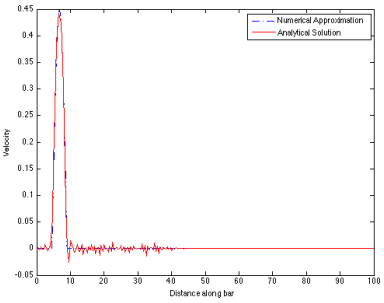
Numerical Approximation
Analytical Solution
Velocity
Distance along bar

(a)

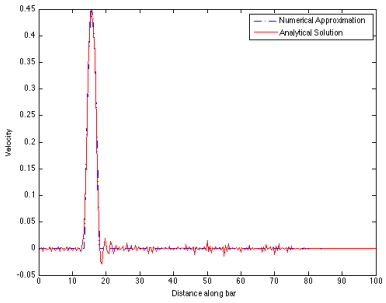
Numerical Approximation
Analytical Solution
Velocity
Distance along bar

(b)

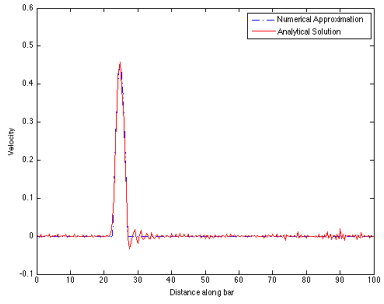
Numerical Approximation
Analytical Solution
Velocity
Distance along bar

(c)

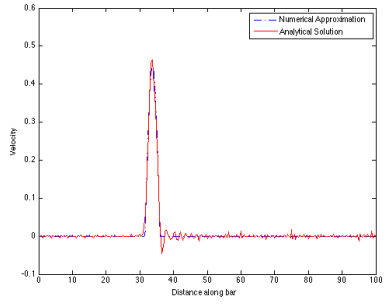
Numerical Approximation
Analytical Solution
Velocity
Distance along bar

(d)

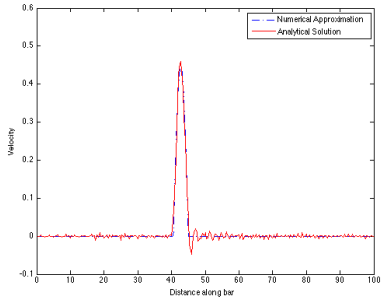
Numerical Approximation
Analytical Solution
Velocity
Distance along bar

(e)

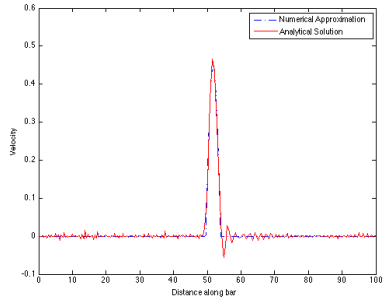
Numerical Approximation
Analytical Solution
Velocity
Distance along bar

(f)

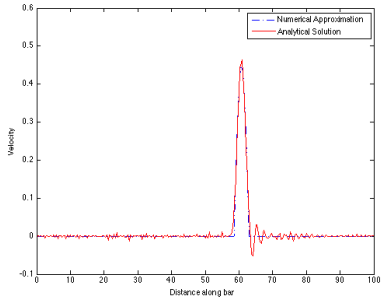
Numerical Approximation
Analytical Solution
Velocity
Distance along bar

(g)

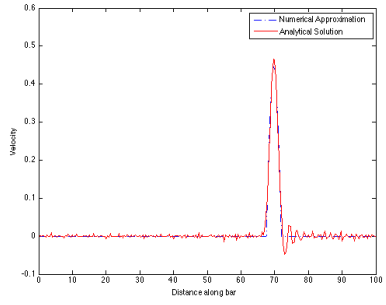
Numerical Approximation
Analytical Solution
Velocity
Distance along bar

(h)

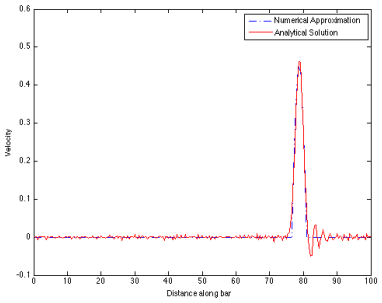

(i)

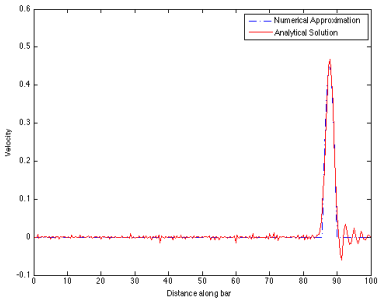

(j)

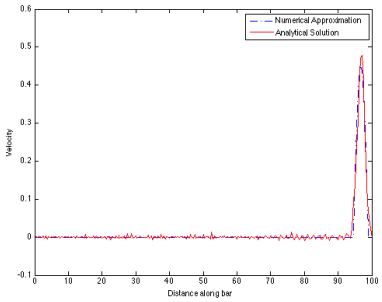

(k)

Figure 5.8: 80 elements with P=3 SE Wave Projection (a)t=.4025 (b)t= 0.8050 (c)t=1.2075 (d)t=1.6100 (e)t= 2.0124 (f) t= 2.4149 (g)t= 2.8174 (h)t= 3.2199 (i)t=3.6224 (j)t=5.0249 (k)t=5.427

5.2.4 SEM using 120 elements based on 3rd order polynomials

This last refining step is performed to see if it is possible to considerably reduce the level of dispersion present in the previous scenario before recurring to increasing our interpolation order. The solution almost removes all traces of dispersion located to the left of the projected wave; however, the traces previously found in the right side are still present, although at a lower level. This means that to completely remove the dispersion present in our system we will have to recur to higher-order interpolation functions and we have done so and the results are presented next.

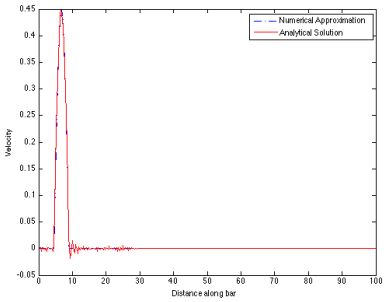
Numerical Approximation
Analytical Solution
Velocity
Distance along bar

(a)

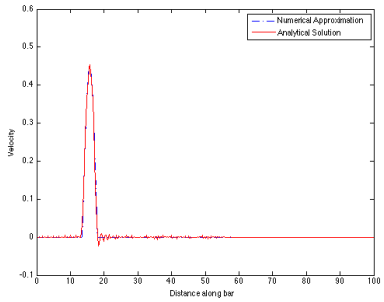
Numerical Approximation
Analytical Solution
Velocity
Distance along bar

(b)

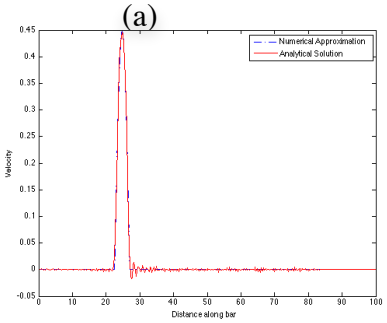
Numerical Approximation
Analytical Solution
Velocity
Distance along bar

(c)

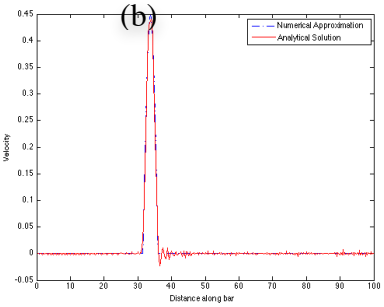
Numerical Approximation
Analytical Solution
Velocity
Distance along bar

(d)

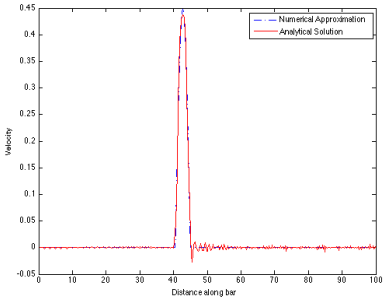
Numerical Approximation
Analytical Solution
Velocity
Distance along bar

(e)

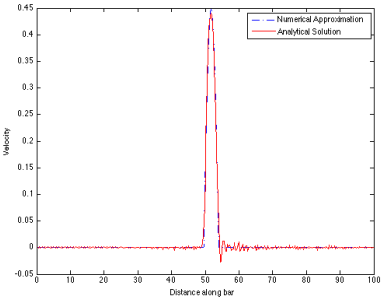
Numerical Approximation
Analytical Solution
Velocity
Distance along bar

(f)

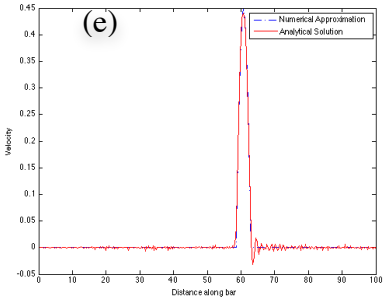
Numerical Approximation
Analytical Solution
Velocity
Distance along bar

(g)

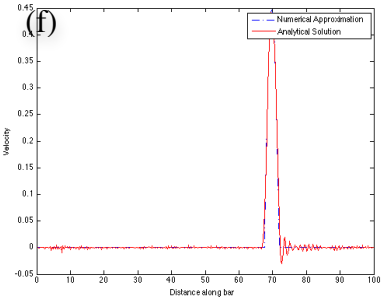
Numerical Approximation
Analytical Solution
Velocity
Distance along bar

(h)

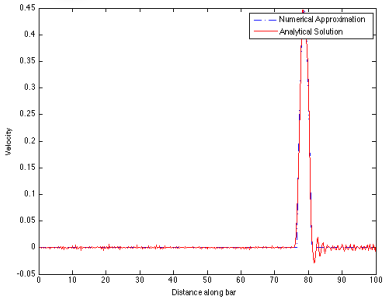
Numerical Approximation
Analytical Solution
Velocity
Distance along bar

(i)

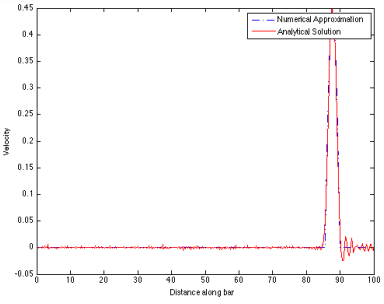
Numerical Approximation
Analytical Solution
Velocity
Distance along bar

(j)

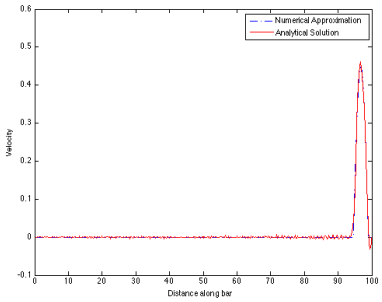

(k)

Figure 5.9: 120 elements with P=3 SE Wave Projection (a)t=.4025 (b)t= 0.8050 (c)t=1.2075 (d)t=1.6100 (e)t= 2.0124 (f) t= 2.4149 (g)t= 2.8174 (h)t= 3.2199 (i)t=3.6224 (j)t=5.0249 (k)t=5.427

5.2.5 SEM using 20 elements based on 4th order polynomials [81 nodes]

The increase in the polynomial order at a low number of elements is analogous to all of our first tries. Both dispersion and dissipation are present in the system perhaps at a lower level but the solution is not very accurate. It is necessary then to refine our mesh and compare the level at which the solution behavior is optimum for the extra work performed.

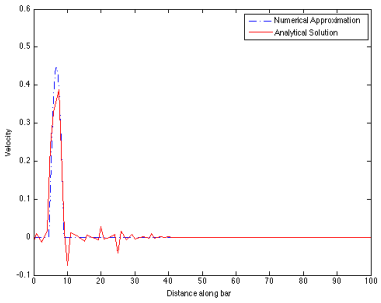

(a)

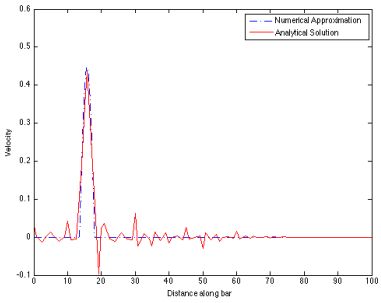

(b)

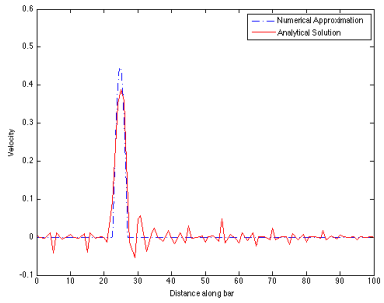
Numerical Approximation
Analytical Solution
Velocity
Distance along bar

(c)

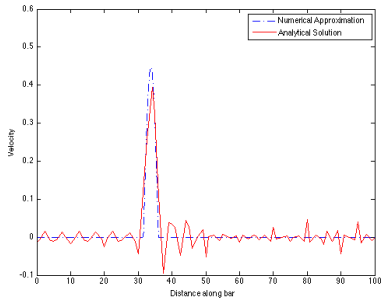
Numerical Approximation
Analytical Solution
Velocity
Distance along bar

(d)

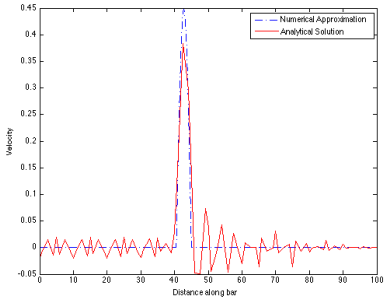
Numerical Approximation
Analytical Solution
Velocity
Distance along bar

(e)

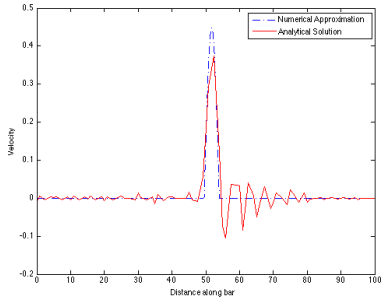
Numerical Approximation
Analytical Solution
Velocity
Distance along bar

(f)

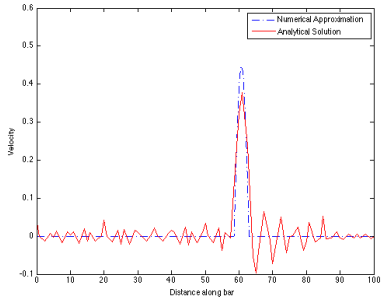
Numerical Approximation
Analytical Solution
Velocity
Distance along bar

(g)

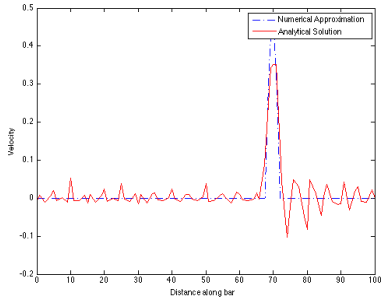
Numerical Approximation
Analytical Solution
Velocity
Distance along bar

(h)

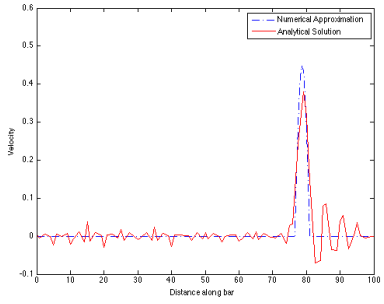
Numerical Approximation
Analytical Solution
Velocity
Distance along bar

(i)

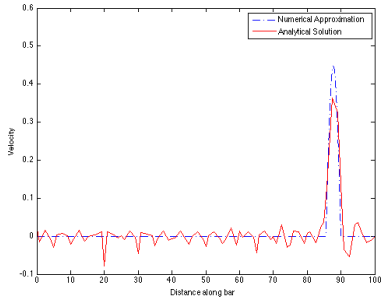
Numerical Approximation
Analytical Solution
Velocity
Distance along bar

(j)

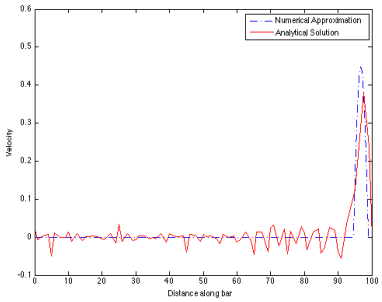

(k)

Figure 5.10: 20 elements with P=4 SE Wave Projection (a)t=.4025 (b)t= 0.8050 (c)t=1.2075 (d)t= 1.6100 (e)t= 2.0124 (f) t= 2.4149 (g)t= 2.8174 (h)t= 3.2199 (i)t=3.6224 (j)t=5.0249 (k)t=5.427

5.2.6 SEM using 40 elements based on 4th order polynomials [161 nodes]

Doubling the element sizes quickly renders a solution whose performance is closer to the level shown by the 3rd degree 80 element SE solution previously presented. The solution is very accurate overall and presents a lower degree of dispersion to the right of the projected wave and little to no dissipation is present.

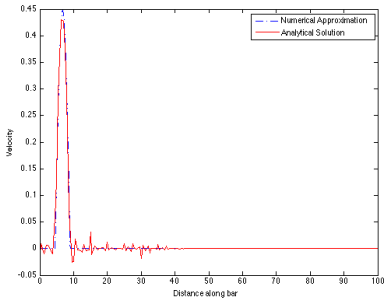

(a)

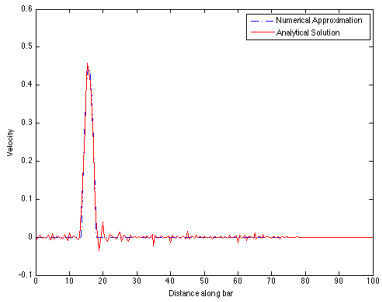

(b)

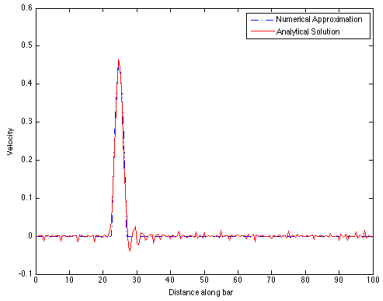

(c)

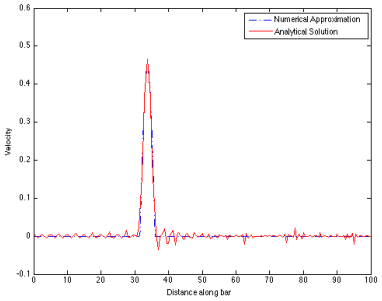

(d)

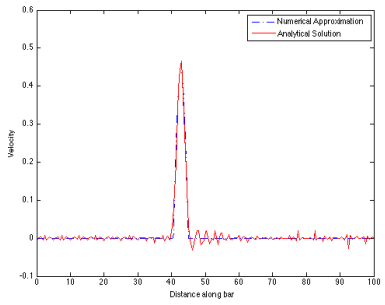

(e)

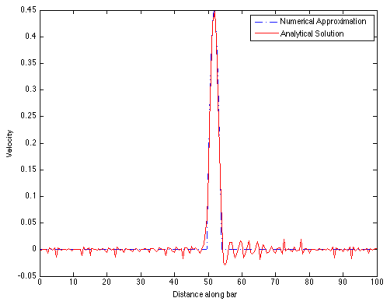

(f)

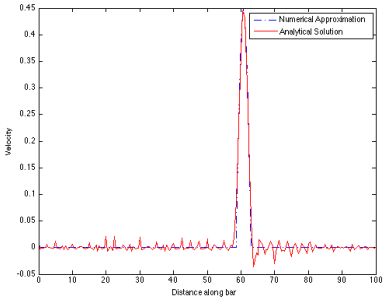

(g)

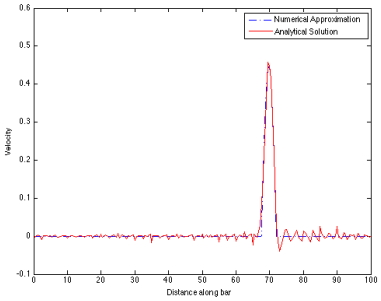

(h)

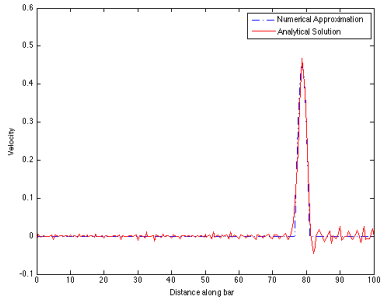

(i)

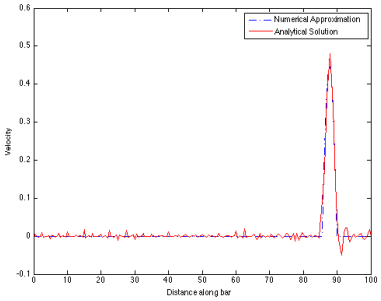

(j)

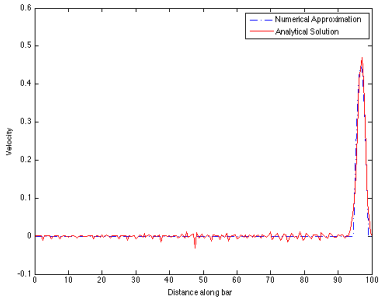

(k)

Figure 5.11: 40 elements with P=4 SE Wave Projection (a)t=.4025 (b)t= 0.8050 (c)t=1.2075 (d)t=1.6100 (e)t= 2.0124 (f) t= 2.4149 (g)t= 2.8174 (h)t= 3.2199 (i)t=3.6224 (j)t=5.0249 (k)t=5.427

5.2.7 SEM using 80 elements based on 4th order polynomials [321 Nodes]

Quadrupling the initial number of elements has resulted in almost completely reducing the level of dispersion to the left of the projected wave and by considerably reducing the level at the right almost to a negligible level. The fit of the solution has been improved at the base of the wave, which in previous scenarios had some slight discrepancies. This is the best accuracy we can level without going into excessive refinement and adding more computational expenses to the procedure. The system's size is almost half the size of the most accurate FE solution presented; this is very interesting we have been able to obtain an excellent solution at half the cost. We still have one scenario left at this polynomial order, let's see how well it behaves.

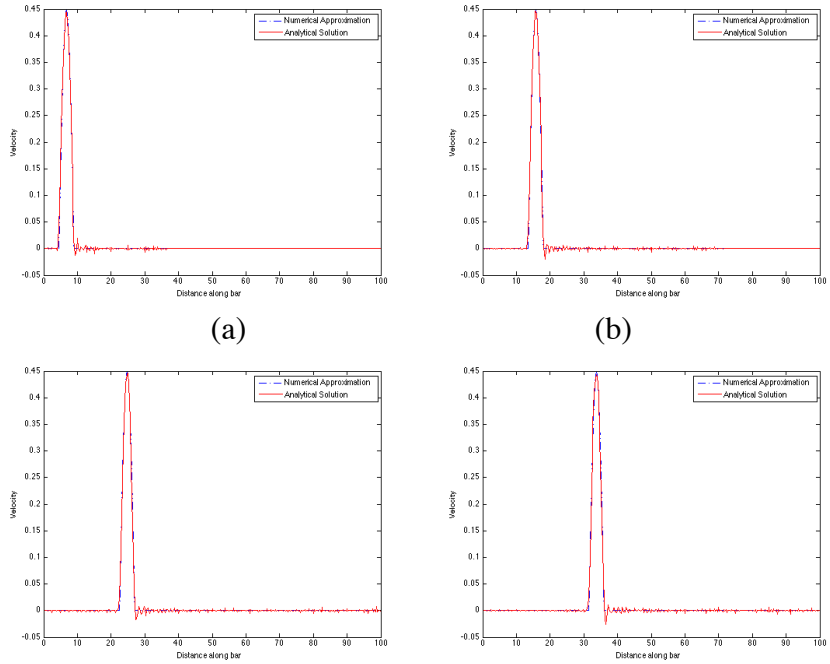

(a) (b)

(c) (d)

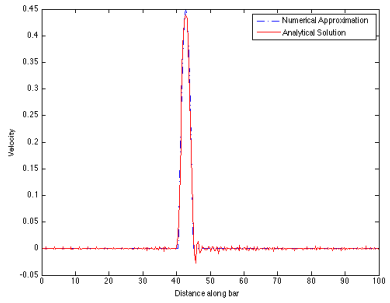

(e)

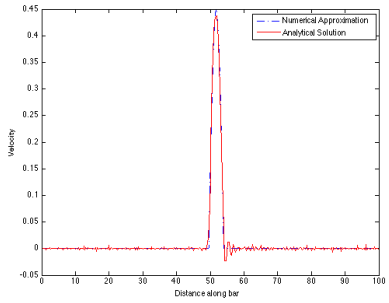

(f)

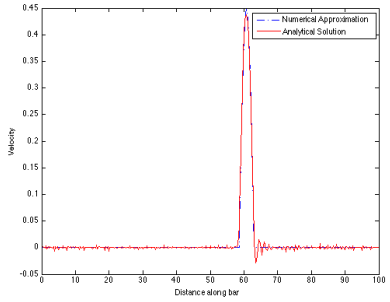

(g)

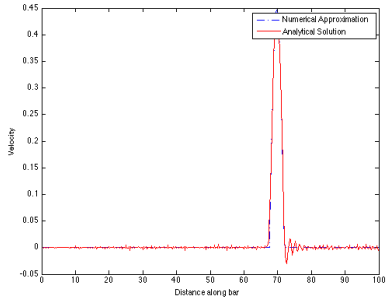

(h)

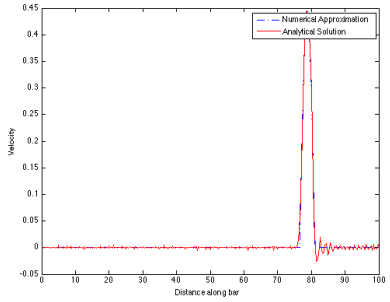

(i)

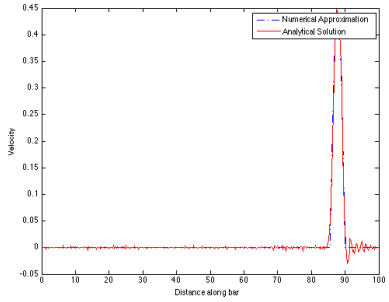

(j)

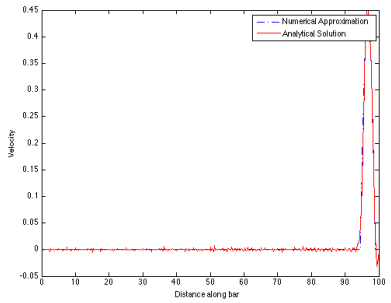

(k)

Figure 5.12: 80 elements with P=4 SE Wave Projection (a)t=.4025 (b)t= 0.8050 (c)t=1.2075 (d)t=1.6100 (e)t= 2.0124 (f) t= 2.4149 (g)t= 2.8174 (h)t= 3.2199 (i)t=3.6224 (j)t=5.0249 (k)t=5.427

5.2.8 SEM using 120 elements based on 4th order polynomials [481 Nodes]

As was expected, the solution initially reduces considerably the dispersion error present to the right of the projected wave; however, it seems to increase slightly as the test is developed. The fit of the approximation to the analytical solution is almost perfect at the base. While still remaining with a system size smaller than the best FE solution our process has rendered an almost perfect solution. We still, nonetheless, will try a higher order interpolation and see if we can make the solution converge to the analytical solution for a smaller system size.

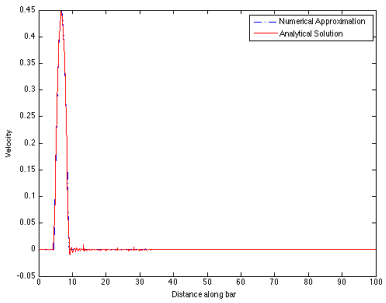

(a)

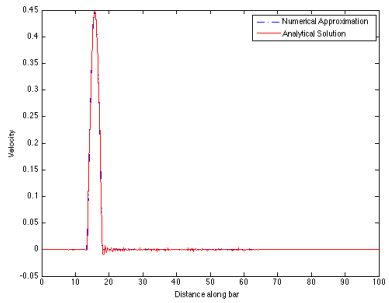

(b)

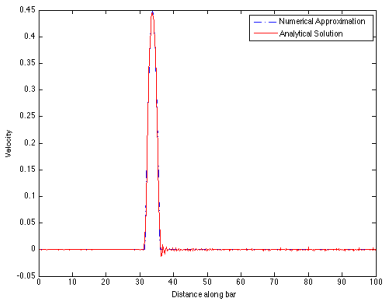

(c)

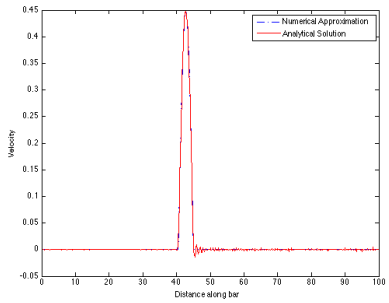

(d)

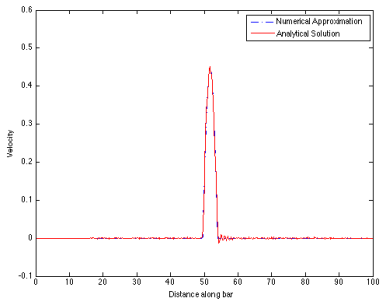

(e)

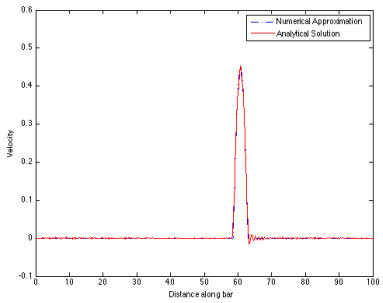

(f)

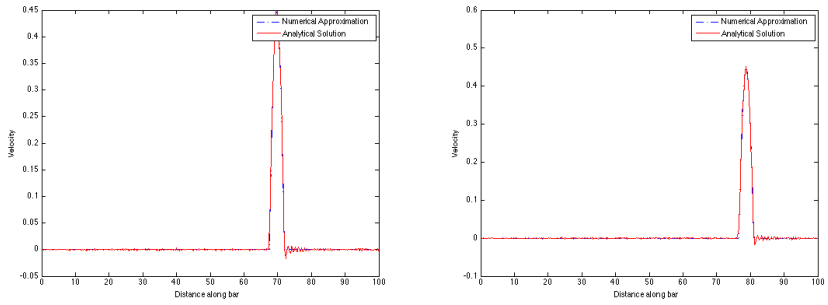

(g) (h)

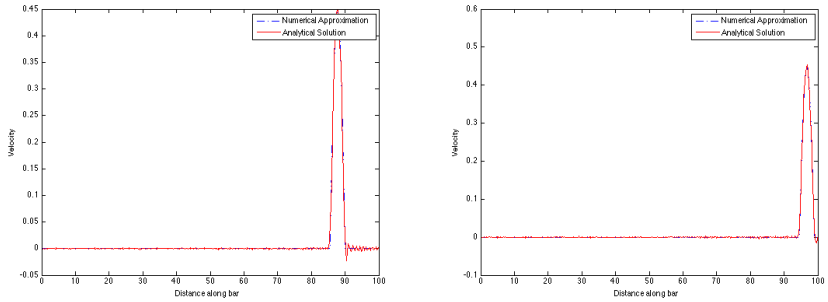

(i) (j)

Figure 5.13: 120 elements with P=4 SE Wave Projection (a)t=.4025 (b)t= 0.8050 (c)t=1.2075 (d)t=1.6100 (e)t= 2.0124 (f) t= 2.4149 (g)t= 2.8174 (h)t= 3.2199 (i)t=3.6224 (j)t=5.0249 (k)t=5.427

5.2.9 SEM using 20 elements based on 6th order polynomials [121 nodes]

For a first scenario consisting of 20 elements only, the solution performs remarkably. The overall levels of dispersion and dissipation are considerably lower than those present in the previously introduced scenarios with a similar total number of nodes. The solution is very accurate overall and behaves in a stable fashion.

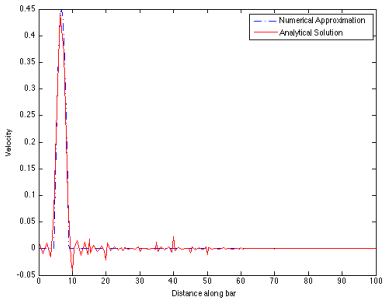
Numerical Approximation
Analytical Solution
Velocity
Distance along bar

(a)

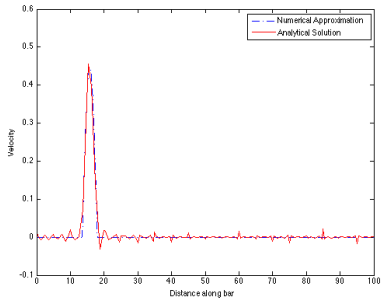
Numerical Approximation
Analytical Solution
Velocity
Distance along bar

(b)

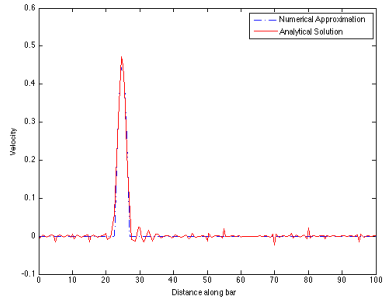
Numerical Approximation
Analytical Solution
Velocity
Distance along bar

(c)

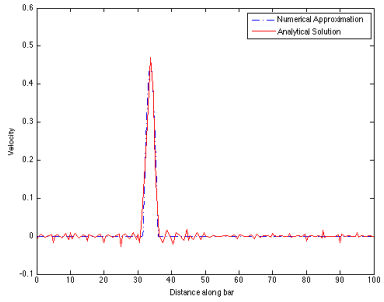
Numerical Approximation
Analytical Solution
Velocity
Distance along bar

(d)

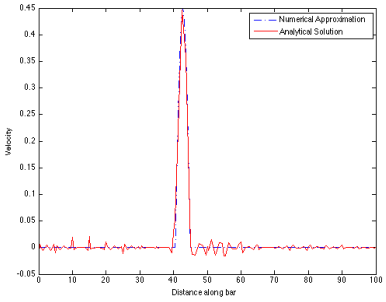
Numerical Approximation
Analytical Solution
Velocity
Distance along bar

(e)

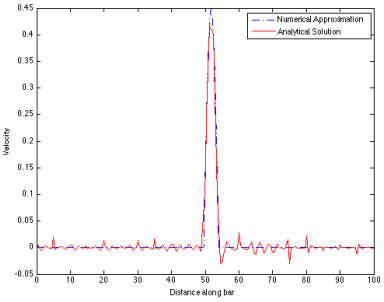
Numerical Approximation
Analytical Solution
Velocity
Distance along bar

(f)

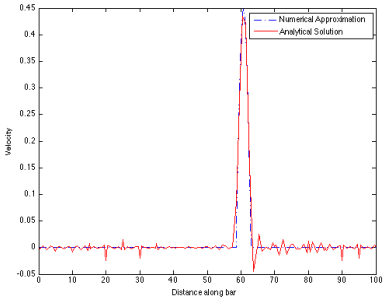
Numerical Approximation
Analytical Solution
Velocity
Distance along bar

(g)

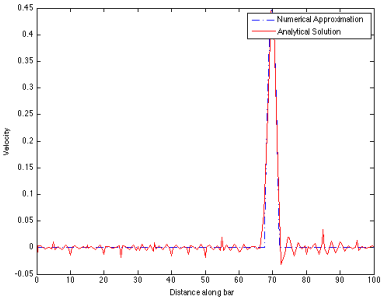
Numerical Approximation
Analytical Solution
Velocity
Distance along bar

(h)

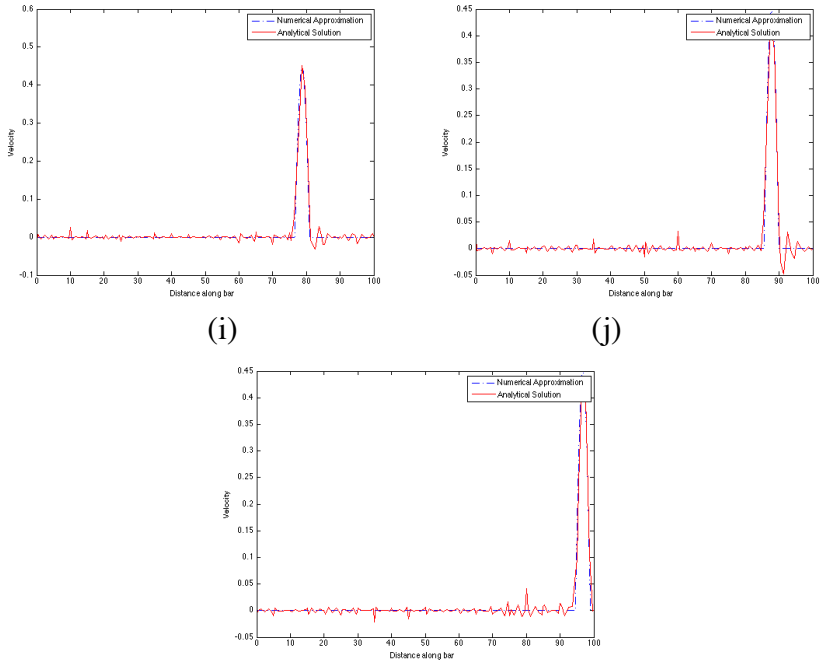

(i) (j)

(k)

Figure 5.14: 20 elements with P=6 SE Wave Projection (a)t=.4025 (b)t= 0.8050 (c)t=1.2075 (d)t=1.6100 (e)t= 2.0124 (f) t= 2.4149 (g)t= 2.8174 (h)t= 3.2199 (i)t=3.6224 (j)t=5.0249 (k)t=5.427

5.2.10 SEM using 40 elements based on 6th order polynomials [241 Nodes]

Doubling the number of elements considerably reduces the dispersion level, however it is still not significant enough to justify the extra effort. The solution compares well to the previously presented scenario, which consisted in a 4th order polynomial approximation using 80 elements. We have been able to accurately model the solution and reduce the system size by more than half, however, we still have some significant presence of dispersion which is always detrimental for our long-range propagation problems, let us try for the last time a higher level of mesh refinement and see if it is possible to reduce almost completely the dispersion presented or if otherwise, other actions should be taken.

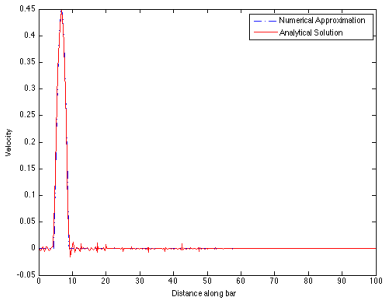
Numerical Approximation
Analytical Solution
Velocity
Distance along bar

(a)

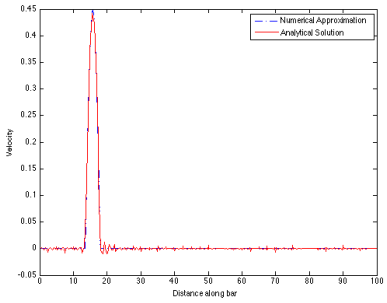
Numerical Approximation
Analytical Solution
Velocity
Distance along bar

(b)

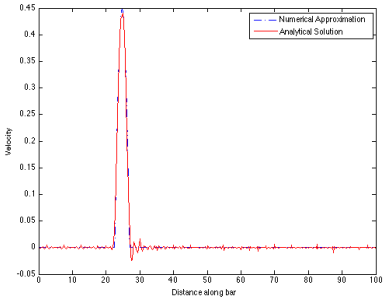
Numerical Approximation
Analytical Solution
Velocity
Distance along bar

(c)

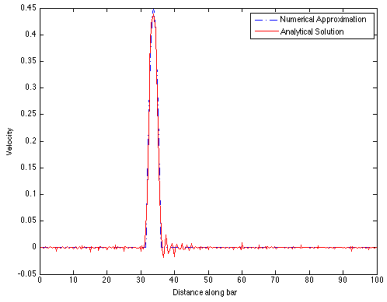
Numerical Approximation
Analytical Solution
Velocity
Distance along bar

(d)

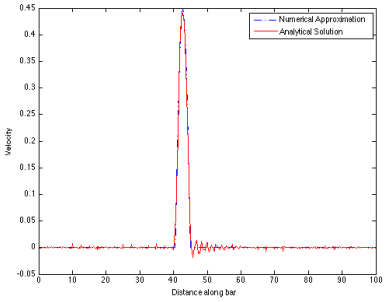
Numerical Approximation
Analytical Solution
Velocity
Distance along bar

(e)

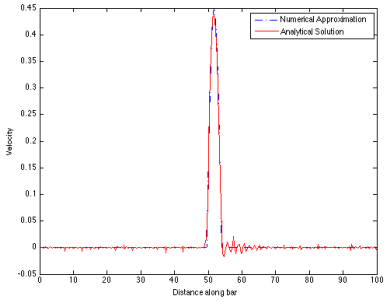
Numerical Approximation
Analytical Solution
Velocity
Distance along bar

(f)

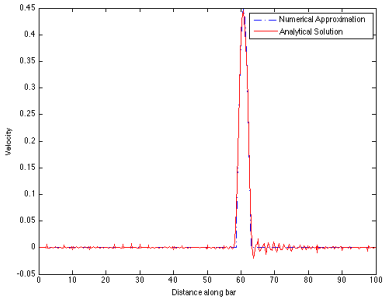
Numerical Approximation
Analytical Solution
Velocity
Distance along bar

(g)

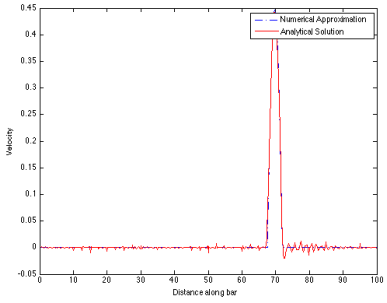
Numerical Approximation
Analytical Solution
Velocity
Distance along bar

(h)

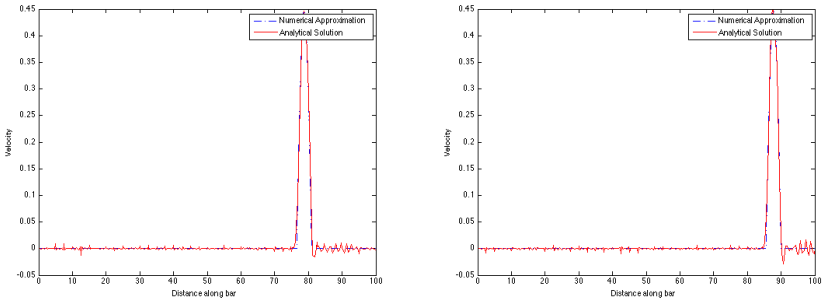

(i) (j)

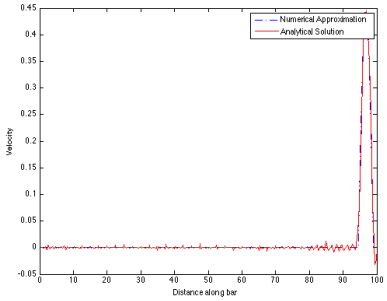

(k)

Figure 5.15: 40 elements with P=6 SE Wave Projection (a) t=.4025 (b)t= 0.8050 (c)t=1.2075 (d)t=1.6100 (e)t= 2.0124 (f) t= 2.4149 (g)t= 2.8174 (h)t= 3.2199 (i)t=3.6224 (j)t=5.0249 (k)t=5.427

5.3.1.1 SEM using 80 elements based on 6th order polynomials

Finally, this last level of discretization has succeeded in reducing the dispersion up to a negligible level. The resulting system is not excessively large; in fact, it is still close to half the size of the system presented for the last FE solution. This is very exciting because we have not use excessively high-order polynomials or an excessively high number of elements and we have been able to reduce both dispersion and dissipation which consequently proves that SEM based solutions perform incredibly well for 1-D long-range propagation problems.

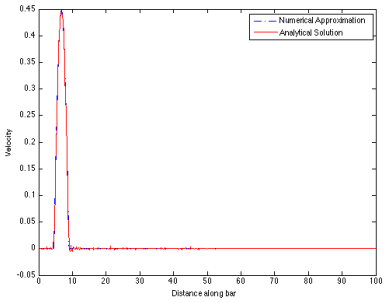
Numerical Approximation
Analytical Solution
Velocity
Distance along bar

(a)

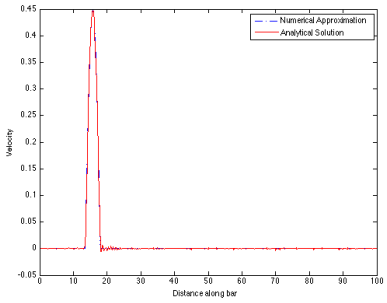
Numerical Approximation
Analytical Solution
Velocity
Distance along bar

(b)

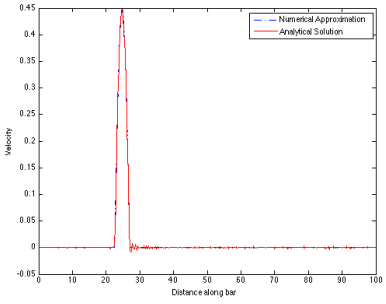
Numerical Approximation
Analytical Solution
Velocity
Distance along bar

(c)

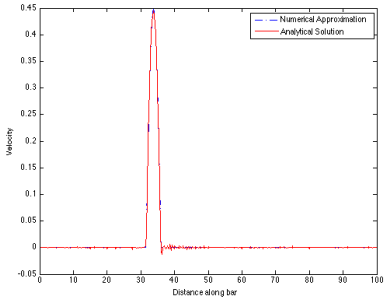
Numerical Approximation
Analytical Solution
Velocity
Distance along bar

(d)

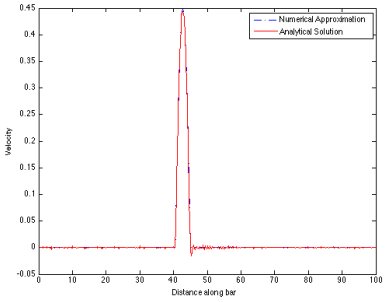
Numerical Approximation
Analytical Solution
Velocity
Distance along bar

(e)

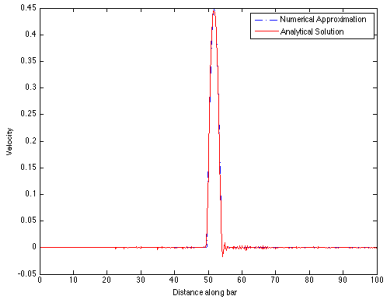
Numerical Approximation
Analytical Solution
Velocity
Distance along bar

(f)

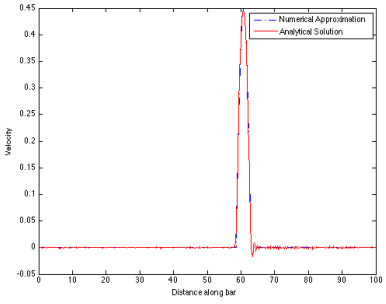
Numerical Approximation
Analytical Solution
Velocity
Distance along bar

(g)

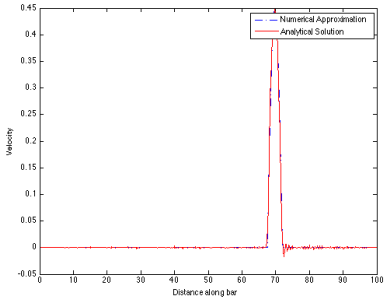
Numerical Approximation
Analytical Solution
Velocity
Distance along bar

(h)

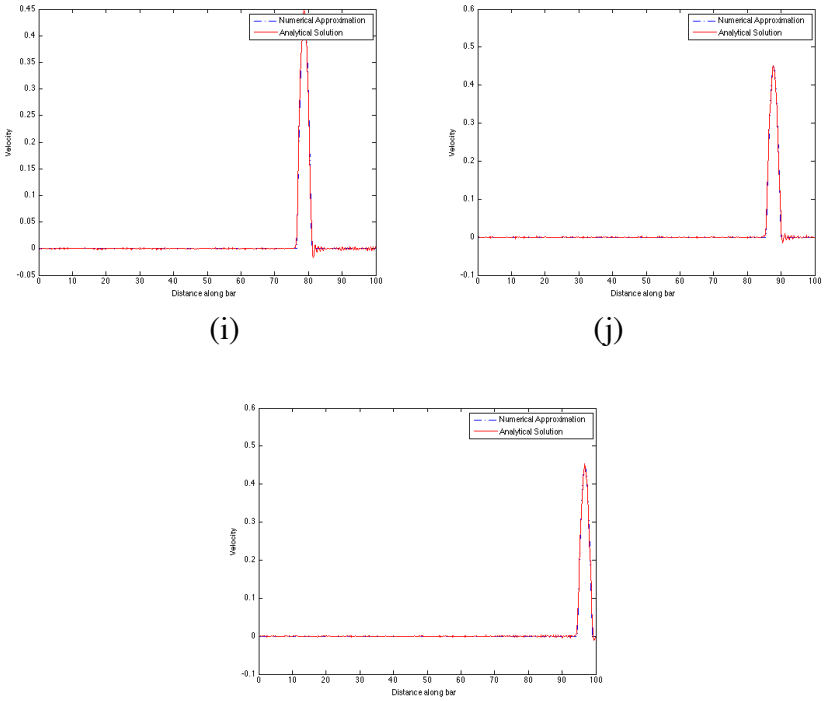

(i) (j)

(k)

Figure 5.16: 80 elements with P=6 SE Wave Projection (a) t=.4025 (b)t= 0.8050 (c)t=1.2075 (d)t=1.6100 (e)t= 2.0124 (f) t= 2.4149 (g)t= 2.8174 (h)t= 3.2199 (i)t=3.6224 (j)t=5.0249 (k)t=5.427

5.3 CONCLUSIONS

It is unnecessary at this stage to state that the spectral element method has exceeded by far the performance presented by the finite element method at a similar number of nodes. The levels of dispersion and dissipation introduced by both numerical procedures have been easily and more effectively reduced by refinement of the spectral elements. For one-dimensional problems the mesh discretization and the interpolation function development is not considerably different which makes the SEM very attractive.

The results just presented and those that had been presented during the previous chapter corroborate the fact that SEM models are remarkably better at handling one-dimensional propagation problems.

Chapter 6: Two-dimensional theoretical background

In the past two chapters we have discussed the fundamental concepts underlying the formulation and implementation of the Finite Element (FEM) and the Spectral Element Method (SEM) for the one-dimensional situation. In this chapter, we turn our attention to the treatment of multiple dimensions. Although the extension procedure is analogous to the one-dimensional case, we will explain how to extend our methodology up to two dimensions to provide a clearer understanding of the construction procedure and the numerical implementation of the multidimensional FE and SE methods. Once the basics have been established, we will proceed to solve the wave equation for the multidimensional case (Eq. 3, shown below).

$$\frac{\partial^2 u}{\partial t^2} = c^2 \nabla^2 u$$

Equation 6.1: Wave equation for multiple dimensions

We will demonstrate one of the most powerful features of the FE method, its adaptability and ability to accommodate to multidimensional solution domains with arbitrary and complex geometries. The extension methodology for multidimensional formulation follows a simple set of instructions that will guarantee a successful solution domain transformation.

1. Formulation of the interpolation functions for the multidimensional domain in question.
2. *Galerkin* formulation of the equation in question. This step will involve the use of Gauss' divergence theorem for reduction of the order of the derivatives.
3. Domain discretization into finite elements. The elements involved must have a proper interpolation function that guarantees C^0 continuity throughout the domain with the exception of the cases where a singularity or discontinuity is known to be present.

4. Transformation of the system of partial differential equations provided by the *Garlerkin* formulation to an algebraic system via the substitution of the finite element expansions.
5. Computation of the element advection, diffusion and mass matrices and the assembly of the general system matrix.
6. Implementation of the Dirichlet and Neumann boundary conditions into the system.
7. Solution of the algebraic part of the system.
8. Application of different time integration methods assuming the problem in question requires it.

Shown next, is the two-dimensional counterpart of the 1-D rod equation presented in the first part of this paper.

$$\frac{\partial^2 u}{\partial^2 t} - c^2\left(\frac{\partial^2 u}{\partial^2 x} + \frac{\partial^2 u}{\partial^2 y}\right) = 0$$

Equation 6.2: Two dimensional Wave Equation

The two dimensional transformation of the equation imposes certain restrictions on the system's formulations. The solution to the wave equation must be situated in a domain, D, that is enclosed by a contour denoted C subjected to the two types of complementary initial boundary conditions which we had previously mentioned. Multidimensional conversion of the system constraints the Neumann boundary conditions to be specified with respect to the inward or outward normal derivative at the solution boundary.

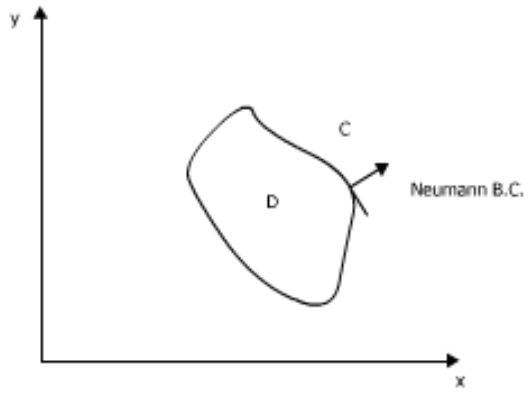

Illustration 6.1: Illustration of an arbitrary system's geometry showing different B.C.'s

The Galerkin projection of the governing differential equation is carried out using as weighting functions the global interpolation functions $N_i(x,y)$. These are assumed known, or in any case to have been previously derived according to the type of element and the degree of the interpolation function desired. The process involves multiplying both sides of the governing partial differential equation by the interpolation function of choice (trial function). The system is then modified using known mathematical manipulation techniques which allow a natural implementation of the Neumann boundary conditions (via Gauss' Divergence theorem) into our formulation and hence system's solution.

$$\iint_D N_i(x,y)\frac{\partial f}{\partial t}dxdy + \iint_D N_i(x,y)u\cdot\nabla f dxdy = (-k\iint_D \nabla N_i(x,y)\cdot\nabla f dxdy + \oint_C N_i(x,y)qdl)$$

Equation 6.2: Galerking Projection in two dimensions

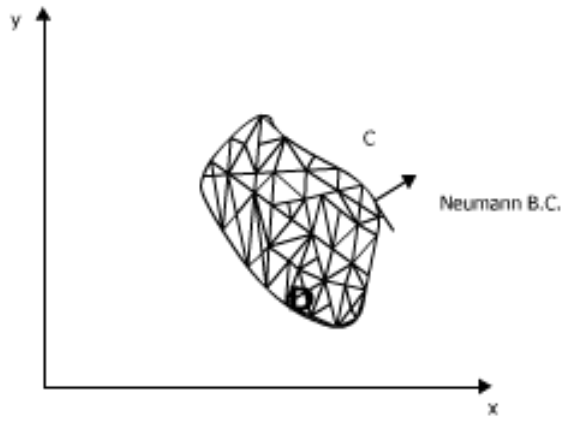

Illustration 6.2: Discretization of the solution domain into N_E elements.

The next step involves the discretization of the domain D into a collection of N_E elements. The formulation of the interpolation formulas (if these have not been formulated already) is performed according to the degree and type of element desired. In practice, the elements involved have triangular or quadrilateral shapes defined by a very few geometrical element nodes since most of these elements have closed-formed solutions ready for the domain integration process. There is no restriction on the shape or number of nodes that conform an element but easy integration across the element domain guarantees a smooth implementation and extension into the system that will provide an overall better performance. Transformation to a *parent* or *master* element shape can be performed via domain mapping which allows the use of integration quadratures that implement a straightforward numerical integration process. Certain restrictions are imposed on the element's geometry due to the mathematical process involved in domain mapping. The elements must be reasonably shaped such that one to one correspondence is guaranteed in the mapping process; mathematically speaking this imposes the restriction on the determinant of the Jacobian (denoted as *surface metric coefficient,* h_s) to be greater than zero throughout the domain in question.

$$h_s \equiv Det\ (J) = \quad Det\left(\begin{bmatrix} \frac{\partial x}{\partial \varepsilon} & \frac{\partial x}{\partial \eta} \\ \frac{\partial y}{\partial \varepsilon} & \frac{\partial x}{\partial \eta} \end{bmatrix}\right) \quad = \quad \left|\frac{\partial x}{\partial \varepsilon} \times \frac{\partial x}{\partial \eta}\right| \quad \geq 0$$

Equation 6.3: Surface Metric Coefficient

In the second stage of implementation we introduce a connectivity matrix with the purpose of mapping the local element nodes to unique global nodes. The need to introduce a boundary flag to specify whether an element, local node or global node is located at the boundary and in consequence is subjected to the boundary conditions rises. Computationally wise, the presence of a boundary flag matrix aids in the automatization process and facilitates the construction of a function that can impose the boundary conditions to a desired level.

Implementation of the finite element method, using linear triangular elements defined by three nodes or quadrilateral elements defined by 4 nodes, imposes a limit on the level of accuracy obtained through h-refinement (element size refinement) techniques. Mesh refinement can be performed throughout the solution domain or specifically at the portions where the solution is known to vary quickly. Refinement of the domain at its curved sections can be performed by decreasing the element size or more accurately by using higher-order elements with a large number of nodes located at the curved section to be modeled. These curved sections will be later transformed via domain mapping to a master or parent element to simplify the numerical integration process. Considerable improvement in the accuracy of the interpolation is provided by augmentation of the order of the interpolation function.

Both SE and FE systems are set up following parallel basic procedures. The Spectral Element Method differs in the sense that the nodal components are judiciously deployed at the positions corresponding to the zeros of certain families of orthogonal polynomials that optimize the interpolation

process by decreasing undesired oscillations that arise due to the mathematical nature of the formulation. Simple translation of the interpolation functions to higher dimensions can be performed via a tensorial product. It is necessary now to make an important distinction between what constitutes a structured and an unstructured domain. Structured domains have a well-*defined* structure or organization, they are arranged by following a pattern and they usually are constituted by quadrilaterals in two-dimensional elements or by hexahedral in three-dimensions. Most structured expansions can be typically constructed from a tensor product since a standard Cartesian coordinate system defines the entrapped regions; this means that a natural and straightforward method of construction involves the *tensor* product between the one-dimensional bases in each of its Cartesian coordinate directions. Unstructured domains are usually represented by triangular elements in two dimensions or by tetrahedral/prismatic elements in three dimensions. Unstructured expansions are usually based on barycentric coordinate systems that are rotationally non-symmetric. Rotationally symmetry is an important consideration that has motivated the use of rotationally invariant barycentric coordinates, unfortunately the use of these types of coordinate systems destroys much of the numerical efficiency that standard structured expansion bases have.

For the structured domains we will denote, from this section and on, the interpolation bases as $\Phi_{ij}(\xi_1, \xi_2)$ or $\Phi_{ijk}(\xi_1, \xi_2, \xi_3)$ for two and three dimensions respectively. If we consider a one-dimensional spectral element basis as a one-dimensional array spanning a linear region (ξ_1-direction) between the vertices A and B depicted in the standard quadrilateral illustrated below, then the indices of the bases within this array correspond to their position within the ξ_1-direction.

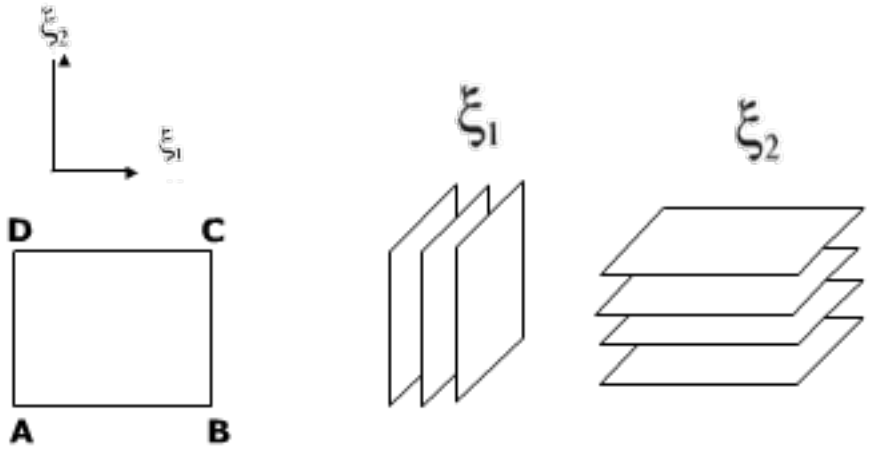

Illustration 6.3: Two-dimensional Interpolation Basis.

The same can be inferred regarding the basis that spans the linear region between A and D in the ξ_2-direction. The basis that spans the region entrapped by vertices A, B, C, and D is formed by applying a tensorial product between the bases of the individual directions that comprise the region.

$$\varphi(\xi_1,\xi_2) = \psi(\xi_1)\psi(\xi_2) \qquad \{A \le \xi_1 \le B, A \le \xi_2 \le D\}$$

Equation 6.4: Two-dimensional basis via a tensor product.

A similar assembly process is possible for three-dimensions with the slight difference that it is now necessary to consider a three-dimensional span comprised by a cube formed by the individual interpolation functions in each of the three directions. We note that the multidimensional polynomial order may differ in each of the Cartesian directions; this means that more flexibility is given as limits are already imposed in the formulation unlike the case with unstructured domains, where the region bounded by the Cartesian coordinates is dependent upon each other. Likewise, certain components of the polynomial result can be suppressed in turn. This can destroy some of the inherent efficiency of the full nodal tension product but at the same time it provides a type of flexibility desirable. This flexibility

provides a natural way to vary the expansion order from one element domain to the other while maintaining C^0 continuity.

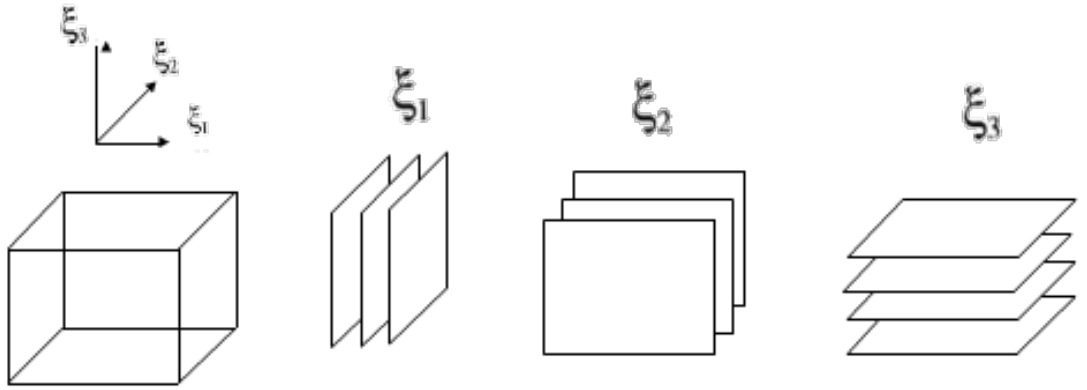

Illustration 6.4: Three-dimensional Basis Formulation.

$$\varphi(\xi_1,\xi_2) = \psi(\xi_1)\psi(\xi_2)\psi(\xi_3) \qquad \{A \le \xi_1 \le B,\ A \le \xi_2 \le D,\ A \le \xi_3 \le E\}$$

Equation 6.5: Three-dimensional basis via a tensor product.

Although most structured expansions are typically constructed from a product of functions as depicted above, it is not so common for unstructured expansions in triangular and tetrahedral domains. As it was previously mentioned, triangular unstructured regions have bounds defined by Cartesian coordinates (ξ_1, ξ_2) that are dependent upon each other; this means that straightforward formulation of the basis via a tensor product is not possible. It is necessary to develop a suitable coordinate system that has independent bounds that will allow the development of a tensorial type basis within the unstructured region. The lack of rotational symmetry does not affect multi-domain construction for triangular expansions, it does, however, impose a restriction on the possible orientations of the elemental regions for tetrahedral domains. The development of suitable coordinate system for unstructured domains offers the advantage that a multi-dimensional system can be defined from a one-dimensional functional basis using a tensorial product. Area and Volume coordinates, otherwise known as barycentric or triangular

tetrahedral coordinates have been used in unstructured domains due to their rotational symmetry. To obtain this symmetry it is required to have an extra (dependent) coordinate that renders the tensor extension process very difficult if not impossible.

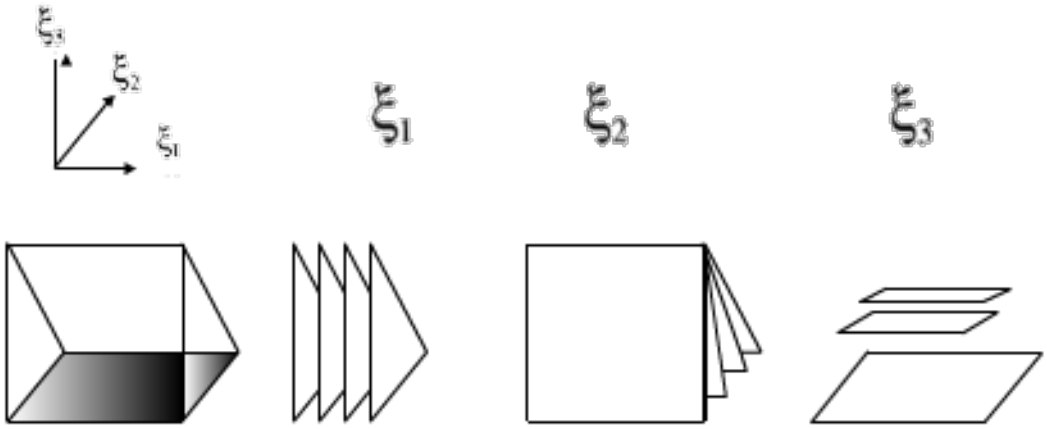

Illustration 6.5: Three-dimensional basis formulation for unstructured domains.

One of the most common methods for treatment of triangular regions is the creation of a collapsed two-dimensional coordinate system. This type of system defines the triangular region in terms of coordinates (η_1,η_2) that are independent of each other and that map back through a set of functions to Cartesian coordinates (ξ_1, ξ_2). This suggests that the definition for a triangular region is identical to the definition of the standard quadrilateral region and that the transformation can be seen as mapping from a triangular region to a quadrilateral through collision of one of its nodal components.

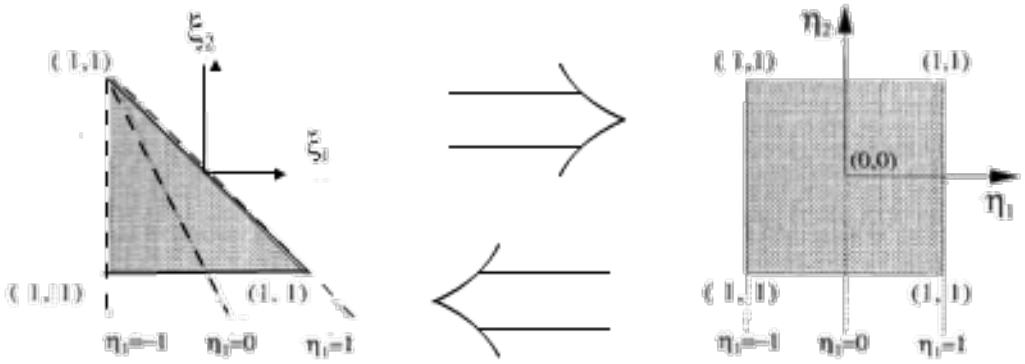

Illustration 6.6: Collapsed two-dimensional coordinate system

There are many considerations that motivate us to select a *proper* expansion basis. Since we are interested in developing computationally efficient algorithms the selection of expansions that have attractive numerical properties, such as matrix conditioning or proper explicit time step restrictions, becomes fundamental for the application and development of a well-posed algebraic system. Unstructured domains may lead to formulation of collapsed systems that suppress a set of polynomial terms from those obtained via tensor product in a quadrilateral domain. This means that some numerical efficiency is lost during the physical formulation of the system and during the computation part through the usage of integration quadratures.

Although finite element expansion bases may be derived in parallel to the SEM procedure previously described, it is more common to find systems composed of low-order elements. As has been already mentioned for one-dimensional cases, an improvement in the computation accuracy is generally achieved by refinement of the mesh rather than by conversion of the system to higher-degree interpolation polynomials. This is in part to take advantage of the existence of well-known closed-form solutions that allow the system to save in computational cost by automatizing the integration process.

In the following sections of this paper we further explain the underlying characteristics of the system that has been set up and we provide the results obtained from the SEM and FEM formulations and their respective conclusions.

Chapter 7: Two-dimensional Wave Propagation Problem Set Up

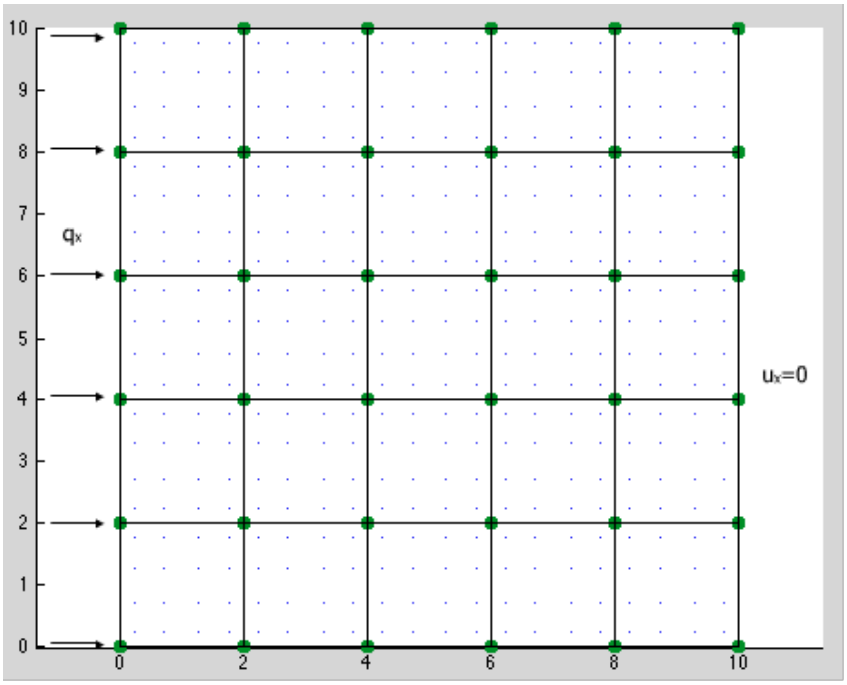

Illustration 7.1: Two-dimensional system set up.

The two-dimensional model for this second part of the paper consists of a square plate of length L=10 and constant thickness of 1. The mechanical properties of the plate include: (i) Elastic Young's modulus $E=10x10^6$ N/m^2 (ii) mass density $\varrho=1.45x10^{-4}$ N/m^3. In parallel to the one-dimensional case, the Dirichlet boundary conditions establish a right fixed. In the other hand, Neumann's boundary conditions do differ for each of the methods performed. For the SEM formulation a sinusoidal pulse with duration of 0.002 s is assumed to take place at the left end of the plate. In the other hand, the FEM formulation involves a steady state force of equal length distributed along the left end of the plate. Careful attention was taken during the formulation and development of the system. It is important to note that special emphasis is made on the assessment of the degree of dispersion, convergence and behavior that each of

the methods provide, in other words, how well they perform numerically and if there is a stability criteria that can be associated to the method of choice. For the conclusion of this paper a final summary describing the behavior and performance of the computed solutions is made.

Damping is not considered for this problem, as the main concern is the natural numerical stability and level of dispersion that Finite Elements and Spectral Elements methods provide. The present concern is to discover some of the aspects and effects that influence the most in the numerical modeling of wave propagation problems. Both the spatial and the temporal discretization introduce errors, which influence the accuracy of the solutions. The combined effects of the procedures performed need to be examined and properly interpreted before a conclusion regarding the selection of the best method for treatment of wave propagation problems can be stated.

One dimensional wave theory and empirical research has provided enough information regarding the wave behavior near fixed boundary conditions. Thanks to one-dimensional theory, it is known that two-dimensional travelling waves reaching fixed boundaries at either end of the material should both reflect and refract. Unfortunately, one-dimensional theoretical formulation cannot be super imposed in both directions for the two-dimensional case and closed-form solutions to the problem are difficult to obtain. Basic theory, however, does give us a basic representation of the behavior the 2D-model should follow in one direction but convergence of the results will not occur, as two-dimensional influence cannot be entirely assessed by this simplified theory. For this second part of the paper, a model based on the conditions described above was tested using FEM with a variable number of linear triangular elements. Similarly, the same model was tested using spectral element methods composed by quadrilateral elements obtained through a tensor product between two interpolation bases of the 5^{th} order based on Lobatto polynomials. The number of elements was allowed to vary using 25, 100, 225, 400,

and 1600 elements across the solution domain. In the case of the finite element model, 228, 857 and 3432 elements were used and the element discretization was performed using commercial software.

The computational effort required by the two-dimensional problem in question imposed, besides a high computational expense, a restriction on the level of domain discretization and a limit to the number of operations that could be performed simultaneously without affecting the modeling time or rendering the computational process numb. It is for this reason that an analytical solution could not be modeled simultaneously and other means of comparison between methods were selected. A general assessment of dispersion, convergence and behavior for the numerical solutions is still possible by graphical means, so the results will be compared in this manner also making use, to a given extent, of the well-known one-dimensional wave theory. During this procedure the displacements, velocities and accelerations of the nodal components were continuously recorded. As a mean of comparison (i) the areas under the wave curve in the numerical approximation, (ii) the difference in magnitude that these present over time and (iii) the differences present between the different levels of discretization are selected to both the base and the starting point for the performance comparison.

Chapter 8: Analysis and Interpretation

8.1 Spectral Element Formulation

For the two-dimensional case treated in this section we have used, as has been previously explained, spectral elements obtained by means of the tensor product between two 5^{th}-degree Lobatto-based polynomials. This type of element is composed by 25 nodes, 16 of them categorized as inner nodes while the remaining nodes are categorized as boundary nodes, this means that C^0 continuity is enforced by the sharing of these nodal components across elements and its high number assures continuity of the solution across the domain up to a certain level. This type of element has no constraints imposed by the domain's geometry so no special provisions have to be taken into account during the element deployment across the domain, however, had the domain been composed by complex geometries, special consideration must have been developed, specially in regards to the degree and geometry of the elements that would be deployed along the distorted part of the domain. It may be sometimes required to do an overall assessment to consider the degree up to which mesh refinement can be performed and whether transitional elements should be present to slowly transition to higher/lower order elements or whether simple mesh refinement is enough to tackle the problem.

8.1.1 SEM Solution Using 25 Elements With One-Dimensional Basis Of P=5 And 26 Nodes Linearly Across

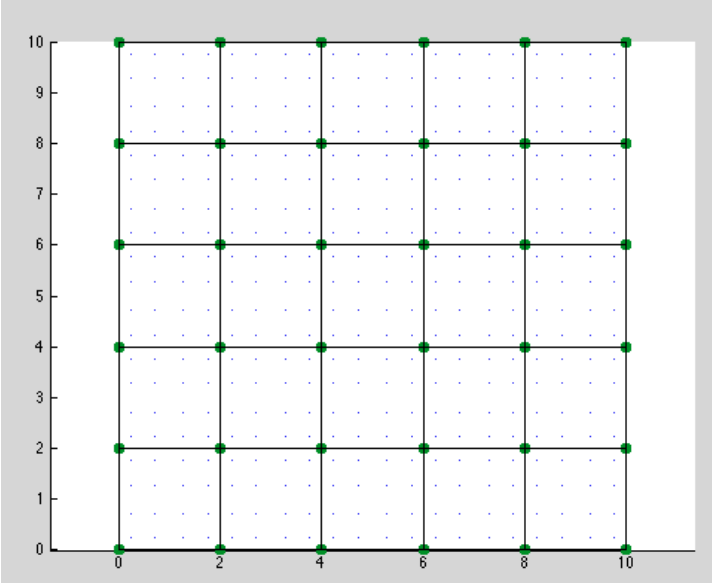

Figure 8.1: SEM: 25 elements obtained from P=5 basis, 26 nodes used linearly across.

For this scenario, 25 elements were distributed evenly across the plate. Twenty-six nodal components lie linearly across in both directions. This characteristic permits the direct comparison to the one-dimensional formulation from previous chapters. Quadrilateral elements allow, up to a given degree, the representation of the wave equation as it spreads across both the x-direction and y-direction individually due to the amount of linear continuity they provide across element, something that is not possible with triangular elements.

The following two figures depict the numerical solution obtained and they represent the wave's behavior as it traverses the longitudinal (x-direction). The representation of the wave across the domain has been accurate to a certain degree, the illustration below does demonstrate, however, that a lower number of nodal components does not satisfactorily captures the material response and that presence of noise (depicted by a bubble/bump in the lower right corner of the illustration) indicates that refinement

should be performed since the magnitude is large in comparison to the represented solution. The reflection imposes an increase in the error present due to the number of elements of choice.

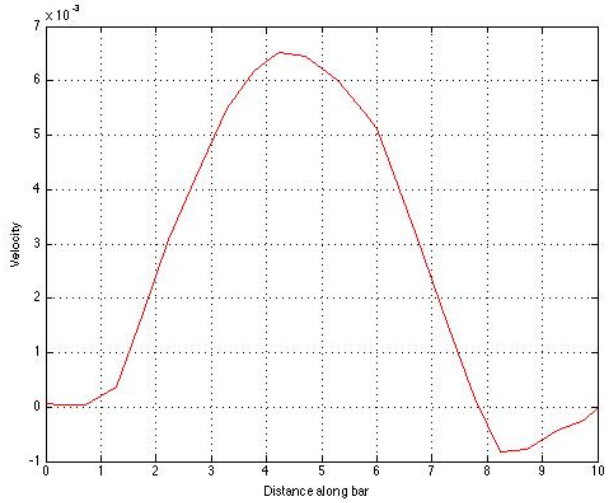

Figure 8.2: Wave preserved in the x-direction.

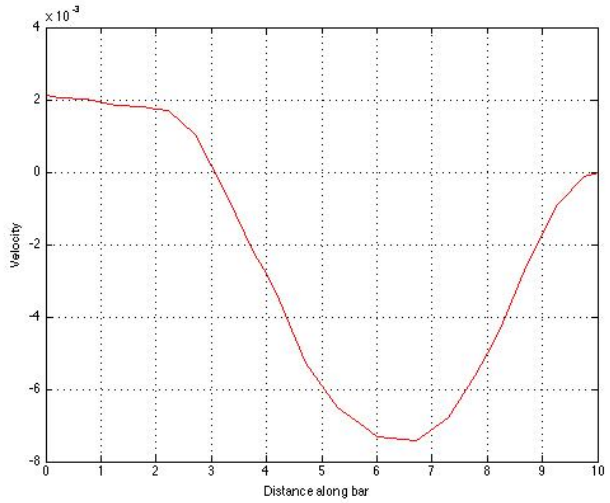

Figure 8.3: Wave preserved in the x-direction after reflection.

The illustration shown below depicts the wave area under the curve as the test progresses. The presence of variation across the computational process can be easily inferred, the solution seems to be oscillating between values when an approximate constant magnitude is desired throughout the test.

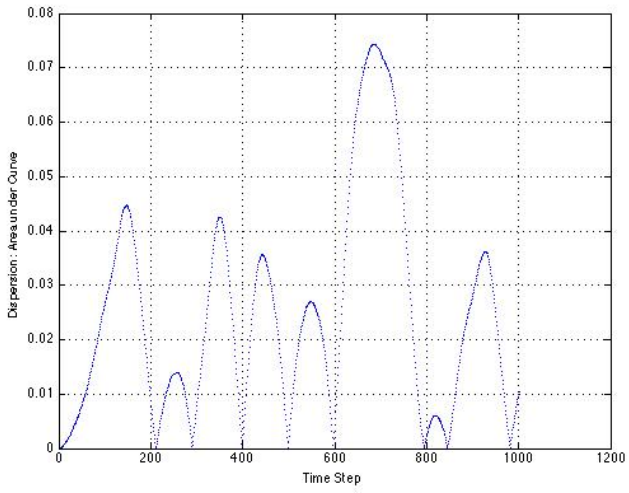

Figure 8.4: Area under the wave curve as a measure of dispersion.

In the other hand, the behavior of the solution in two-dimension was satisfactorily that expected. In fact, as it will be seen over the course of this section, the accuracy of the solutions improves as mesh refinement takes place. The following illustration depicts a colored plot depicting the varying velocity magnitudes across the plate at a given time period of the test. The test is able to capture the higher velocity values at the nodal positions where the point loads/pulses took place; likewise the model captures the wave propagation in two-directions and recreates the reflection effect accurately. Given the degree of the elements and the amount of computational time the result obtained is satisfactory but room for improvement is present.

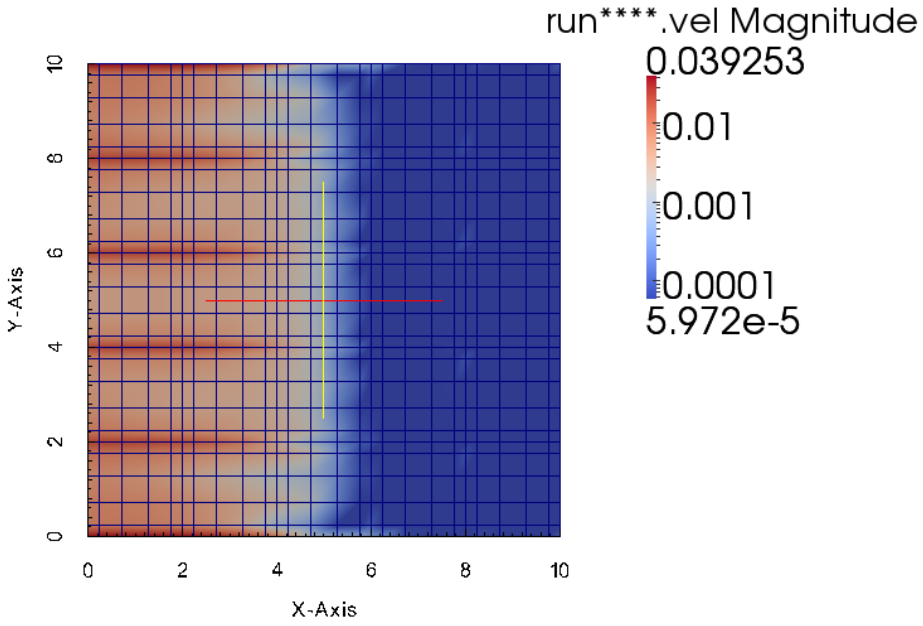

Figure 8.5: Velocity magnitude at t=0.00124 s.

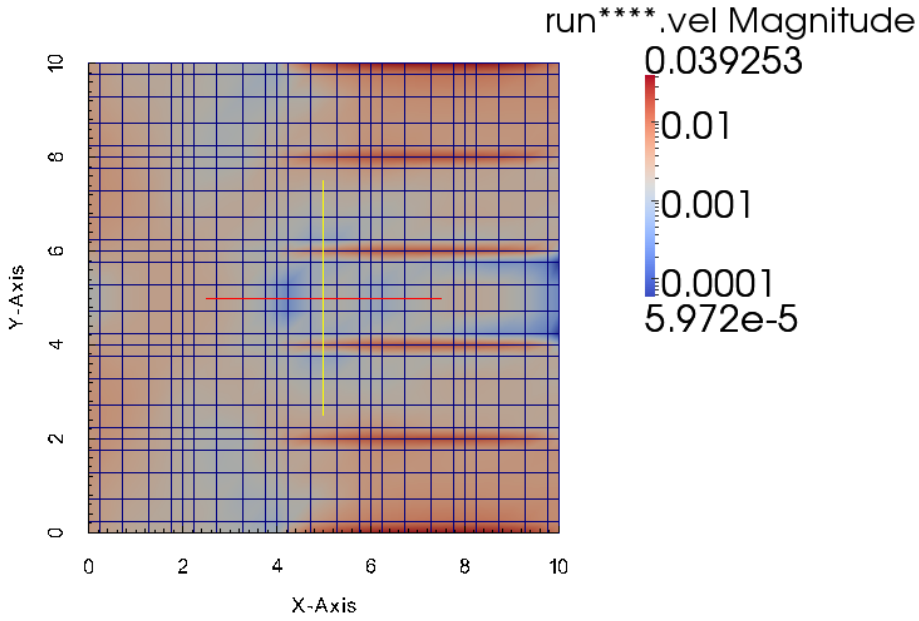

Figure 8.6: Reflection of the wave taking place at 0.00316 s.

8.1.2 SEM Solution Using 100 Elements With One-Dimensional Basis Of P=5 And 51 Nodes Linearly Across

For this second scenario, 100 elements where distributed evenly across the plate. Fifty-one nodal components lie linearly across in both directions. Computationally wise the problem has been more expensive that the preceding model and the solution has taken considerable more time to obtain size the system size has been quadrupled. Physically wise, the system has not changed and for this reason we will focus the discussion on the computational changes in dispersion, convergence and accuracy that the new model provided rather than repeating the technical changes that the code suffered in order to accommodate for the new charactersistics.

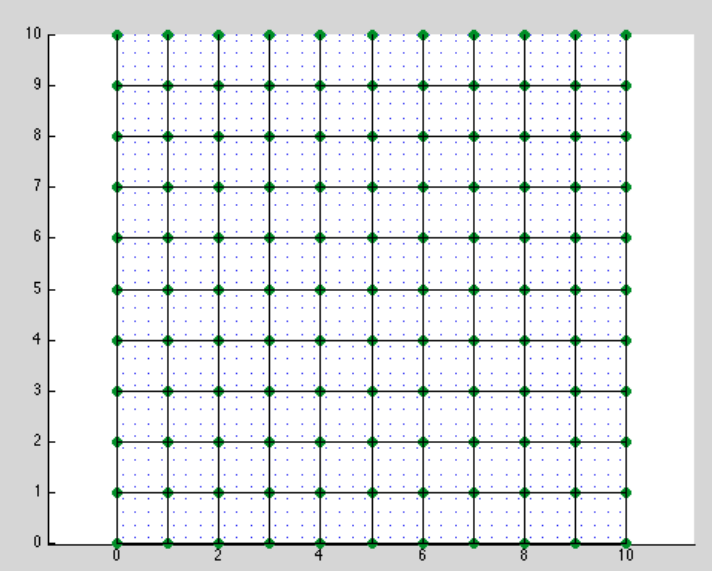

Figure 8.7: SEM: 100 elements using a 5th degree 1D basis and 51 nodes linearly across.

The following two figures depict the numerical solution obtained and they represent the wave's behavior as it traverses the longitudinal (x-direction). The representation of the wave across the domain differs considerably from the solution previously calculated. The illustration below does demonstrate, however, that raising the number of nodal components has not satisfactorily reduced the noise presence in the numerical approximation (depicted by the area increase in the bubble/bump that we had first

perceived in the previous scenario.) This indicates that refinement has not been exactly successful in reducing the error introduced by lack of mesh refinement and special attention should be paid to tracing back its origin and finding out whether any possible solutions exist and these involve the mathematical foundations on the model rather than the physical distribution of the elements.

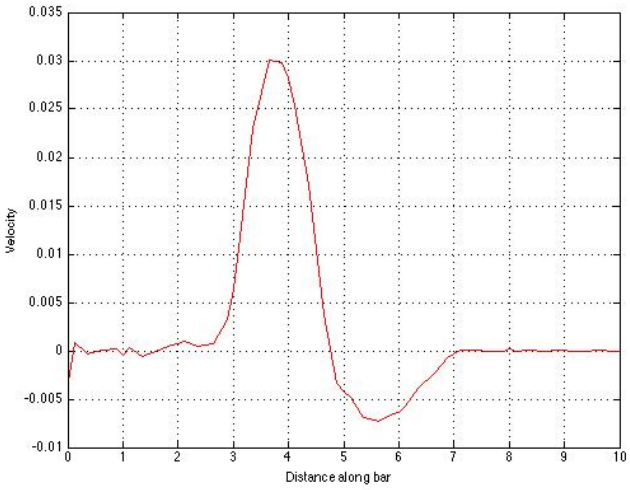

Figure 8.8: Wave Propagation using 100 elements, 51 nodes spread linearly across in both directions.

The level of dispersion satisfactorily shows some reduction. The magnitude of the area seems to be following a pattern with periods of constant magnitude, which indicate less presence of numerical dispersion in the model. It is necessary to keep refining the mesh to see if a higher number element can show more considerable improvement and in this way render a solution to the problems that have come across so far.

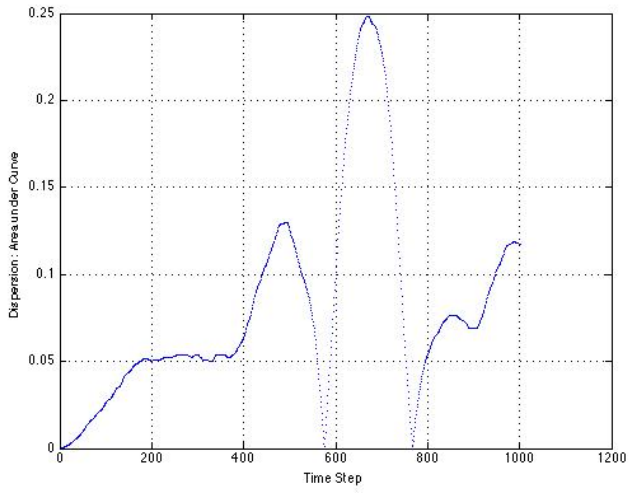

Figure 8.9: Dispersion measurement using the area under the curve.

The solutions in two-dimensions, similarly appear to be correct even though the magnitude order is quite different, this is something that at this point may be attributed to the original level of refinement used, however, as the modeling scenarios progress a broader picture of what is actually occurring will be obtained and a more educated treatment of the problem can be assessed.

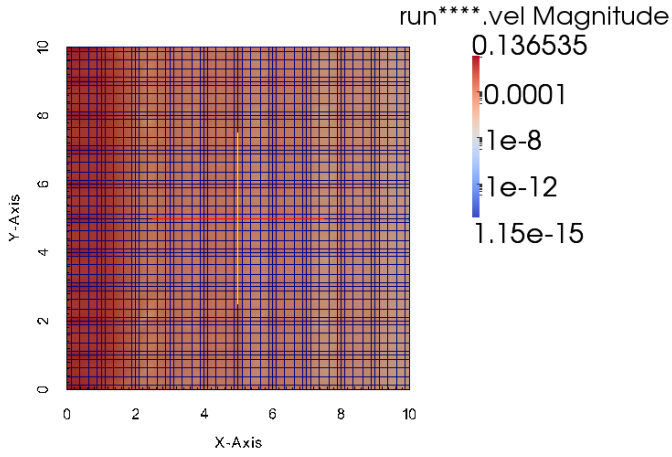

Figure 8.10: Velocity magnitude at t= 0.00125 s for a 100-element.

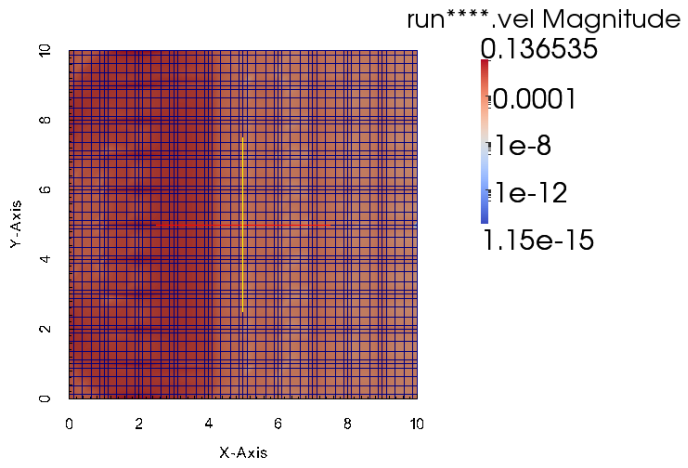

Figure 8.11: Velocity magnitude at t=0.00316 for 100-elements.

8.1.3 SEM Solution Using 225 Elements With One-Dimensional Basis Of P=5 And 76 Nodes Linearly Across

For this second scenario, 225 elements where distributed evenly across the plate. Seventy-six nodal components lie linearly across in both directions. Once more the solution has taken more time to obtained since the system size had almost doubled. It is important to note that the system has not suffered any fundamental changes within its theoretical background or B.C's. The process of assessing the computational changes in dispersion, convergence and accuracy that the new model provided is still the area of attention. From this point and on, the explanations will be more brief and oriented toward the graphical description that accompanies it. This in part is because the nature of the problem is not changing across scenarios only the system responses, our sole concern, and in order not to render the writing of this report dull for both reader and writer and by this lose focus on the task we were set out to do. We will now shorten our explanations and emphasize on the difference and on what can be directly inferable both computationally and theoretically wise from the illustration. In this manner, we will wait

to the end of this section to produce a summary of the findings that we have encountered accompanied by a proper interpretation of these.

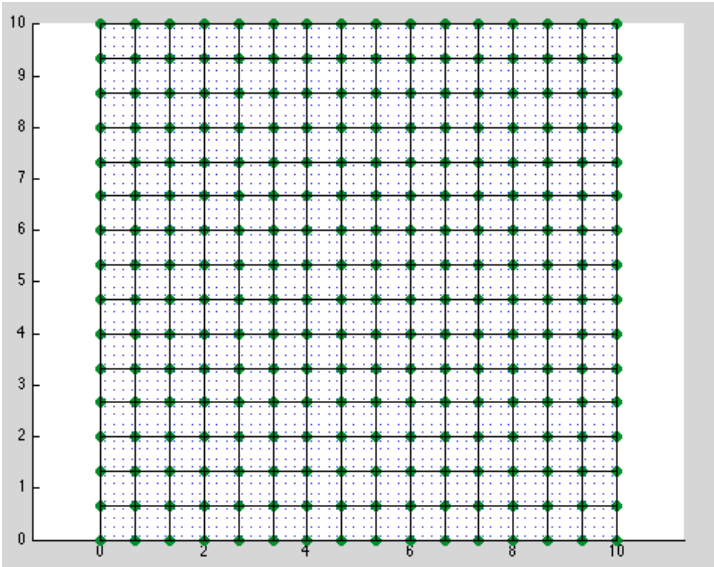

Figure 8.12: SEM: 225 elements (76 nodes across in both directions).

This scenario has been able to offer a series of very encouraging results. Comparing the magnitudes obtained for the wave propagation representation in the x-direction for this and the previous model demonstrates a considerable degree of convergence present. Numerical noise is still present in what can be perhaps equal degree but a must important factor is the existent presence of wave oscillations that lag behind the wave propagation across the plate and increase with respect to time. It is important to mention that some of these situations may have been introduced by the time-scheme procedure of choice, since no change in time step length was accompanied by the mesh refinement and the type of time-integration scheme is well known to be conditionally stable, that is accuracy of the numerical approximation and presence of noise within the solutions are directly tied to the magnitude of the time step of choice. Unfortunately, it has been very unpractical to modify this variable, as delays in the computation times are extremely unpractical and detrimental both for numerical modeling purposes and for the graphical representations that are created for each of the scenarios modeled. It is most important to mention that exact convergence of the solution will not occur regardless of the degree of

mesh refinement attained by any of the modeling scenarios. The tensor formulation has rendered the computation of the boundary conditions located at the left end of the plate rather complex, in the sense that unequal distribution is taking place and the process to allocate the real values is time-consuming. Since the purpose of this paper is to assess the numerical properties and behavior of both SE and FE method, we have assumed equally distributed forces applied across the nodal components at the left end of the plate. This is something that should be kept in mind since a considerable degree of error has been introduced in the solution due to the simplification of the physical model.

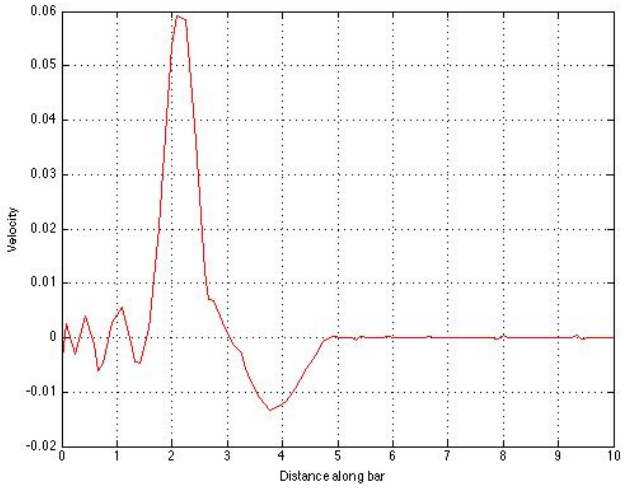

Figure 8.13: SEM: wave propagation using 225 elements, 76 nodes across in both directions.

Important improvement is shown in the area of numerical stability. Dispersion seems to have decreased and the illustration below shows how the wave behavior has been rendered more stable/constant.

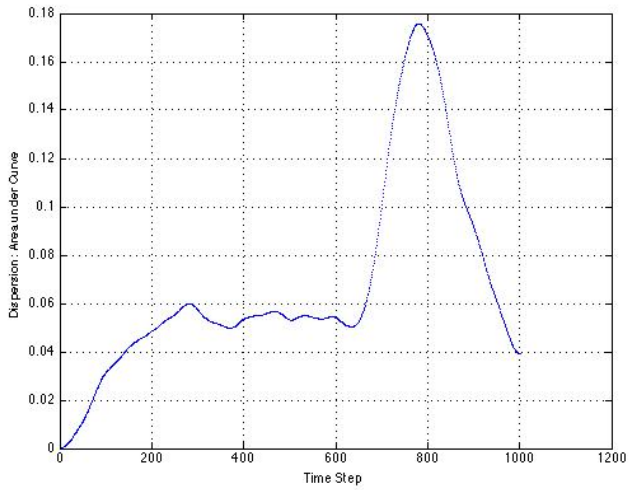

Figure 8.14: Area under the wave curve as a measure of dispersion.

The solutions in two-dimensions, depicted in the illustration below, similarly corroborate. The solution behaves as expected and most importantly, the degree of convergence can be more easily perceived.

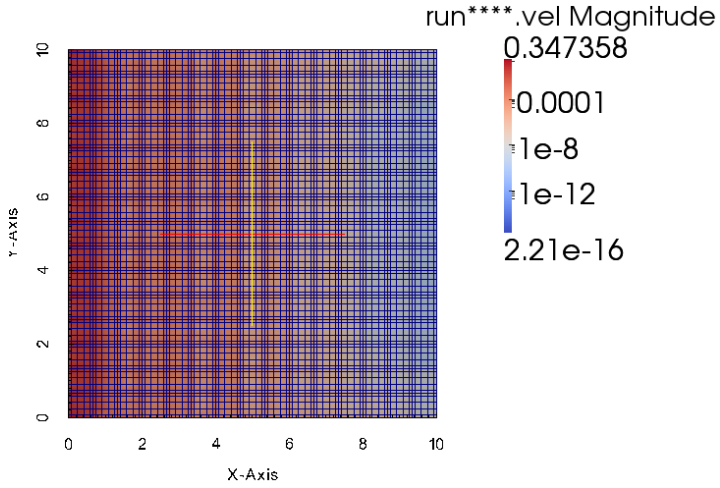

Figure 8.15: Velocity magnitude at t= 0.00125 s for a 225-element model.

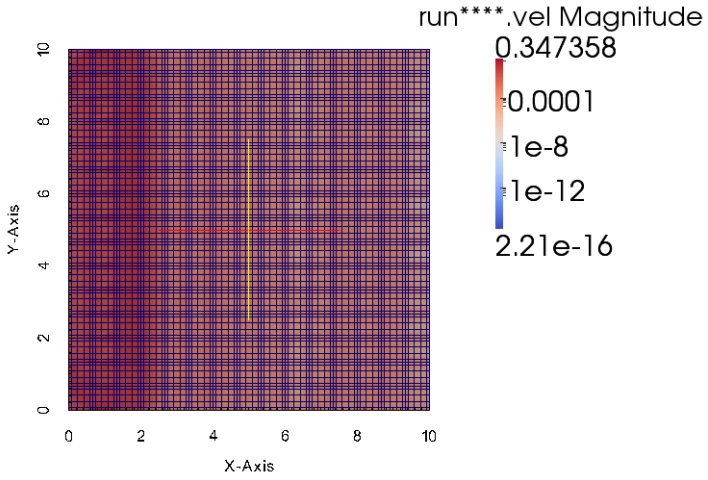

Figure 8.16: Velocity magnitude at t= 0.00316 s for a 225-element model.

8.1.4 SEM Solution Using 400 Elements With One-Dimensional Basis Of P=5 And 101 Nodes Spread Linearly Across

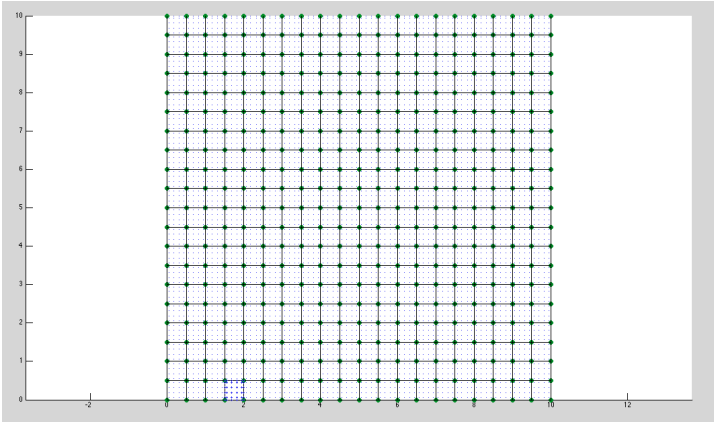

Figure 8.17: SEM: 400 elements (101 nodes across in both directions).

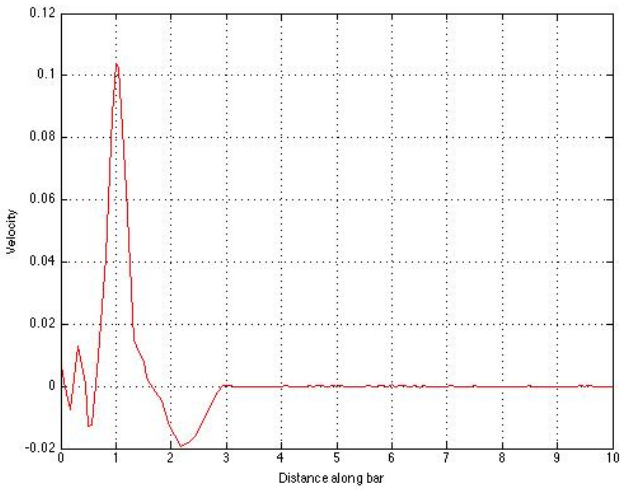

Figure 8.18: Wave Propagation using 100 elements, 51 nodes spread linearly across in both directions.

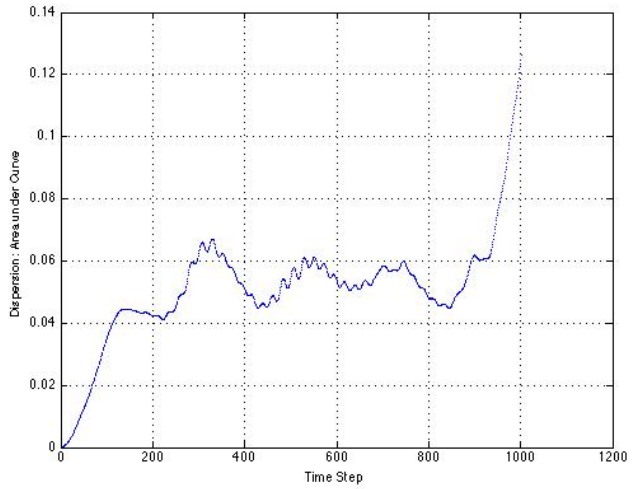

Figure 8.19: Area under the wave curve as a measure of dispersion.

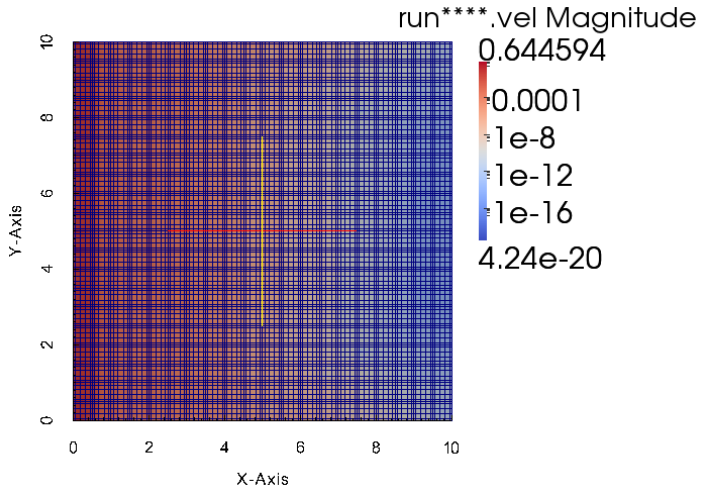

Figure 8.20: Velocity magnitude at t=0.00124 s.

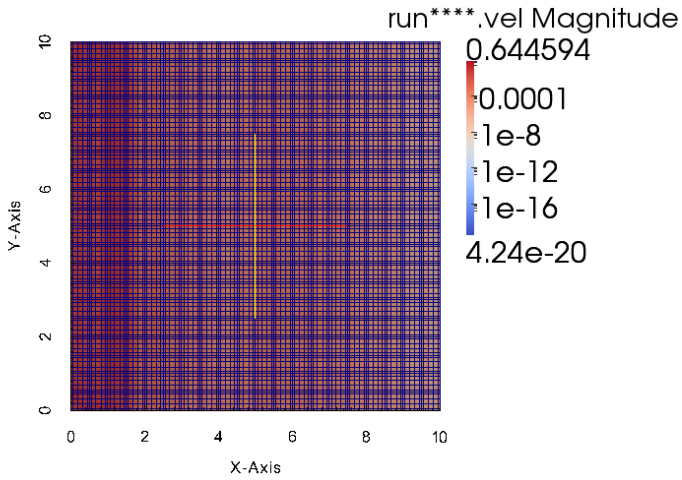

Figure 8.21: Velocity magnitude at t=0.00316 s.

8.1.5 SEM Solution Using 1600 Elements With One-Dimensional Basis Of P=5 And 201 Nodes Spread Linearly Across Both Directions

This last scenario has resulted with very interesting considerations. The wave propagation in the x-direction has resulted in values considerable close together. It had been previously mentioned that actual convergence to a solution was not possible due to the underlying formulation the system was set

up on top of. Numerical noise is still present in what can be considered its lowest level throughout what has been our set of models. Lagging wave oscillations seemed to have augmented, however, not much information regarding this can be inferred as the duration of the test has been rendered unpractical due to the high computational cost (model ran for approximately two hours to model 0.01 seconds of the wave propagation behavior.) In consequence, the reader is suggested to find different techniques to assess in a more practical manner the correct behavior of the material.

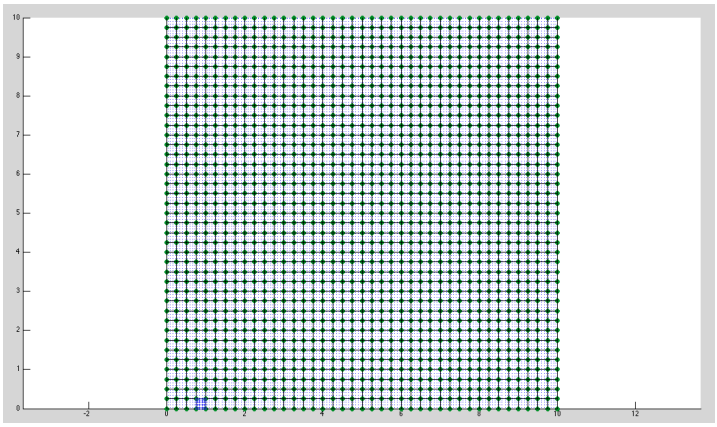

Figure 8.22: SEM: 1600 elements (201 nodes across in both directions).

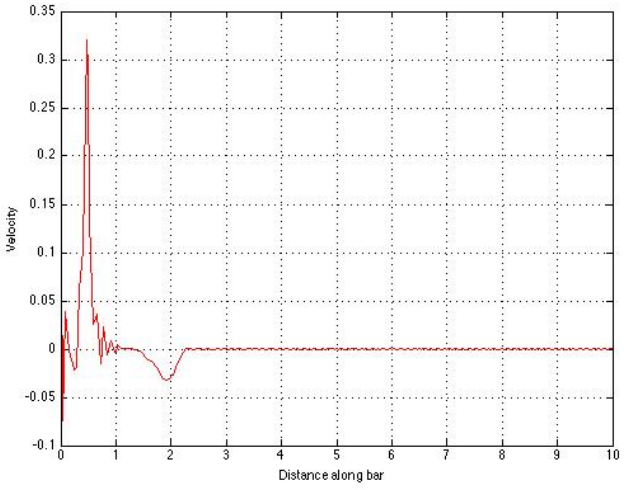

Figure 8.23: Wave Propagation using 1600 elements, 201 nodes spread linearly across in both directions.

The dispersion level seem to have suffered an augmentation from the previous scenarios, this may in part be consequence of the time-integration scheme, whose direct influence on the solution and the system's behavior has been already a focus of discussion.

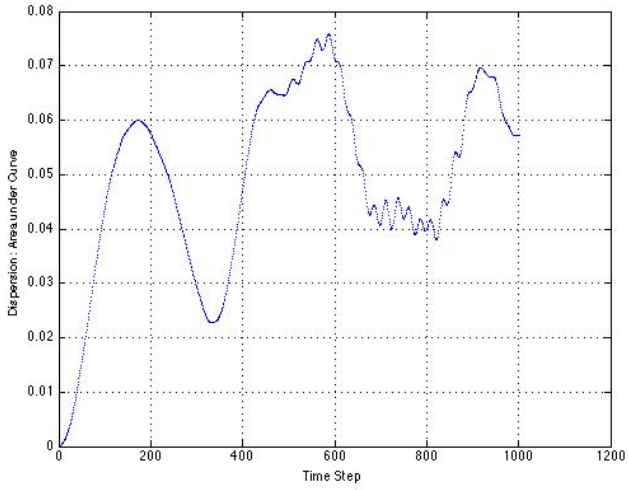

Figure 8.24: Area under the wave curve as a measure of dispersion.

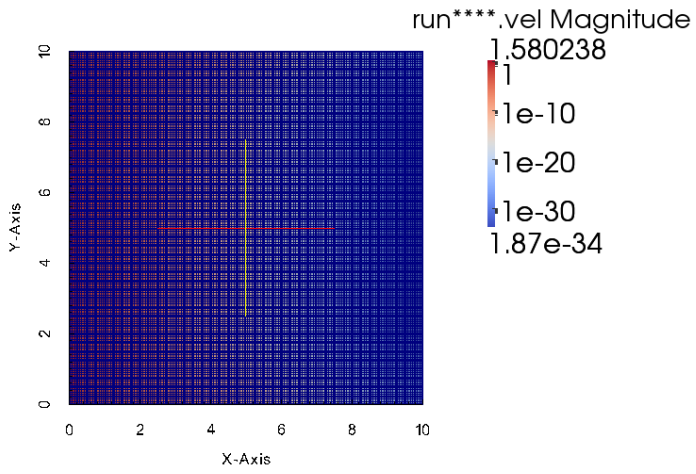

Figure 8.25: Velocity magnitude at t=0.00124 s.

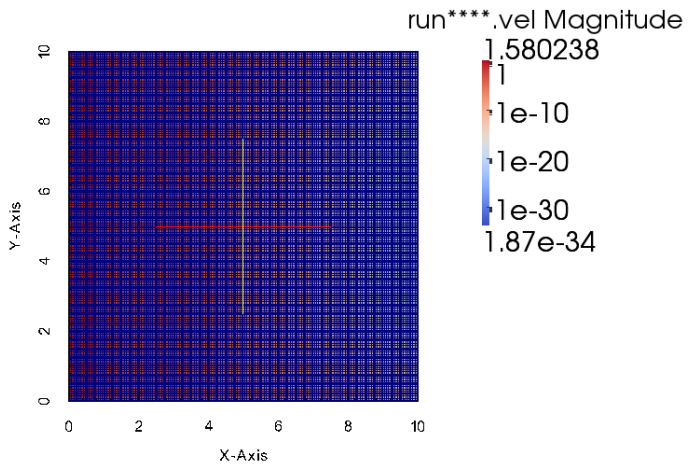

Figure 8.26: Velocity magnitude at t=0.00316 s.

8.2 FINITE ELEMENT METHOD

The turn has come to test our system using the finite element method. Due to the nature of the meshing refinement utilized and lack of the graphical tools we have previously made use of (x-directional wave propagation and dispersion by area) the results are more generally assessed and interpreted, however, the possibility for actual solution convergence is now at the door. The presence of evenly spaced nodes at the left plate boundary allows a correct and effective distribution of the boundary forces.

8.2.1 FEA 228 linear triangular elements

Certain advantages arise from the use of simple linear triangular elements. From a computational point of view, operational time is saved because triangular elements do not have to be mapped to a *master* or *standard* shape in order to be numerically integrated using quadratures. Triangular elements have the advantage of having nice closed-form solutions to the integrals as well as constant-valued B matrices that accelerate the element's stiffness matrix assembly process.

Some of the problems that arise from the use of triangular elements are that high levels of discretization are needed to obtain accurate solutions. Since nodal deployment is often arbitrary, dynamic information conveyed by the system may not be handled effectively. Assessment of the mesh refinement technique in use becomes necessary. The system of choice must be continuously tested to see if the dynamic part of the system is handled correctly, areas that have a larger rate of change in comparison to others demand a higher level of refinement. Likewise, highly-geometrically distorted sections must allocate a higher number of elements or allocate higher-degree triangular elements in order to be correctly processed and modeled.

The FEA model using 228 linear triangular elements is able to quickly generate a model for the two-dimensional wave propagation occurring in the plate. The low number of elements used, however, affects considerably the average values that are obtained through the triangulation of the element's nodal components. This in part forces the system to diverge considerably from the actual results. Values across elements differ considerable so further refinement is suggested. No statements can be made at this point regarding the accuracy of the FE system; this is in part because of the lack of an analytical solution to the problem or a different model to compare against.

Let us now get away from the main topic to introduce another very important subject. Often times, computing an analytical solution is very difficult if not impossible. The analysis is performed by first assuming that the equation is analytically intractable. Our analysis is mainly interested in the relationship between computational effort and the quality of the approximation to the governing PDE. The results of the analysis must be given in terms of cost-benefit. These benefits do not only include the computed numerical approximation but a *quantification* of the quality of the approximation, in other words, an error estimate.

To put things in perspective, let us assume a function y (t) that obeys the ordinary differential equation with its corresponding initial boundary conditions:

$$\frac{\partial y}{\partial t} + \Gamma(y,t) = 0$$

FE and SE methods approximate numerically the value of Y by discretizing the space-time domain into small segments. We select, from a finite dimensional space, the function that approximates the governing differential equation the best at a local level. This means that the best solution is that whose accumulated error has the minimum value within our restricted domain of all possible solutions. For this example, the error calculation would be quantified by the formula e= y-Y, where y is the analytical value and Y is the value of the approximation, however, as we had previously stated we are not always lucky enough to have an analytical solution to the problem in question. This is where norms come into place. A norm is a function that assigns a length or size to all vectors in a vector space. The norm may be chosen to quantify an error at a particular point in the space-time domain or an average over the continuum.

In classical *a priori* error theory, the error estimation is calculated before computing any solutions. This can be done by bounding the error produced in the first calculation step by means of Taylor's theorem. This allows the error accumulation (total error) to be similarly bounded. The effect of the perturbation in a solution can be analyzed by linearizing the differential equations within the bounds of the solution space. The *Jacobian* (whose importance we had previously discussed) is the coefficient matrix for the linearized solution system. The Jacobian matrix allows us to state the error bound as:

$$\|e\| \leq e^{J_{Max}t} \max \tau$$

Equation 8.1: Global Error Bound

where τ represents the interpolation error. This is the traditional form of the *a priori* error bound. A list of unknowns and intractable quantities arise. Among these, we encounter the higher-order derivatives from the Taylor approximation and the range of the solution required to calculate J_{max}. This type of quantification method offers us a bound that is different in hundreds of orders of magnitude, we need to describe an alternative way to compute the error bound such that the difference is in a factor of two or three within the true error. This means that the linear system must be solved for each error estimate, it is an *a posteriori* bound, this means that the error is computed after the solution has been approximated. *A posteriori* bounds are composed of two parts. The first parts measures the error at a local level while the other part measures the effects of error accumulation.

How well do we approximate the actual solution? This question can only be answered through the use of Taylor's theorem; unfortunately its computation is difficult and often impractical. We can, nonetheless, rephrase the question without losing the information that we wish the answer to convey, "How well do we approximate the differential equation?" the answer is simple and lucky enough for us, it is also easy to compute. The residual R describes the amount of error in the approximation to the governing differential equations by our computed solution.

$$R = \left\| \quad \dot{Y} + f(y,t) \quad \right\|$$

Equation 8.2: Residual

The quantity is fully compatible and it is naturally decomposed into space and time residual errors. There is a relationship between the residual and the error bound. It generally summarized with the following formula:

$$\|e\| = S(t) \max R$$

Equation 8.3: Error bound

where S is the stability factor. There are different stability factors depending on the type of error. There are errors due to meshing or spatial discretization and errors due to incorrect modeling of initial conditions.

We will now take some time to draw an analogy between the recently explained error bounds and the process of solving a generic system of linear equations of the form Ax = b, where A is a coefficient matrix and x and b are column vectors. In order to determine the quality of our approximation the direct approach would involve computing the error || X-x ||, where X is the approximate solution, which we have explained is often not computable. The alternative method is to focus on the residual || AX-b ||. The relationship between the error and the residual is determined by the conditioning number. The stability factor plays out the same role when referring to differential equations. Stability factors are not explicitly computable because they are a function of the unknown solution, we can nonetheless approximate stability values using the numerical approximation to the differential equations. The study of why and how these approximations work is a topic of current research.

The assessment of a system's performance cannot be based solely on mesh refinements and/or modification to the time steps size until the system seems to have converged. A system's performance analysis must be conformed by an accurate numerical approximation supported by enough numerical evidence to prove that the approximate solution will not change considerably if further discretization of both the spatial and temporal domains occurs. Even inaccurate systems, after a certain level of discretization, may give the false impression of convergence. Brute-forcing systems to show convergence by discretizing the system excessively both spatially and temporally is counterproductive since the approximation may result excessively accurate, this would mean that more resources than needed were allocated to the operation and had there been correct identification of the system state it could have been possible to make the operation more cost-efficient.

Now it's time to return to the discussion of our finite element model focusing on its accuracy assessment. For the system that we have been developing, two main problems arise due to the lack of an analytical solution or a simplified method of obtaining it. Lack of an exact solution means that recovery based error estimators are not available, unless a thorough and exhaustive analysis is performed to "recover solutions" using Superconvergent Patch Recovery techniques (SPR). This only permits us the use residual based error estimators. The second problem is that residual based error involves approximating an equilibrium flux by minimizing the residuals and it can only be done so up to an undetermined constant. We note that the non-uniqueness of the solution represents the non- uniqueness of the equilibrium status of the element residuals. The choice of the arbitrary constant in solving will certainly affect the accuracy of the recovered solution and therefore the accuracy of the error estimator.

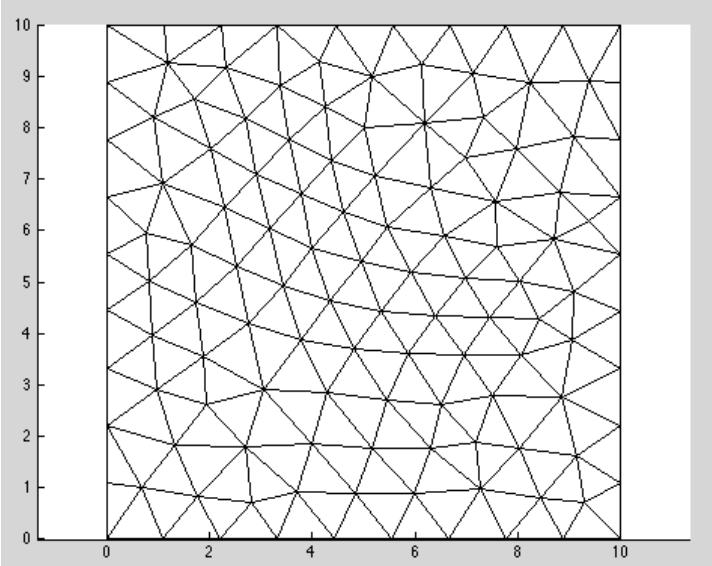

Figure 8.27: FEA: 228 linear triangular elements.

The following set of figures (Fig.[8.28-30]) were taken at exact times in order to graphically compare how the system was behaving. It is important to mention that at the low level of discretization presented the system is able to provide a well-behaved solution at a low computational expense.

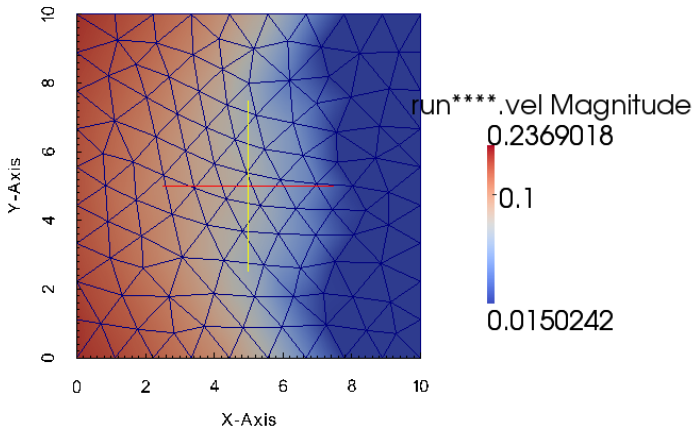

Figure 8.28: Velocity Magnitude in the plate at t=2.5e-5s

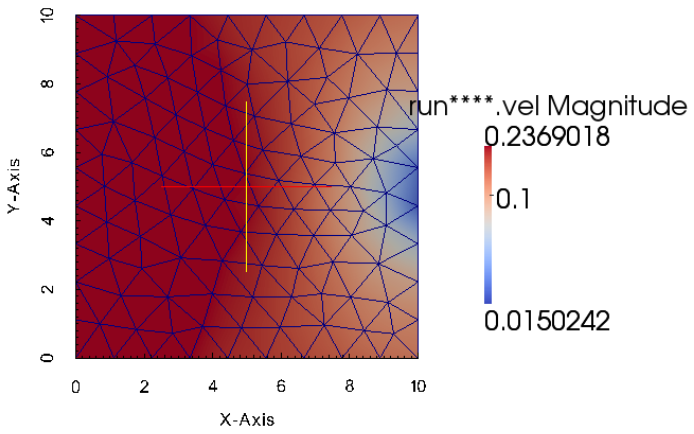

Figure 8.29: Velocity Magnitude in the plate at t=0.000134s

The need for mesh refinement results immediately obvious during the graphical analysis of the velocity values in the x-direction. Values near the boundary condition should be null due to the fixed condition of the right end of the plate, but due to the triangularization between the nodal components to obtain the element's average value the results quickly scalades and is no longer able to recreate the boundary conditions.

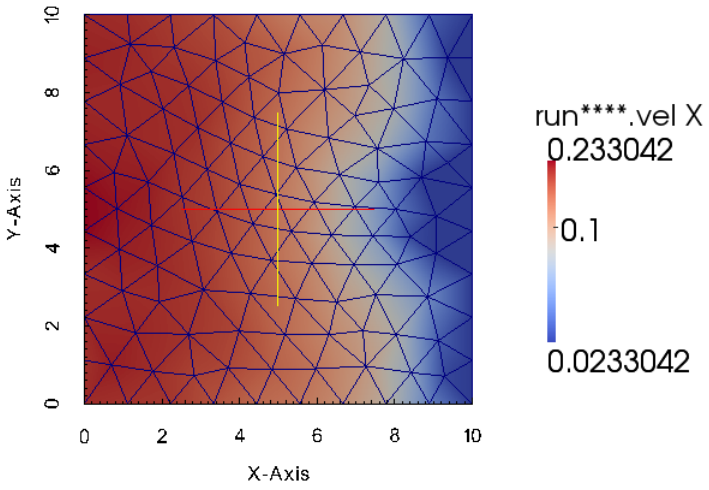

Figure 8.30: Velocity (X-direction) in the plate at t=0.000394s

8.2.2 FEA 857 linear triangular elements

The next mesh refinement that takes place doubles the number of elements distributed across the boundaries and almost quadruples the number of elements across the domain. Significant improvement in the representation of the wave propagation is immediately shown. The system is now able to recreate the boundary conditions more accurately for both velocity plots. It is even possible to see traces of convergence up to at least two significant figures, however, further spatial and temporal refinement are encouraged since the conditioning number increases with the number of elements and the solution systems become more unstable and difficult to predict.

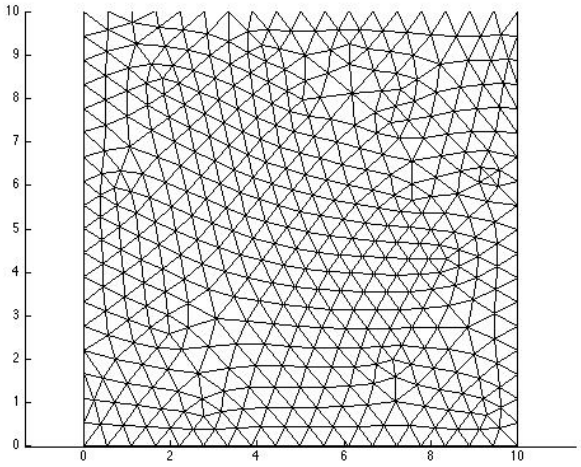

Figure 8.31: FEA: 857 linear triangular elements.

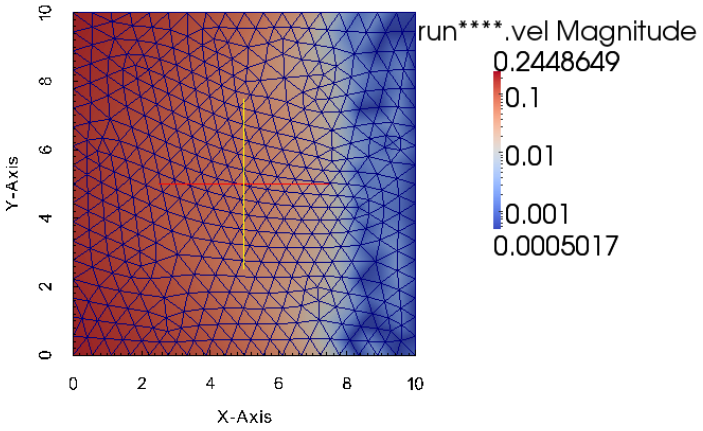

Figure 8.32: Velocity Magnitude in the plate at t=2.5e-5s

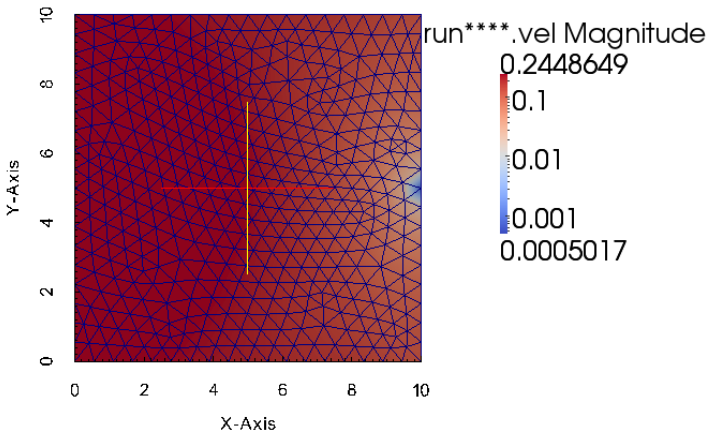

Figure 8.33: Velocity Magnitude in the plate at t=0.000134 s

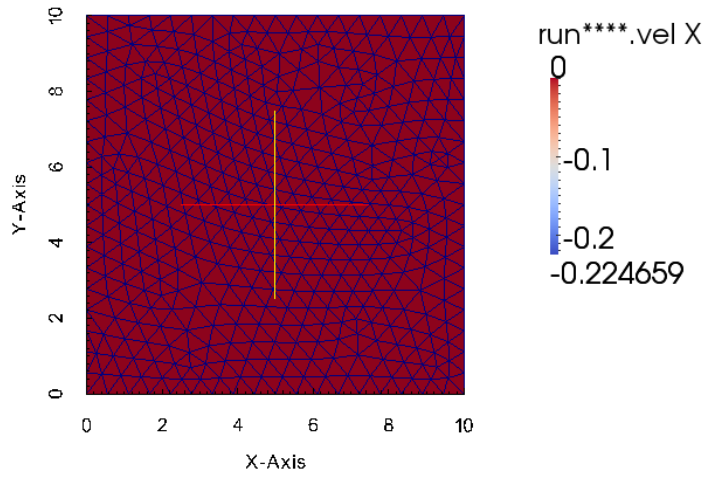

Figure 8.34: Velocity Magnitude in the plate at t=0.000394 s

The solution seems to behave differently than at the previously depicted time steps. The mesh refinement had to be accompanied by a significant reduction in the order of the time step. This was able to reduce the erratic behavior presented when only the spatial discretization had taken place. The computational expense was considerably larger and the solution time was several orders of magnitude larger than for the original 228 triangular elements.

8.2.3 FEA 3432 linear triangular elements

Further discretization took place. The system was increased by a factor of almost 15. The first figures depict that the boundary conditions were recreated almost perfectly, however, the convergence state we had previously reached is no longer present. The magnitude of the velocity calculated is several orders smaller. The solution does seem to behave with respect to the governing wave equation. It is important to mention that to obtain the solution the time step was further reduced which increased considerably the computational time, it might have even rendered the whole process little to non-practical.

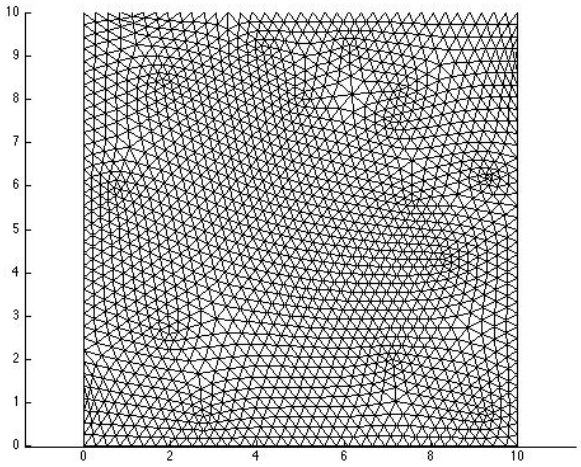

Figure 8.35: FEA: 3432 linear triangular elements.

A new method to assess the model's performance must be developed. The solution process involves many factors other than spatial discretization. To properly assess the model's performance it becomes necessary to modify the time step and perhaps to even consider the modification of the type of time integration scheme used to see if any conditioning problems will exist if further refinement takes place because of compatibility issues.

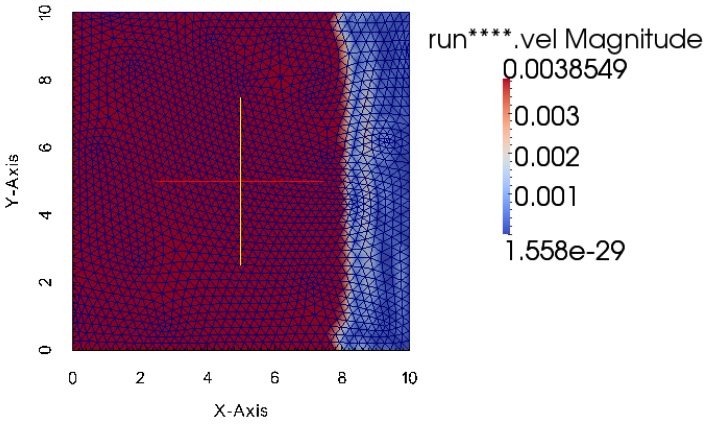

Figure 8.36: Velocity Magnitude in the plate at t=2e-5s

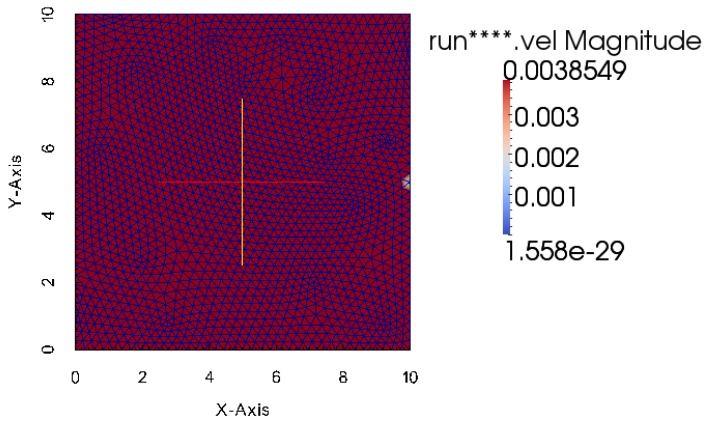

Figure 8.37: Velocity Magnitude in the plate at t=0.000134

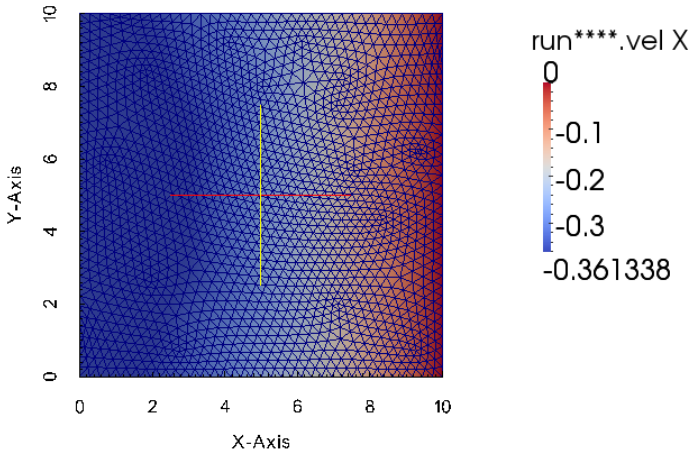

Figure 8.38: Velocity Magnitude in the plate at t=0.00015s

It is necessary to conclude that as further refinement of both the temporal and spatial domain took place overall improvement of the solution behavior occurred. Unfortunately, this can only be stated up to a certain point. As the system's size increases, conditioning problems become too significant to ignore. A proper assessment cannot be casually performed by checking if values converge or reach a certain threshold. There are too many factors that need to be described and quantified to add credibility to the system's response assessment.

Graphical analysis methods are easy to perform but they lack the fundamental tools of numerical analysis. Error estimation methods based on a strong theoretical background should be implemented because they convey much more information regarding the underlying numerical performance of the system. Unfortunately, for this last section no definite answer exists. A statement regarding which method is better at handling wave propagation problems in two dimensions would be irresponsible at this point. Further analysis must be performed. This in-depth analysis should involve domains with

complex geometries, different time integration schemes, different temporal and spatial discretization techniques, proper error estimation methods, and if possible, testing of the models using well-known scenarios that have a closed-form solution, this would in part direct our attention to the recovery-based error estimation approach since there would be already expected values to compare with.

Chapter 9: 2-D Dissipation and Dispersion

For this section we will present an analysis on the dissipative/dispersive performance based on a two-dimensional long-range wave propagation scenario. The scenario is basically analogous to that previously presented for the one-dimensional case, however, we now deal with a tenfold increase in longitudinal plate's direction. As was previously explained, this increase is in part to have a wavelength that is considerably smaller such that boundary conditions do not affect the wave propagation inside the domain in question, which is in turn a rough representation of wave propagation through an infinitely large medium.

To compare the performance, we will once again make use of a time series but this time it will consist of a two-dimensional colored plot that allow us to see the wave propagation pattern followed by the models at specific time intervals.

Since we do not have an analytical solution to compare against, we will try to look for certain characteristics that indicate a good solution performance. If the method is performing correctly, there should be some convergence of the resulting values between each of the scenarios. Likewise, a wave propagation that is not significantly subjected to dispersion/dissipation errors should be depicted graphically by a shifting uniform color that does not change considerably in shape and that shows no exaltations in color near the travelling wave.

9.1 FEM

For the FEM, we have tested the scenario using 78, 308, and 1224 linear triangular elements. The images that compose the time series were captured at the following times: t= 1e-5, 0.0001, 0.0002, 0.0003, 0.0004, and 0.00045 seconds.

9.1 FEM: 78 Triangular Linear Elements

The solution using a very coarse mesh behaves relatively well, however presence of dispersion is shown by the exaltation in color following close behind the portion with the highest velocity (projected wave), this is depicted in illustration shown next, more specifically in parts d, e, and f. Presence of dispersion is likewise presented and it's considerable. This can be quickly perceived by sudden changes in color and by the continuously changing shapes and sizes of the propagating 'spot.'

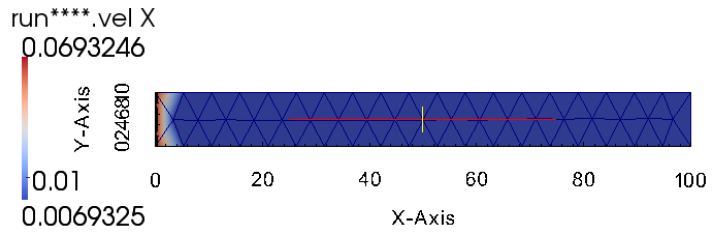

a)

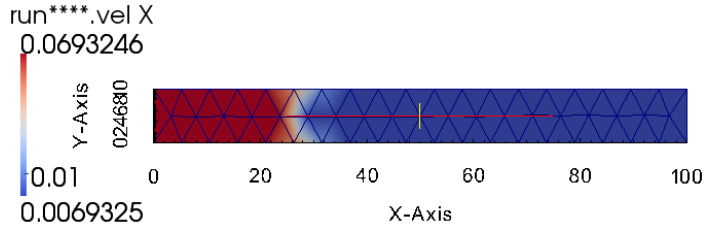

b)

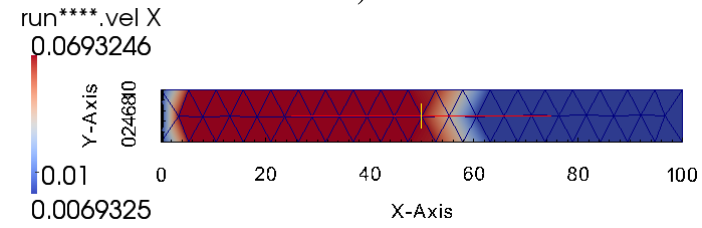

c)

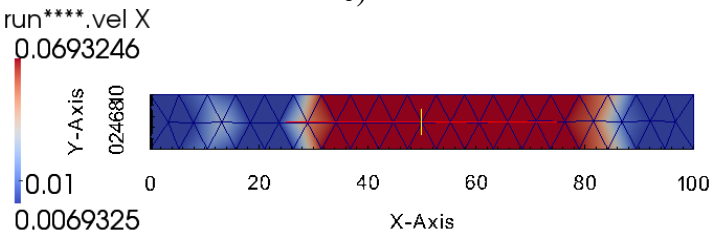

d)

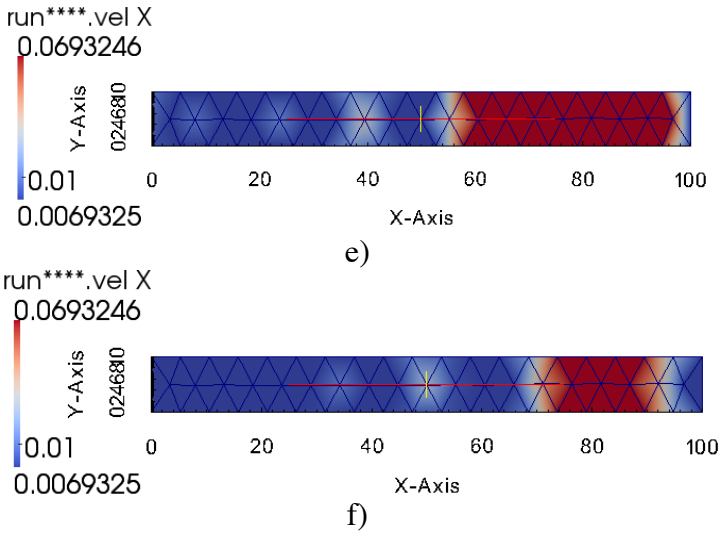

Figure 9.1: 78 linear triangular elements a) t= 1e-5s b) t= 0.0001 c) t= 0.0002 d) t= 0.0003 e) t=0.0004 f) t= 0.00045 seconds.

9.2 FEM: 308 Triangular Linear Elements

Further discretization of the domain in question, almost a fourfold increase in this case, does not effectively reduce the presence of dispersion, it does, however, improve the dissipation level by allowing a more constant-sized and uniformly-colored shape traverse the plate. The maximum velocity seems to be in the same order as that previously presented which indicates some level of convergence, which is always an indicator we are heading in the right direction.

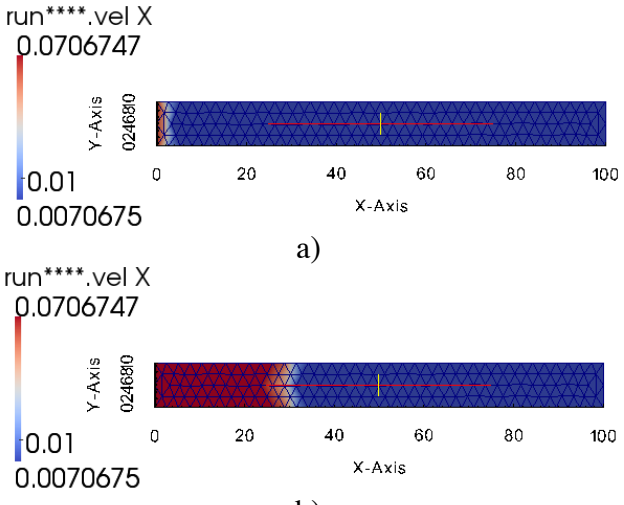

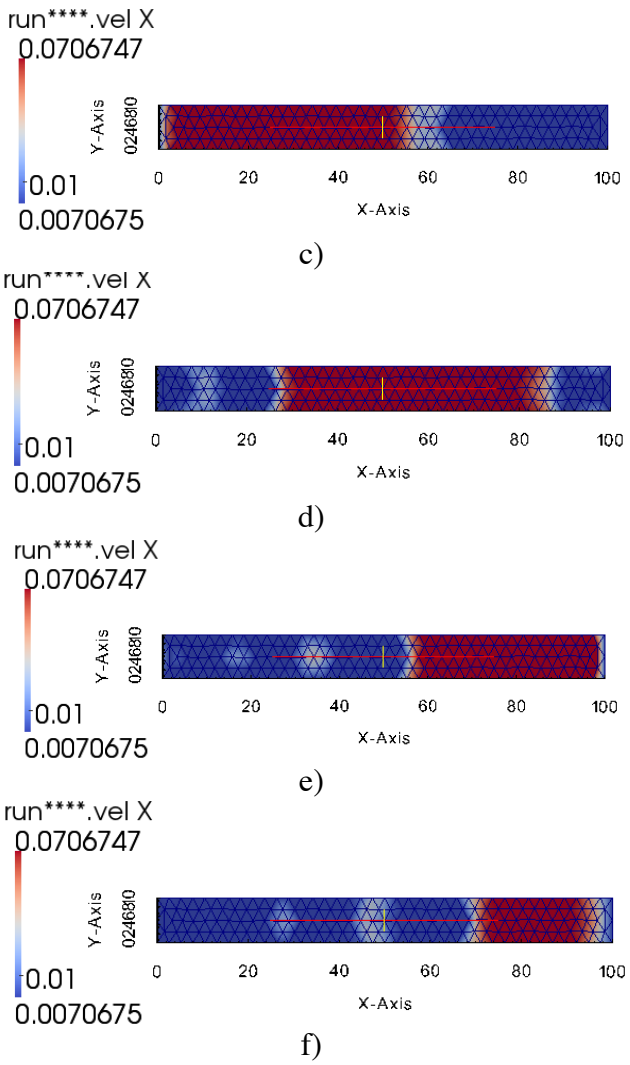

Figure 9.2: 308 linear triangular elements a) t= 1e-5s b) t= 0.0001 c) t= 0.0002 d) t= 0.0003 e)t=0.0004 f) t= 0.00045 seconds.

9.4 FEM: 1224 Triangular Linear Elements

By quadrupling the number of elements from those used in the previous scenarios we are able to reduce the level of dispersion presented and there is an improve in the overall dissipation, the traversing wave seems to keep a constant-sized and uniformly-colored shape. An important note must be made here. Even though the maximum value shown is of a considerable higher order than those that had previously resulted, this is 'error' is to be attributed to the post-processing software as strange behavior tends to take place as the system size increases. This is a continuous indication that two-dimensional

problems indeed pose a high computational expense and that should be dealt with using effective computational tools.

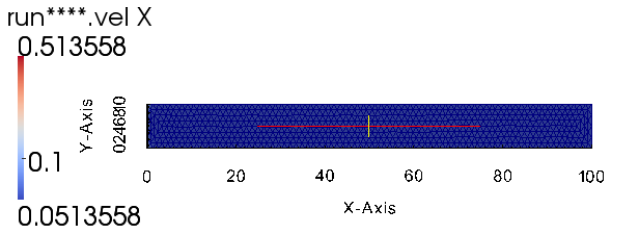

a)

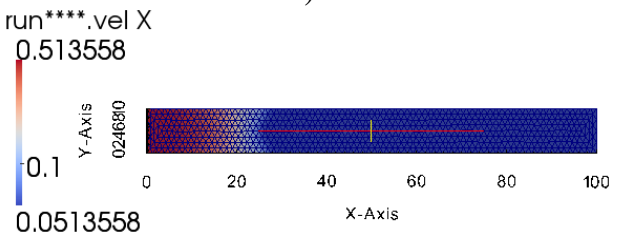

b)

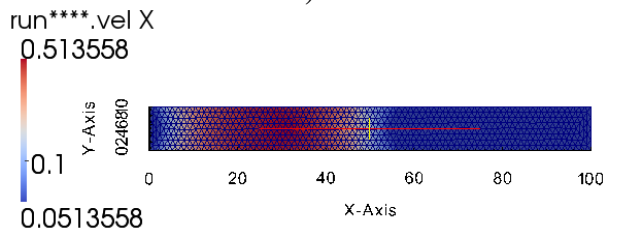

c)

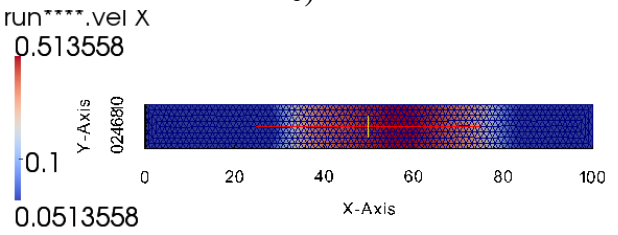

d)

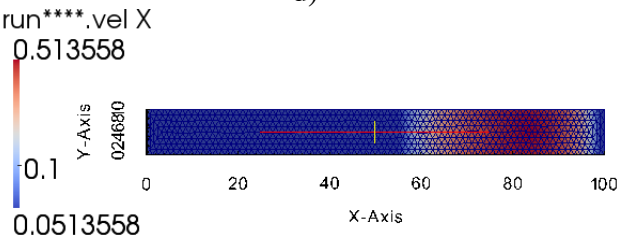

e)

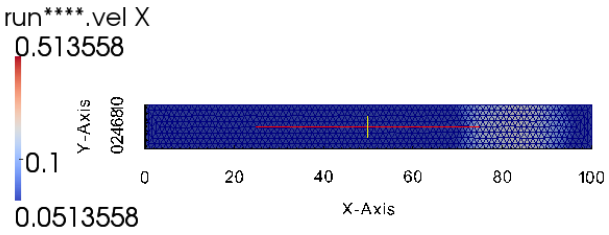

f)

Figure 9.3: 1224 linear triangular elements a) t= 1e-5s b) t= 0.0001 c) t= 0.0002 d)t=0.0003 e) t= 0.0004 f) t= 0.00045 seconds.

9.2 SEM

As we mentioned during the introductory part of this chapter, a response to the presence of dispersion and dissipation has been the use of spectral elements. The spectral elements are high-order elements that are able to detect the quick changes in the behavior of the solution, which in turn results in a higher accuracy level. Needless to say, the models here presented are analogous to those previously described. The scenarios tested were the following:

1. 400 SE model based on a 1-D 3rd order polynomial basis.
2. 900 SE model based on a 1-D 3rd order polynomial basis.
3. 400 SE model based on a 1-D 4th order polynomial basis.

The spectral elements for this section are composed by 16 and 36 nodal points depending on the interpolation order. The resulting systems are consequently very large in size and the computational expenses are considerably larger than those for the FE solutions. Let us analyze now if the extra effort is compensated by a more accurate and stable solution.

9.2.1 400 SE model based on a 1-D 3rd order polynomial basis

As can be seen in the following illustration, spectral elements do have a lower dissipative behavior. The low dissipation can be identified by the uniformly colored shapes that propagate parallel to the wave direction [illustrated in b, c, d, and f]. It is immediately obvious, however, that the system

contains a high level of dispersion that increases considerably as the simulation progresses. Common indicators of dispersive behaviors, as was previously mentioned, are depicted by the multiple color exaltations that appear that lag behind the travelling wave. This spectral element solution is not very efficient in the long run. The traversing waves seem to merge together and distinction between the original wave and the numerical noise is no longer possible.

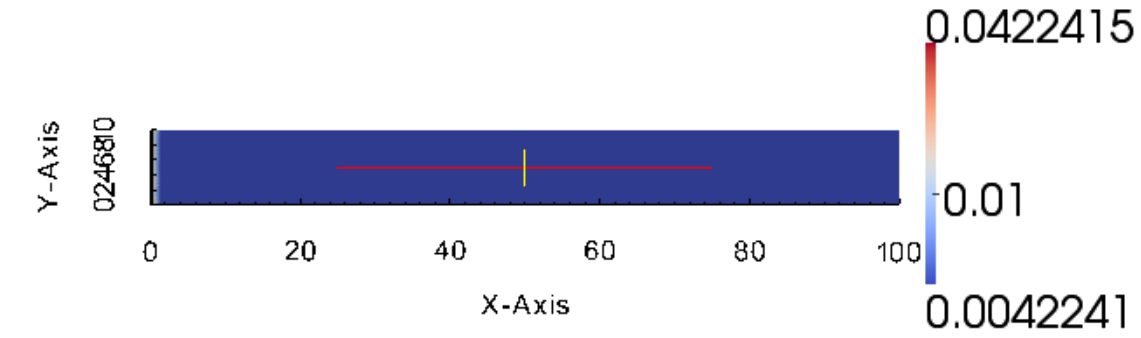

(a)

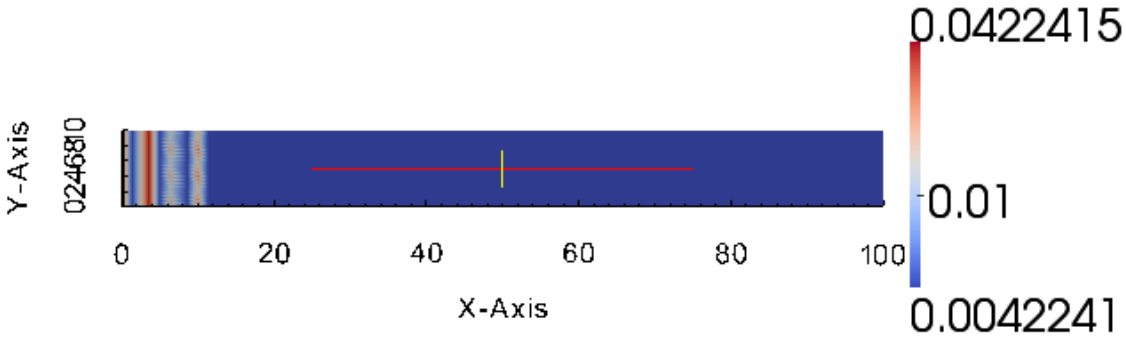

(b)

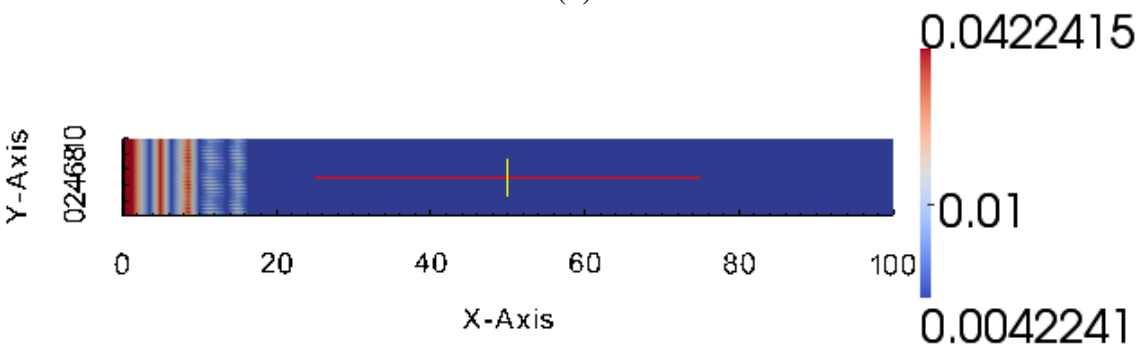

(c)

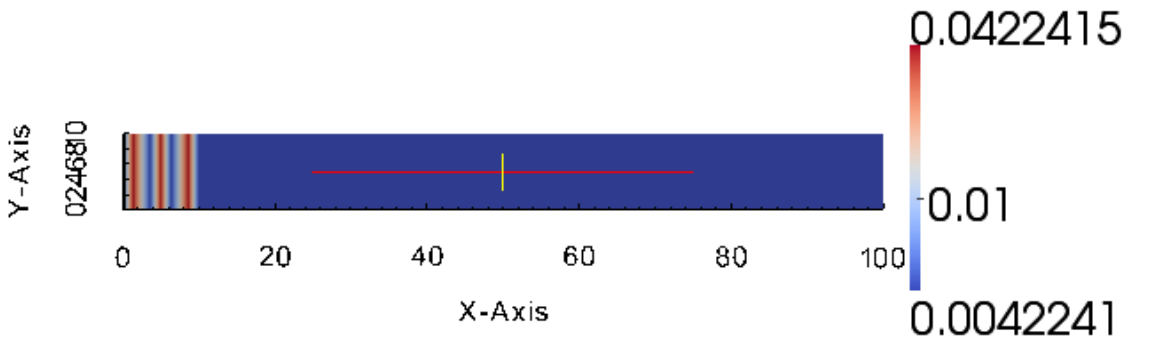
Y-Axis
0246810
0
20
40
60
80
100
X-Axis
0.0422415
0.01
0.0042241

(d)

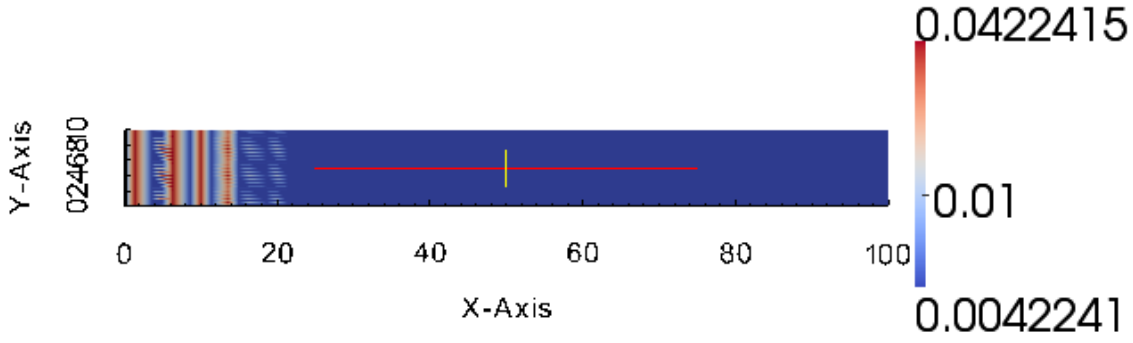
Y-Axis
0246810
0
20
40
60
80
100
X-Axis
0.0422415
0.01
0.0042241

(f)

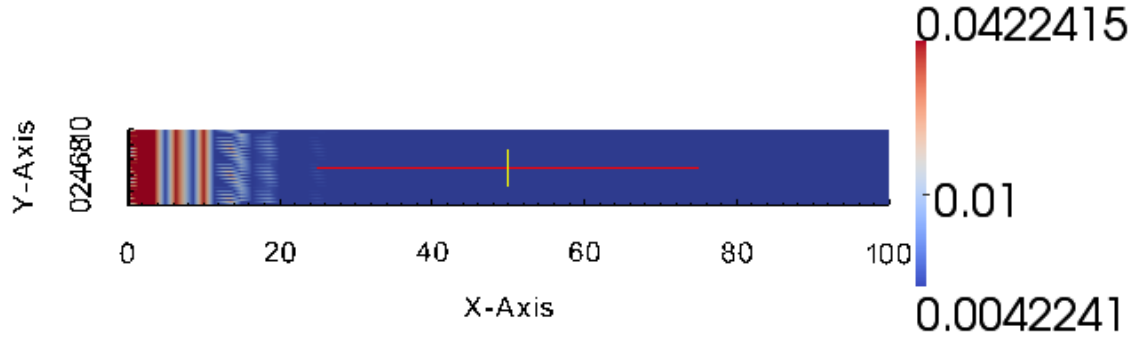
Y-Axis
0246810
0
20
40
60
80
100
X-Axis
0.0422415
0.01
0.0042241

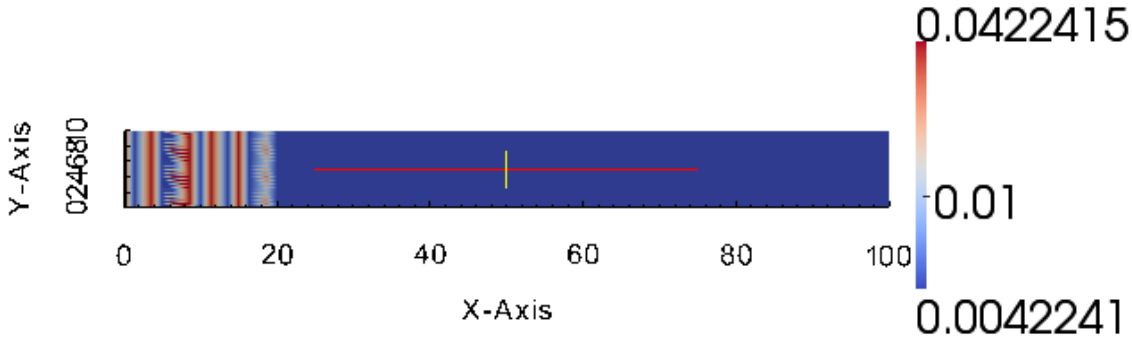
Y-Axis
0246810
0
20
40
60
80
100
X-Axis
0.0422415
0.01
0.0042241

(g)

(h)

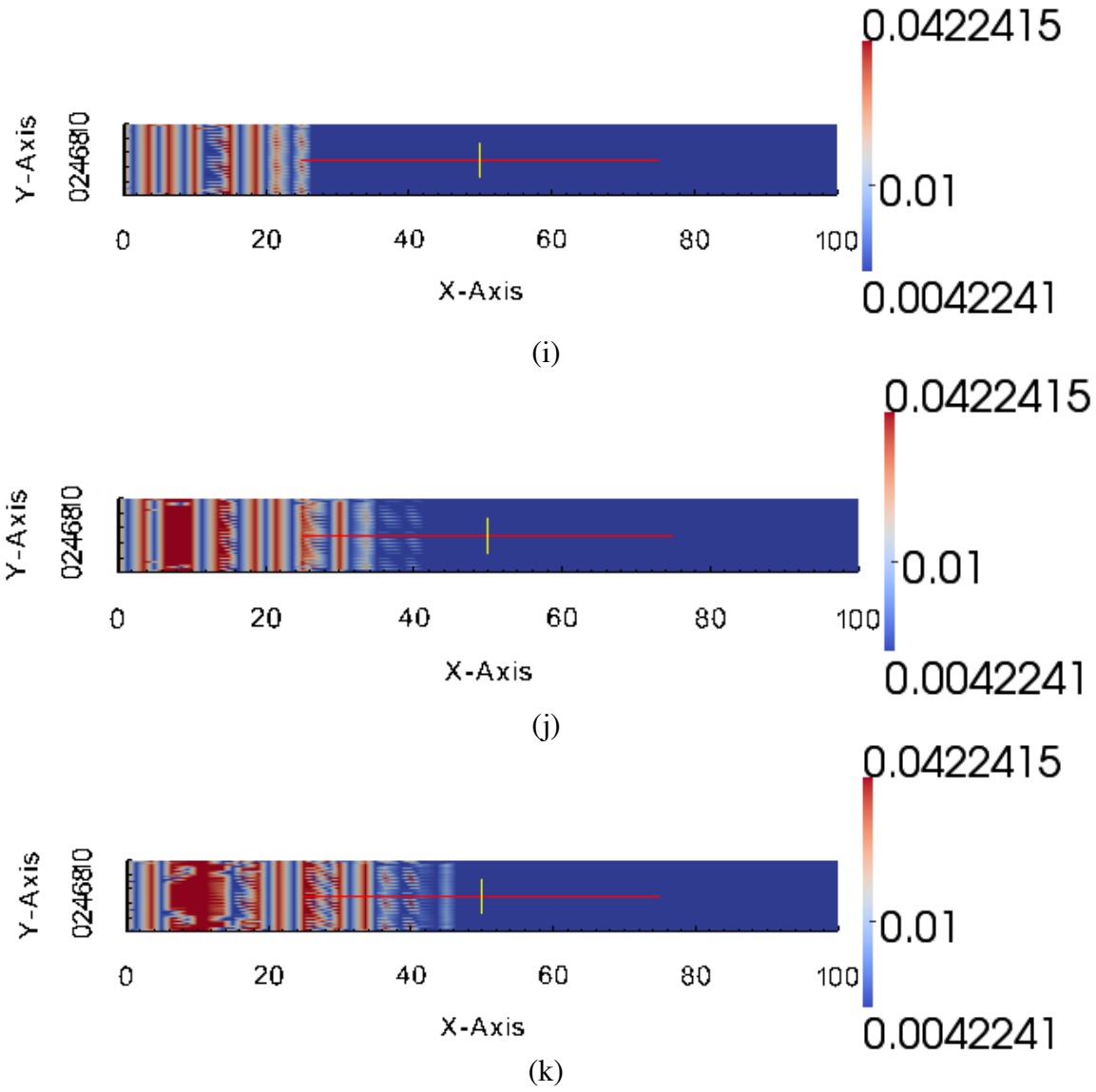

Figure 9.4: 400 SE model based on a 1-D 3rd order polynomial basis a)t=1e-5s b)t=0.0001 c)t=0.0002 d)t=0.0003 e)t=0.0004 f)t=0.0005 g)t=0.0007 h)t=0.001 i)t=0.0015 j) t=0.002 k)t=0.0025

9.2.2 900 SE model based on a 1-D 3rd order polynomial basis.

Further mesh refinement is able to reduce the magnitude of dispersion considerably; it attenuates the exaltations but only for a short period of time. Dissipative behavior is still present and is significant enough to deteriorate the traversing shapes in the long run. Computational cost increase is significant enough in comparison to the previous scenario, overall improvements are not. Let us now test the last

scenario by increasing the polynomial order basis and analyze whether significant improvements take place.

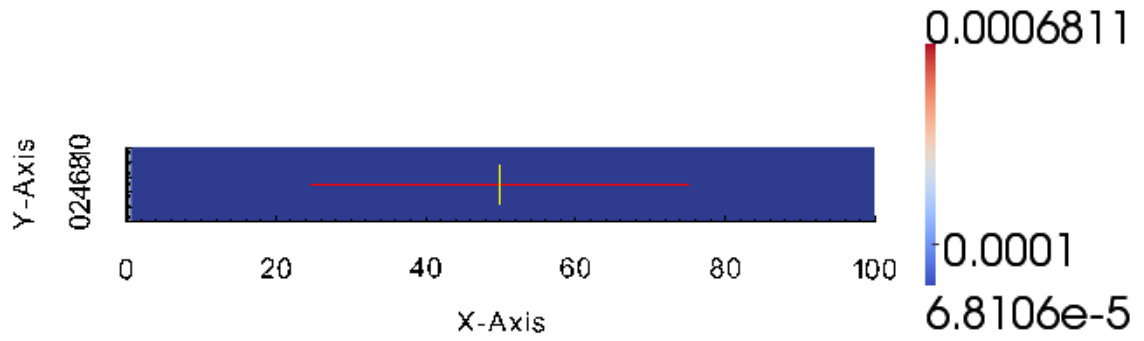

(a)

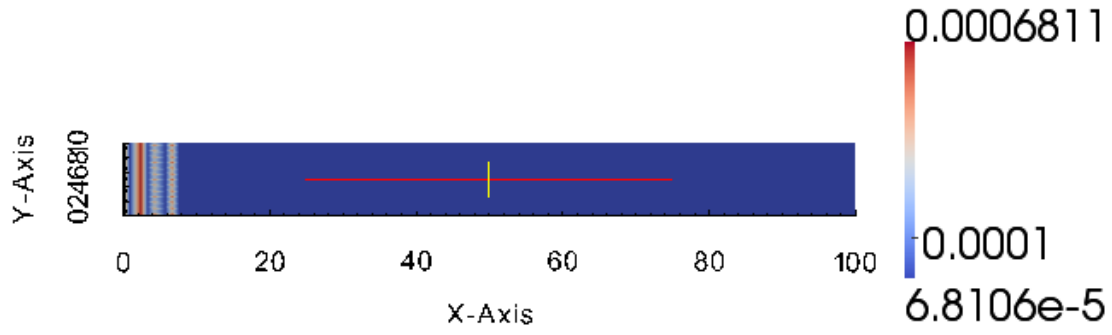

(b)

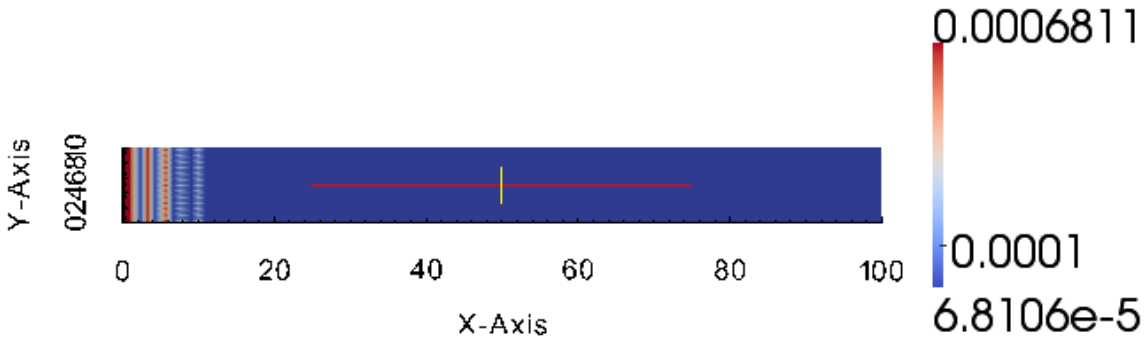

(c)

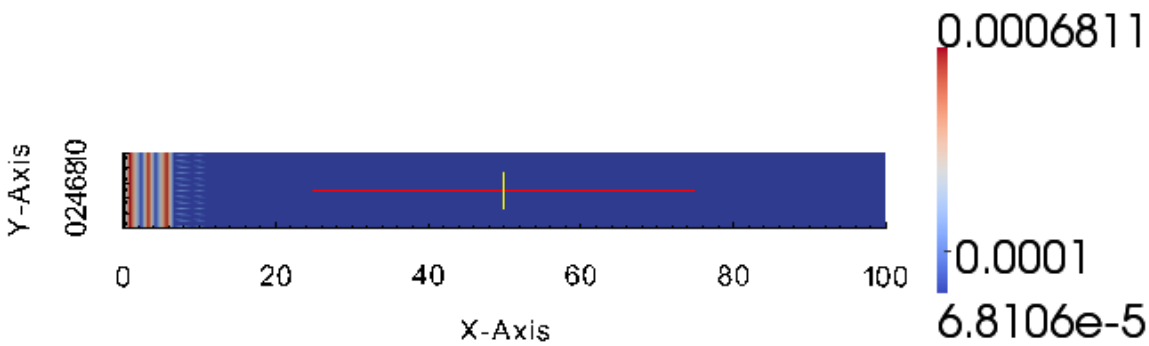

(d)

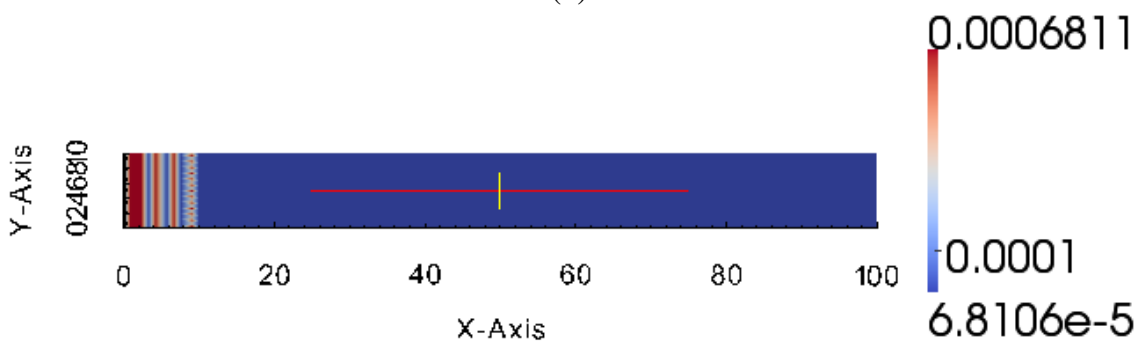

(e)

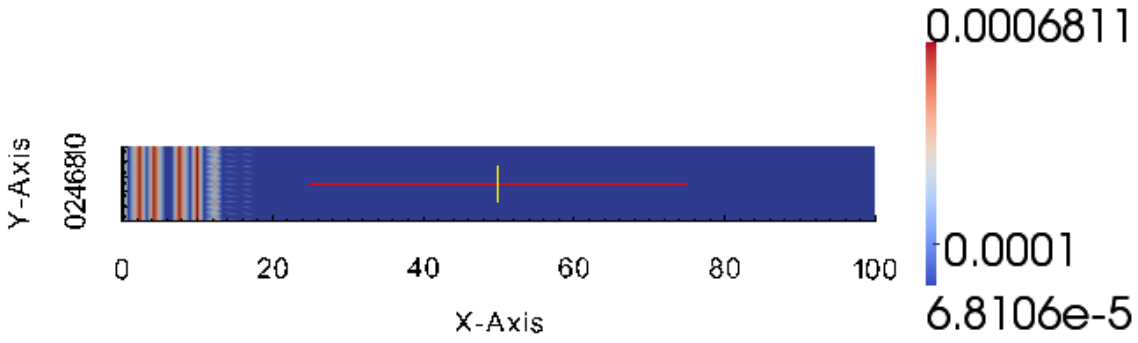

(f)

Figure 9.5: 900 SE model based on a 1-D 3rd order polynomial basis a)t=1e-5s b)t=0.0001 c)t=0.0002 d)t=0.0003 e)t=0.0004 f)t=0.0005

9.2.4 400 SE model based on a 1-D 4th order polynomial basis

The resulting solution has a nice overall behavior, it has decreased dissipation but unfortunately, erratic behavior still seems to increase with respect to time. In order to counteract this, it would be necessary to further discretize the domain. Unfortunately, by increasing the system's size we are forced to decrease the time step considerably. This renders the system very unstable and the computational cost too high. It is important to mention, once again, the visualization problems that arise because of the system size. The resulting plots need continuous updating and rescaling otherwise the information displayed does not accurately capture what is actually taking place. This may lead to

incredible loss of information in the plot and consequently an incorrect perception and interpretation of the actual behavior.

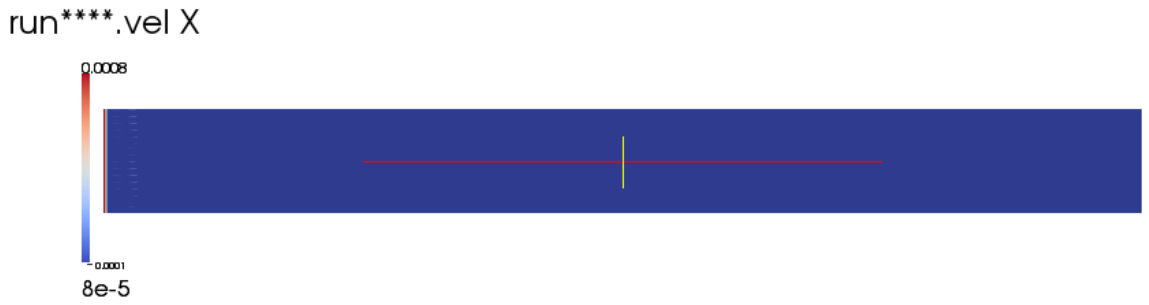

(a)

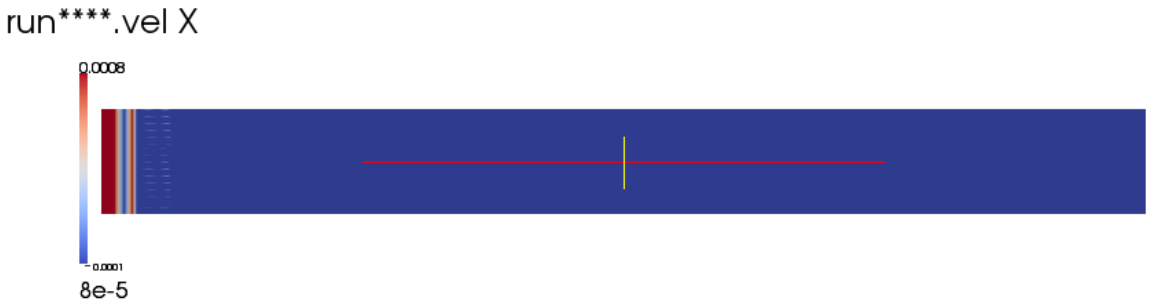

(b)

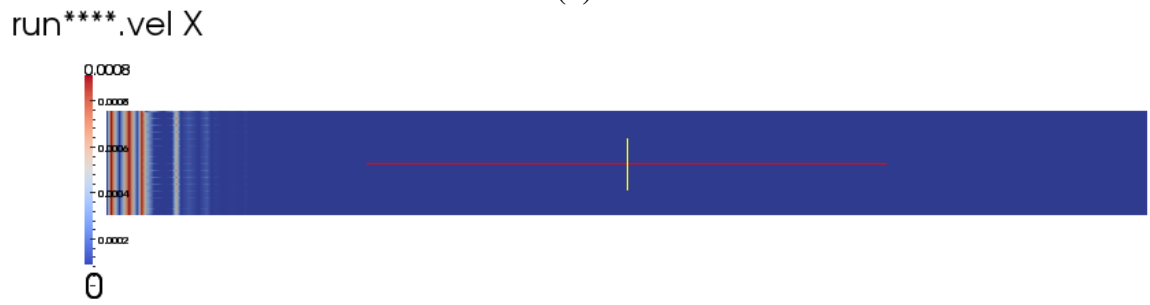

(c)

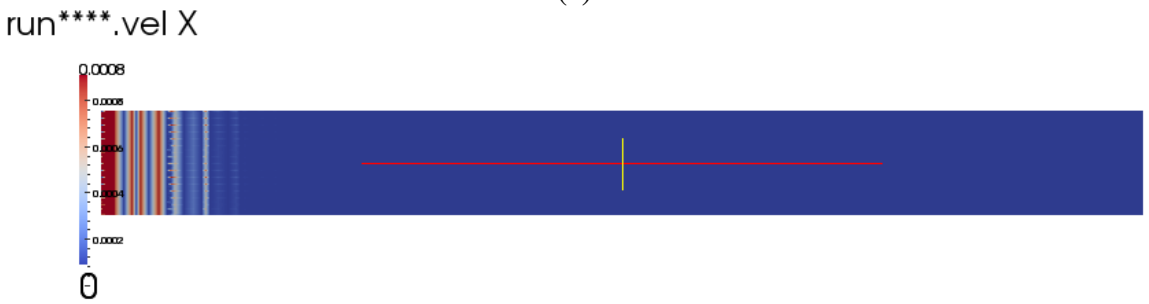

(d)

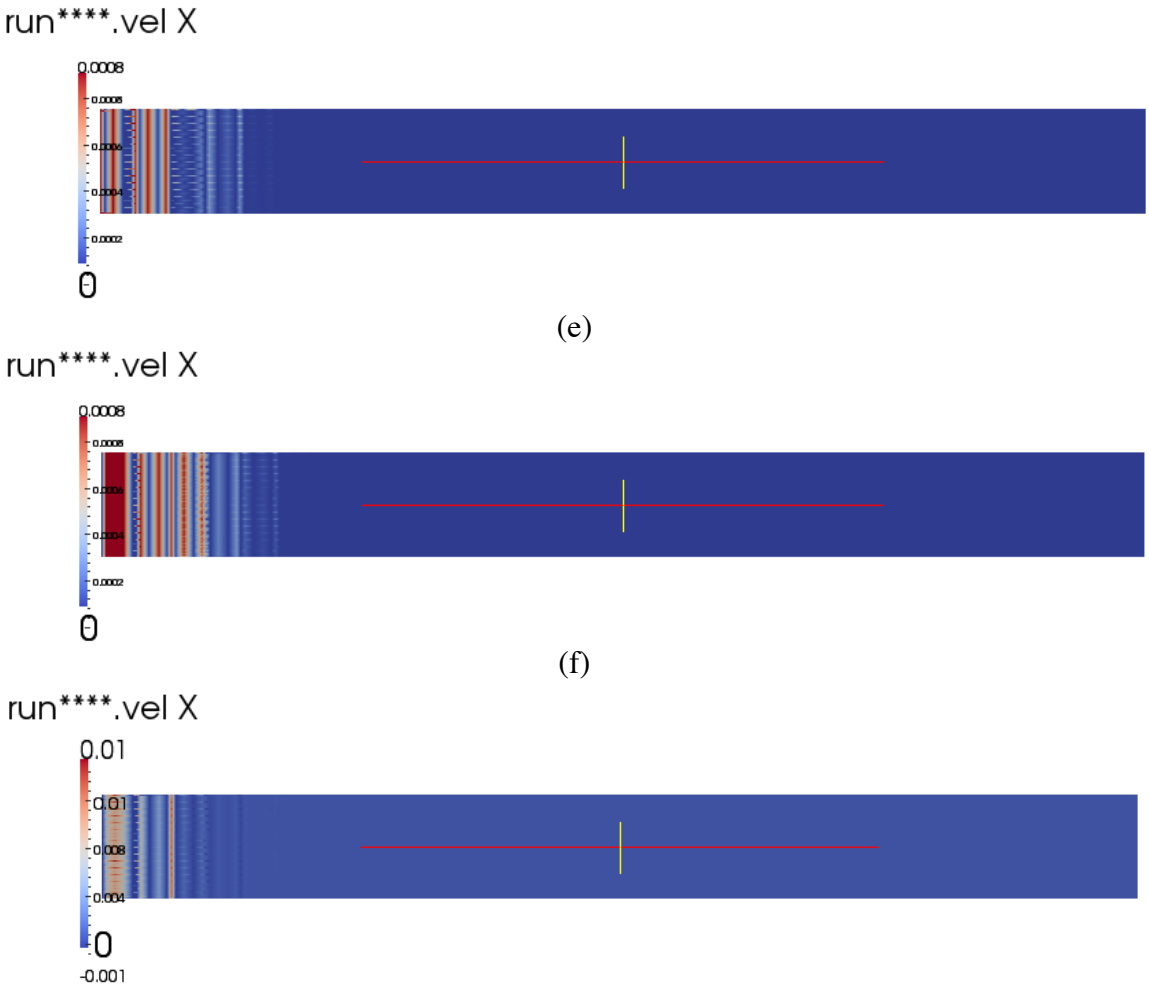

Figure 9.6: 400 SE model based on a 1-D 4th order polynomial basis a)t=1e-5s b)t=0.0001 c)t=0.0002 d)t=0.0003 e)t=0.0004 f)t=0.00045 g)t=0.0005

9.3 CONCLUSIONS

The results for the two-dimensional case are harder to interpret. The spectral element solution, although it has shown a lower tendency to dissipate or disperse, has required a considerably increase in the system's size and the computational time. In the other hand, the finite element solution results in a faster computational time but the solution does not perform very well for long-range propagation problems unless a significantly fine mesh is used.

The SEM performs best numerically wise but a more computationally powerful system is suggested. Given a fixed number of elements, the spectral elements system based on a 3rd order basis can get easily to be more than 5 times larger than a finite element system composed by linear triangular elements. Thus, unless a higher-end computational system is possessed, working on smaller domains is suggested.

Chapter 10: Conclusions

The Spectral Elements have put in evidence their efficiency at treating wave propagation problems in comparison to conventional FEA for the one-dimensional case. They do pose certain problems that involve their sometimes-complex formulation as the order of interpolation is increased. This problem overturns the nice numerical properties and efficiency that SEM provides in comparison to FEM for the treatment of one-dimensional wave propagation problems. Among the problems we often encounter, we find that if the order of the interpolation largely exceeds the value that would render the solution exact, the system becomes considerably unstable. Further temporal discretization would be needed to somewhat overcome the conditioning problems that arise from the system's increase in size. Unfortunately, this would mean longer-than-needed computational times and the whole idea behind using spectral elements would vanish.

One-dimensional spectral elements do have in comparison to conventional FE a lower dispersion degree regardless of the time scheme chosen. In the other hand, they may have a more limiting stability number, which is something to reflect upon about since it may overturn the time computational advantages.

As for two-dimensional wave propagation problems certain advantages arise from the use of simple linear triangular elements. From a computational point of view, operational time is saved because triangular elements do not have to be mapped to a *master* or *standard* shape in order to be numerically integrated using quadratures. Triangular elements have the advantage of having nice closed-form solutions to the integrals as well as constant-valued B matrices that accelerate the element's stiffness

matrix assembly process. Computational times are faster but require fine meshing to reach a high-accuracy level.

The analysis was performed by first assuming that the equation was analytically intractable. Our analysis was mainly interested in the relationship between computational effort and the quality of the approximation to the governing PDE. The results of the analysis must be given in terms of cost-benefit. These benefits do not only include the computed numerical approximation but a *quantification* of the quality of the approximation, in other words, the error estimate.

The assessment of a system's performance cannot be based solely on mesh refinements and/or modification to the time steps size until the system seems to have converged. A system's performance analysis must be conformed by an accurate numerical approximation supported by enough numerical evidence to prove that the approximate solution will not change considerably if further discretization of both the spatial and temporal domains occurs. Even inaccurate systems, after a certain level of discretization, may give the false impression of convergence. Brute-forcing systems to show convergence by discretizing the system excessively both spatially and temporally is counterproductive since the approximation may result excessively accurate, this would mean that more resources than needed were allocated to the operation and had there been correct identification of the system state it could have been possible to make the operation more cost-efficient.

It is necessary to conclude that for both SEM and FEM models as further refinement in the temporal and spatial domain took place overall improvement of the solution behavior occurred. Unfortunately, this can only be stated up to a certain point. As the system's size increases, conditioning problems become too significant to ignore. A proper assessment cannot be casually performed by

checking if values converge or reach a certain threshold. There are too many factors that need to be described and quantified to add credibility to the system's response assessment.

Graphical analysis methods are easy to perform but they lack the fundamental tools of numerical analysis. Error estimation methods based on a strong theoretical background should be implemented because they convey much more information regarding the underlying numerical performance of the system. Unfortunately, for the two-dimensional case no definite answer exists. A statement regarding which method is better at handling wave propagation problems in two dimensions would be irresponsible at this point. Further analysis must be performed. This in-depth analysis should involve domains with complex geometries, different time integration schemes, different temporal and spatial discretization techniques, proper error estimation methods, and if possible, testing of the models using well-known scenarios that have a closed-form solution, this would in part direct our attention to the recovery-based error estimation approach since there would be already actual values to compare with.

Future looks brighter for spectral element based methods, especially on the area of Computational Fluid Mechanics (CFD) where the need for high-response systems that can be easily adapted to the continuous dynamic changes in the numerical data is one of the main considerations. Models are being developed as we speak and equal attention is focused on the development of error estimation methods to correctly assess the accuracy of the solutions. No great change will occur, however, until major breakthrough in the spectral element method development occurs which in turn will cause the shift of the commercial software industry to readily perform these methods. In any case, many options to choose from are still available in order to solve these types of systems; the selection of systems will depend largely on the equipment available, the desired degree of accuracy and the computational time to be invested.

References

Bathe, K. (1982). *Finite element procedures in engineering analyses.* Englewood Cliffs, NJ, USA: Prentice Hall.

Bhatti, M. A. (2005). *Fundamental Finite Element Analysis and Applications.* Hoboken, NJ, USA: John Wiley & Sons.

Gopalakrishnan, S., Chakraborty, A., & Roy Mahapatra, D. (2007). *Spectral Finite Element Method: Wave propagation, Diagnostics and Control In Anisotropic and Inhomogeneous Structures.* Cambridge, MA, USA: Springer.

Hughes, T., & Belytschko, T. (1983). Analysis of transient algorithms with particular reference t o stability behavior. *Computational methods for transient analysis* , 67-155.

Karniadakis, G. E., & Sherwin, S. J. (1999). *Spectral/hp Element Method For CFD.* New York, New York, US: Oxford University Press.

Kwon, J., Ryu, S., Kim, P., & Kim, S. D. (2012). Finite Element Preconditioning on Spectral Element Discretizations for Coupled Elliptic Equations. *Journal of Applied Mathematics , 2012*, 16.

Lee, U. (2009). *Spectral Element Method in Structural Dynamics.* Singapore, Asia: Wiley.

Li, F., Peng, H., Sun, X., Wang, J., & Meng, G. (2012). Wave Propagation Analysis in Composite Laminates Containing a Delamination Using a Three-Dimensional Spectral Element Method. *Mathematical Problems in Engineering , 2012*, 19.

Mitchell, A., Kokotoff, D. M., & Austin, M. W. (2001). Closed-Form Expressions for the Numerical Dispersion and Reflection in FEM Simulations Involving Biaxial Materials. *IEEE TRANSACTIONS ON ANTENNAS AND PROPAGATION , 49* (No. 2).

Pozrikidis, C. (2010). *Introduction to Finite and Spectral Element Methods using MATLAB.* San Diego, California, USA: Chapman & Hall.

Pozrikidis, C., & Blyth, M. (2005 йил 16-March). A Lobatto interpolation grid over the triangle. *IMA Journal of Applied Mathematics* , 1-17.

Schwarz, C., Werner, E., & Dirschmid, H. (2010). 1D wave propagation in a rod: analytic treatment for non-trivial boundary conditions. *Procceedings in Applied Mathematics and Mechanics , 10*, 525-526.

van Hoof, J. (1994). *One- and Two-Dimensional Wave Propagation in Solids.* University of Technology at Eindhoven, Department of Fundamental Mechanics. Eindhoven: University of Technology at Eindhoven.

Yue, B., & Guddati, M. N. (2005). Dispersion-reducing finite elements for transient acoustics. *Acoustical Society of America , 118* (No.4), 2132–2141.

Vita

Shaddy C. Ponton describes himself in the words of James Joyce, as an *engineering* student, an oarsman, a tenor, an amateur actor, a shouting politician, a small landlord, a small investor, a drinker, a good fellow, a storyteller, somebody's secretary, something in a distillery, a taxgatherer, a bankrupt and at present a praiser of his own past. Born two minutes behind schedule, he has been trying to catch up ever since.

Shaddy finished top of his class and during his master he was lucky enough to be a recipient of the Eisenhower fellowship for transportation students even though he chose not to engage in that path. Ever since, Shaddy has engaged in a first and hopefully last attempt at establishing a software design company that specializes on DBMs.

Permanent address: PMB 381 500 W University ave.
El Paso, TX. 79968

This thesis/dissertation was typed by Shaddy C. Ponton.